

# Application of Atypical Acetyl-Lysine Methyl Mimetics in the Development of Selective Inhibitors of the Bromodomain-Containing Protein 7 (BRD7)/Bromodomain-Containing Protein 9 (BRD9) Bromodomains

*Michael A. Clegg,<sup>†,‡</sup> Paul Bamborough,<sup>†</sup> Chun-wa Chung,<sup>†</sup> Peter D. Craggs,<sup>†</sup> Laurie Gordon,<sup>†</sup>  
Paola Grandi,<sup>§</sup> Melanie Leveridge,<sup>†</sup> Matthew Lindon,<sup>†</sup> Gemma M. Liwicki,<sup>†</sup> Anne-Marie  
Michon,<sup>§</sup> Judit Molnar,<sup>†</sup> Inmaculada Rioja,<sup>†</sup> Peter E. Soden,<sup>†</sup> Natalie H. Theodoulou,<sup>†,‡</sup> Thilo  
Werner,<sup>§</sup> Nicholas C. O. Tomkinson,<sup>‡</sup> Rab K. Prinjha,<sup>†</sup> Philip G. Humphreys<sup>†\*</sup>*

<sup>†</sup>GlaxoSmithKline R&D, Stevenage, Hertfordshire SG1 2NY, United Kingdom

<sup>‡</sup>WestCHEM, Department of Pure and Applied Chemistry, Thomas Graham Building,  
University of Strathclyde, 295 Cathedral Street, Glasgow, G1 1XL, United Kingdom

<sup>§</sup>Cellzome GmbH, R&D MST GlaxoSmithKline, Meyerhofstrasse 1, 69117 Heidelberg,  
Germany

**KEYWORDS:** BRD9, BRD7, chemoproteomics, Bromodomain, Bromodomain Containing  
Protein, acetyl-lysine mimetics, Epigenetics

**Abstract**

Non-BET bromodomain containing proteins have become attractive targets for the development of novel therapeutics targeting epigenetic pathways. To help facilitate the target validation of this class of proteins, structurally diverse small molecule ligands, and methodologies to produce selective inhibitors in a predictable fashion are in high demand. Herein we report the development and application of atypical acetyl-lysine (KAc) methyl mimetics to take advantage of the differential stability of conserved water molecules in the bromodomain binding site. Discovery of the n-butyl group as an atypical KAc methyl mimetic allowed generation of **31** (GSK6776) as a soluble, permeable and selective BRD7/9 inhibitor from a pyridazinone template. The n-butyl group was then used to enhance the bromodomain selectivity of an existing BRD9 inhibitor and to transform pan-bromodomain inhibitors into BRD7/9 selective compounds. Finally, a solvent exposed vector was defined from the pyridazinone template to enable bifunctional molecule synthesis and affinity enrichment. Chemoproteomic experiments were used to confirm several of the endogenous protein partners of BRD7 and BRD9 which form part of the chromatin remodelling PBAF and BAF complexes, respectively.

## **Introduction**

Bromodomains are structurally conserved epigenetic reader modules found within bromodomain containing proteins (BCPs) which selectively bind to context-sensitive acetylated lysine residues, thereby recruiting cellular transcriptional machinery to a specific histone mark and regulating gene expression.<sup>1,2</sup> The structure of the 61 human bromodomains is comprised of four antiparallel alpha helices ( $\alpha Z$ ,  $\alpha A$ ,  $\alpha B$ , and  $\alpha C$ ) connected by two flexible loop regions (ZA and BC), which together form the hydrophobic pocket for acetylated lysine binding (Figure 1). Within the binding site of typical human bromodomains (48/61) are two

conserved amino acid residues, Asn and Tyr, which form a direct and a water mediated hydrogen bond to the acetyl-lysine (KAc) residue. The water molecule involved in the latter interaction is one of four highly conserved water molecules also located in the binding site of the bromodomain.

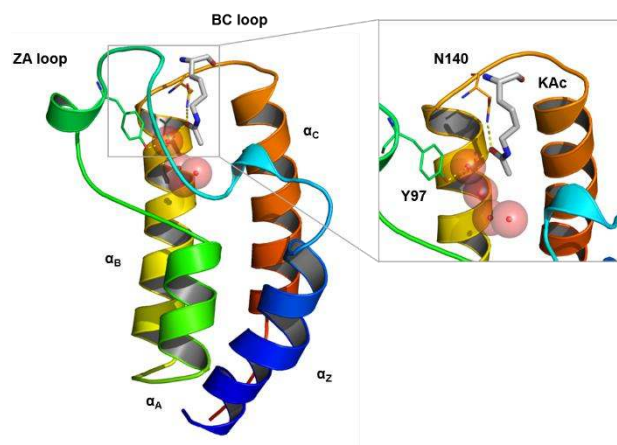


**Figure 1.** X-ray crystal structure of the N-terminal bromodomain of BRD4, BRD4(1), bound to KAc (PDB: 3uvy),<sup>3</sup> highlighting the four antiparallel alpha helices, loop regions, four conserved water molecules, and the key interactions formed between typical bromodomains and acetylated lysines.

Over the past decade bromodomains have emerged as tractable therapeutic targets for immuno-inflammation, neurological disorders, metabolic disease and oncology.<sup>4,5</sup> The bromodomain drug discovery landscape has been dominated by inhibitors of the bromodomain and extra terminal (BET) subfamily of proteins,<sup>6-8</sup> for which a strong and exciting biological phenotype is known. The remaining 53 non-BET BCPs have also been linked with a multitude of diseases, and as demonstrated by the first non-BET bromodomain inhibitor recently entering the clinic (CREBBP inhibitor CCS1477),<sup>9,10</sup> are attractive targets for future therapeutics. To help elucidate the role that BCPs play in modulating healthy and disease states, a variety of chemical and chemical biology approaches are being utilized for the pre-clinical target validation of their bromodomain regions.<sup>11,12</sup> One such approach is chemical probes, small

molecules that selectively binds to a target and are used to interrogate its biological function.<sup>13-</sup>  
<sup>15</sup> Used in conjunction with techniques such as gene knockdown, chemical probes can provide complementary information into the modulation of individual protein domains, particularly prevalent with multidomain BCPs.<sup>16</sup> Fundamental to the success of target validation is the assignment of an observed phenotype to inhibition of the target in question, so access to multiple ligands of divergent chemotypes and structurally related negative controls helps to facilitate this. Although significant advances have been made in populating the bromodomain small molecule toolbox,<sup>17</sup> several BCPs lack the sufficient chemical equity required for robust target validation and would benefit from a deeper more diverse selection.

BRD9 and BRD7 have been reported to be components of the mammalian chromatin remodeling complexes BRG1/BRM-associated factor (BAF) and polybromo associated BAF (PBAF), respectively, two of the most frequently mutated complexes in cancer malignancies,<sup>18,19</sup> making BRD7 and BRD9 attractive targets for oncology.<sup>20</sup> BRD9 has been shown to be involved in multiple cancers,<sup>21</sup> and has recently emerged as a therapeutic target for rhabdoid tumors,<sup>22</sup> whilst BRD7 has been found to function as a tumor suppressor across various cancers.<sup>23-26</sup> To enable investigations into the biology of the BRD7 and BRD9 bromodomains in 2015 the Structural Genomics Consortium (SGC) and the University of Oxford reported the first micromolar BRD7/9 bromodomain inhibitor, LP99 (**1**) (Figure 2).<sup>27</sup> Since then, several BRD7/9 small molecule tools have been reported (Figure 2) spanning multiple chemotypes, although an unsaturated bicyclic system is common throughout. iBRD9 (**2**) was the first BRD9 inhibitor disclosed to display selectivity over the closely related BRD7 with nanomolar potency for BRD9.<sup>28</sup> TP-472 (**3**),<sup>29,30</sup> BI-9564 (**4**) and BI-7273 (**5**) have since been developed by SGC/Takeda and Boehringer Ingelheim, respectively.<sup>31</sup> dBRD9 (**6**), the first BRD9 degrader, has also been disclosed utilizing **5** as a BRD9 selective binder.<sup>32</sup> Degradation of BRD9 may find application in the treatment of strongly BRD9 dependent cancers such as

synovial sarcoma.<sup>33</sup> Finally, selective BRD9 inhibitor GNE-375 (7) has recently been developed by Genentech and Constellation Pharmaceuticals.<sup>34</sup> Small molecule bromodomain inhibitors typically mimic the hydrogen bond acceptor motif and methyl group of the endogenous KAc ligand. The KAc methyl mimetic found most commonly in bromodomain small molecule binders is the methyl group (Figure 2, methyl mimetic highlighted in blue).<sup>17</sup> Chlorine and bromine groups have been used as methyl mimetics, however, the *E*-crotyl group found in GNE-375 (7) is particularly atypical as a KAc methyl mimetic, as is the mechanism by which it drives BRD7/9 selectivity (vide infra).<sup>35</sup>

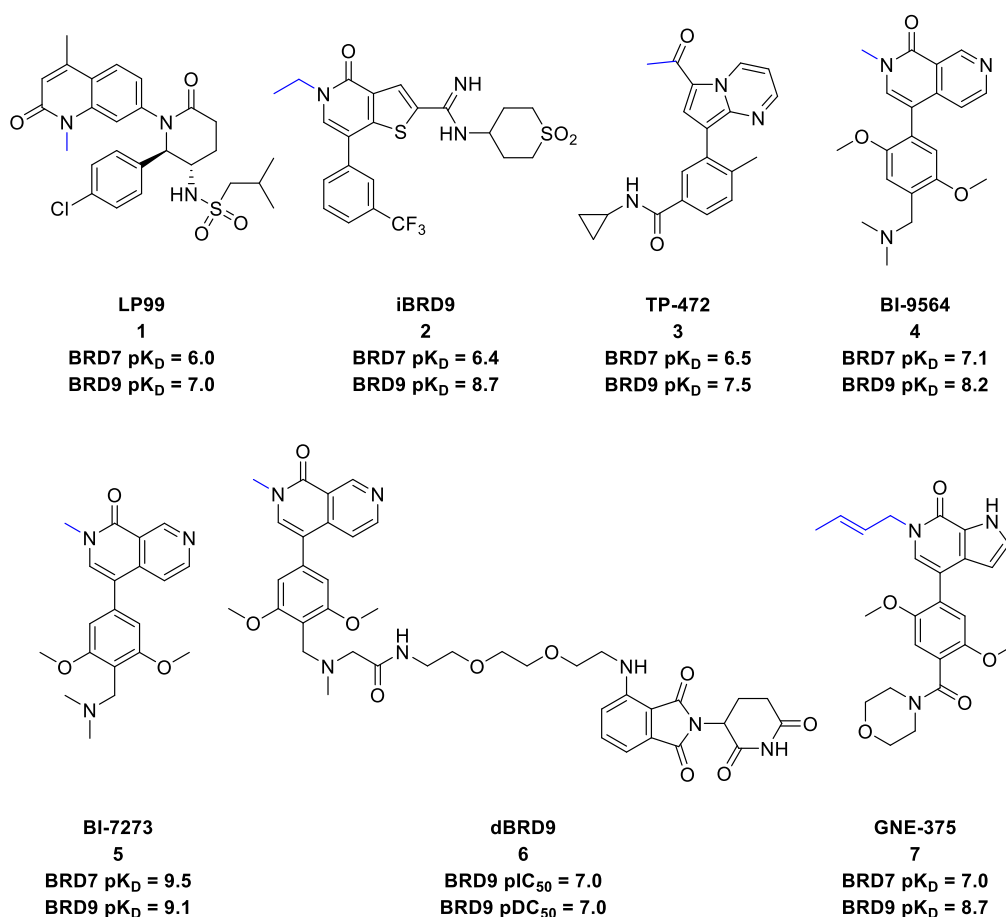


**Figure 2.** Existing BRD7/9 inhibitors and their reported BRD7/9 potencies. The KAc methyl mimetic is highlighted in blue.

Selectivity is heavily scrutinized in medicinal chemistry and is particularly important when considering linking a biological phenotype induced by a small molecule to a target. As

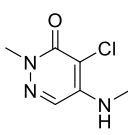
such, methods to obtain selectivity for a given target in a predictable and facile manner is valuable. Herein, we report the discovery and application of the n-butyl group as an atypical KAc methyl mimetic during a research programme to obtain BRD7/9 inhibitors. The n-butyl group was critical to achieve the desired bromodomain selectivity profile and enabled delivery of a potent, selective, soluble and cell-penetrant BRD7/9 inhibitor from an unselective pyridazinone start point bearing a chlorine KAc methyl mimetic. The n-butyl KAc methyl mimetic was then readily applied across diverse chemotypes to identify BRD7/9 selective inhibitors. Finally, a solvent exposed vector was identified from the pyridazinone template to create a linkable analogue for bifunctional applications and chemoproteomic affinity enrichment experiments were used to confirm the endogenous proteins partners of BRD7 and BRD9, which form part of the PBAF and BAF complexes.

## Results and discussion

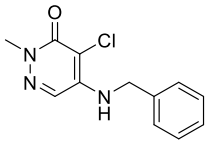
**Discovery of the pyridazinone series as BRD9 inhibitors.** As reported previously, pyridazinones **8** and **9** were identified via a biochemical screen of molecules that were predicted to contain acetyl lysine mimetics during work developing PCAF/GCN5 bromodomain inhibitors.<sup>36</sup> During the course of this work, activity against BET family of bromodomains, using the N-terminal bromodomain of BRD4, BRD4(1), as a representative example, was monitored as an anti-target due to the profound biological phenotype associated with BET inhibition. Fragment **8** is five-fold biased over BRD4(1) and is equipotent against both PCAF and BRD9 (Table 1). In contrast, benzyl **9** demonstrates increased activity and selectivity for BRD9 over both PCAF and BRD4(1). Although both BRD9 and PCAF possess Tyr gatekeeper residues, producing similar deep and narrow binding pockets, they possess significantly different WPF shelf motifs (PCAF: Trp746, Pro747, Phe748; BRD9: Gly43, Phe44, Phe45) (Figure 3b). The impact on the binding site is manifested with Phe44 in BRD9,

which sits almost perpendicular to Trp746 in PCAF and provides a more sterically confined pocket in BRD9 (Figure 3a).

**Table 1.** Biochemical profiling of pyridazinones **8** and **9**.



**8**



**9**

	<b>8</b>	<b>9</b>
BRD9 pIC <sub>50</sub>	4.6	5.7
PCAF pIC <sub>50</sub> (selectivity) <sup>a</sup>	4.7 (-)	4.9 (×6)
BRD4(1) pIC <sub>50</sub> (selectivity) <sup>a</sup>	3.9 (×5)	4.7 (×10)

<sup>a</sup>Selectivity determined from the difference between PCAF or BRD4(1) pIC<sub>50</sub> and BRD9 pIC<sub>50</sub>.

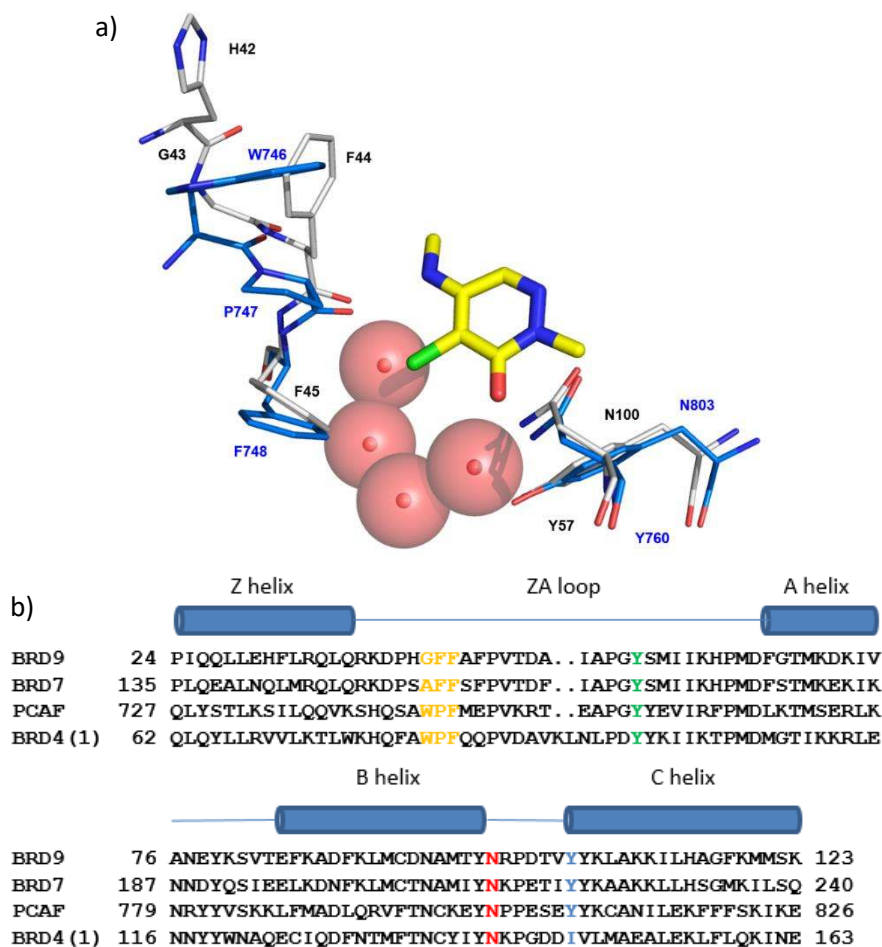
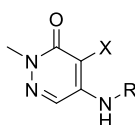


**Figure 3.** a) Crystal structures of pyridazinone fragment **8** (yellow) bound to BRD9 (grey, PDB: 6YQW) and PCAF (blue, PDB: 5MKX) highlighting the different ‘WPF’ shelf motif residues. BRD9 amino acid residues labelled in black, PCAF amino acid residues labelled in blue; b) Sequence alignment of BRD9, BRD7, PCAF and BRD4(1). The WPF moiety is colored orange, the conserved acetyl-lysine-binding asparagine and tyrosine are colored red and green, respectively, and the gatekeeper residue is colored blue.

With numerous pyridazinones synthesized and profiled across several bromodomain assays from PCAF/GCN5 studies,<sup>36</sup> interrogation of the unpublished data revealed a trend between BRD9 selectivity over both PCAF and BRD4(1) and  $sp^2$  hybridization at the amine  $\beta$ -position carbon. On the assumption that selectivity between BRD7 and BRD9 was unlikely due to the high bromodomain homology (Figure 3b), it was hypothesized that selective BRD7/9 inhibitors could be developed from the same pyridazinone template using  $sp^2$  hybridization at the amine  $\beta$ -position as the start point, e.g. compound **9**.

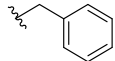
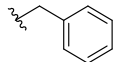
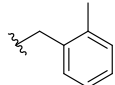
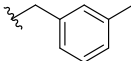
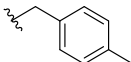
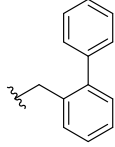
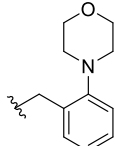
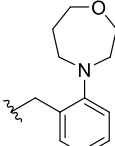
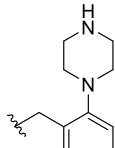
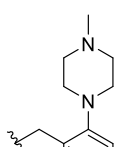
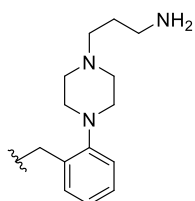
**Benzyl ring SAR investigation.** SAR was initially focused around exploring the different vectors of the benzene ring in compound **9** to gain further interactions with BRD9 and improve potency (Table 2). Bromodomain potency for BRD9 and BRD4(1) was measured via a Time-Resolved Fluorescence Resonance Energy Transfer (TR-FRET) competition assay, where displacement of a fluorescent ligand from the bromodomain binding site provided  $pIC_{50}$  values as measurement of affinity.

**Table 2.** BRD9/BRD4(1) SAR table.  $pIC_{50}$  values refer to potency within TR-FRET assays.



Compound	X	R	BRD9 $pIC_{50}$	BRD9 LLE <sup>a</sup>	BRD4(1) $pIC_{50}$ (selectivity) <sup>b</sup>	Chrom $LogD_{pH7.4}$
----------	---	---	--------------------	--------------------------	---	-------------------------



<b>9</b>	Cl		5.7	2.5	4.7 (×10)	3.2
<b>10</b>	Me		5.9	3.0	4.6 (×20)	2.9
<b>11</b>	Me		6.4	2.8	4.6 (×63)	3.6
<b>12</b>	Cl		5.6	1.6	4.7 (×8)	4.0
<b>13</b>	Cl		6.1	2.1	4.9 (×16)	4.0
<b>14</b>	Me		7.0	2.2	4.9 (×125)	4.8
<b>15</b>	Me		7.0	3.8	4.7 (×200)	3.2
<b>16</b>	Me		7.0	3.5	4.9 (×125)	3.5
<b>17</b>	Me		6.7	6.0	<4.3 (>×250)	0.7
<b>18</b>	Me		6.7	5.1	<4.3 (>×250)	1.6
<b>19</b>	Me		7.2	6.0	4.8 (×250)	1.2

<sup>a</sup>LLE = pIC<sub>50</sub> – ChromLogD<sub>pH7.4</sub>. <sup>b</sup>Selectivity determined from the difference between BRD4(1) pIC<sub>50</sub> and BRD9 pIC<sub>50</sub>.

As shown in Figure 3a, the chloro group of the pyridazinone core functioned as the KAc methyl mimetic in compound **8**. On the assumption that the same was true for compound

**9**, the Cl and Me KAc methyl mimetic matched molecular pair (**9** and **10**) demonstrated broadly similar activity at BRD9 and BRD4(1), although the Me group showed improved BRD9 lipophilic ligand efficiency (LLE) as a result of the reduced lipophilicity. Methyl substitution at the *ortho*, *meta* and *para* positions of the benzene ring were tolerated (compounds **11-13**), with *ortho*-substituted **11** providing the most attractive combination of increased BRD9 potency, LLE and selectivity over BRD4(1). Substitution of the *ortho*-methyl group for a benzene ring with **14** provided an increase in both potency against BRD9 ( $pIC_{50} = 7.0$ ) and lipophilicity. Although activity against the BET bromodomains increased slightly (BRD4(1)  $pIC_{50}$ : 4.9), >100-fold selectivity was achieved for the first time.

To understand the binding modes of compound **14** in both proteins and to gain insights into avenues for further optimisation, X-ray crystallography in both BRD9 and BRD4(1) was obtained (Figure 4). In BRD9, the gatekeeper residue Tyr106 rotates relative to the published apo structure (PDB: 3hme)<sup>3</sup> to make a face-to-face aromatic interaction with the pyridazinone core (Figure 4a), an interaction not possible in BRD4(1) due to the isoleucine gatekeeper (Figure 3b). The pyridazinone carbonyl group forms the canonical direct and water mediated hydrogen bond interactions to Asn100 and Tyr57 respectively. The pyridazinone C-Me group functions as the KAc methyl mimetic, positioning the phenyl ring in the narrow cleft discussed previously with the *ortho* phenyl ring twisted 67.6° to sit on the protein surface (Figure 4b). The pyridazinone NH forms a direct hydrogen bond to the backbone carbonyl of Pro44, whilst the pyridazinone sp<sup>2</sup> hybridized N forms a water mediated hydrogen bond to the backbone carbonyl of Ile53. In contrast, crystallography of **14** bound to BRD4(1) revealed a dramatically different binding mode (Figure 4c). Whilst the canonical hydrogen bond interactions between the pyridazinone carbonyl and Asn140 together with a through-water hydrogen bond to Tyr97 are present, the pyridazinone core flips 180° resulting in the N-Me group functioning as the KAc methyl mimetic. This allows the benzyl group to make partial hydrophobic interactions

with the lipophilic WPF shelf. The *ortho*-phenyl group is directed into the narrow ZA channel formed between Leu92 and Trp81 with a 60.8° dihedral angle to avoid steric clashes with the protein (Figure 4d). Presumably, the lower activity of **14** against BRD4(1) is driven by the lack of pyridazinone core face-to-face aromatic stacking with an aromatic gatekeeper residue, lack of NH hydrogen-bond to the protein and incomplete occupancy of the WPF shelf.

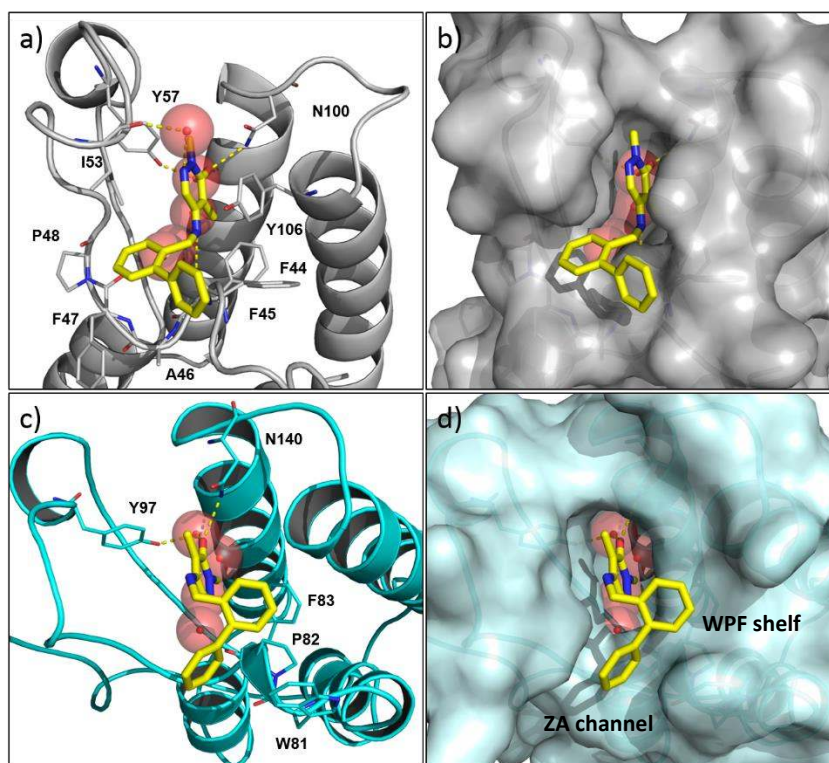
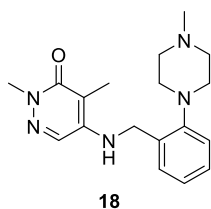


**Figure 4.** a) X-ray crystallography of compound **14** (yellow) bound to a) BRD9 (grey, PDB: 6YQR); b) BRD9 (grey, PDB: 6YQR) highlighting the protein surface; c) BRD4(1) (cyan, PDB: 6YQZ); d) BRD4(1) (cyan), PDB: 6YQZ highlighting the protein surface.

While **14** demonstrated that >100 fold selectivity over BRD4(1) was obtainable from the pyridazinone template, the molecule was unacceptably lipophilic (ChromLog $D_{pH7.4}$ : 4.8) with a less than desirable LLE (BRD9 LLE: 2.2). As the *ortho*-phenyl ring sat in the narrow ZA cleft in BRD4(1), its replacement with polar saturated heterocycles was considered to not only further improve the selectivity over BRD4(1) via steric clashing, but also improve BRD9

LLE.<sup>37</sup> This work-package was not anticipated to impact BRD9 potency drastically as the *ortho*-vector placed such substituents onto the BRD9 protein surface (Figure 4b). Supporting the design hypothesis, morpholine **15** demonstrated improved BET selectivity ( $\times 200$ ) whilst maintaining potency against BRD9 ( $\text{pIC}_{50} = 7.0$ ) and lowering lipophilicity (Table 2). Expansion to the 7-membered oxazepane **16** showed similar properties, whereas basic piperazine **17** showed a further reduction in BET activity ( $\text{pIC}_{50} < 4.3$ ), together with a dramatic drop in lipophilicity and concomitant improvement in the BRD9 LLE to 6.0. Due to concerns over the low lipophilicity of **17** ( $\text{ChromLog}D_{\text{pH}7.4}: 0.7$ ) and the likely impact on passive permeability,<sup>37</sup> methyl piperazine **18** was accessed in order to remove the additional hydrogen bond donor present in **17** and improve permeability while maintaining BRD9 potency, BRD4(1) selectivity and lipophilicity within acceptable ranges. Compound **18** achieved these goals with no change in BRD9 potency, a small drop in BRD9 LLE and desirable chemiluminescent nitrogen detection (CLND) solubility and artificial membrane permeability (AMP) indicating likely cell penetration via passive permeability (Table 3). Further selectivity screening of piperazine **18** against the DiscoverX BROMOscan panel of 34-bromodomains not only confirmed the expected comparable potency between BRD9 and BRD7, but also revealed generally desirable selectivity against the BET (630-fold) and non-BET bromodomains (50-fold) (Table S3).<sup>38</sup> The notable exception to this was BRPF1 where almost equipotency was observed (BRPF1  $\text{pK}_i = 6.6$ ) resulting in only 6-fold bias.

**Table 3.** BROMOscan activity and physicochemical profile for compound **18**.  $\text{pIC}_{50}$  values refer to potency within a TR-FRET assays.  $\text{pK}_i$  values refer to potency within the DiscoverX BROMOscan assay.

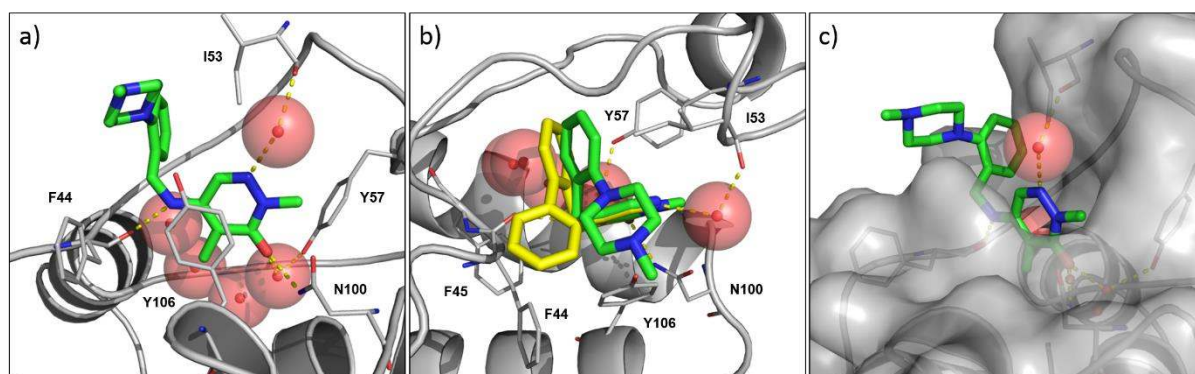


<b>18</b>	
BRD9 pIC <sub>50</sub>	6.7
BRD9 LE <sup>a</sup> /LLE <sup>b</sup>	0.38 / 5.1
BRD9 pK <sub>i</sub>	7.4
BRD7 pK <sub>i</sub>	7.6
BRD4(1) pK <sub>i</sub>	4.6
BRPF1 pK <sub>i</sub>	6.6
BROMOscan selectivity <sup>c</sup>	BET > × 630 All others ≥ ×50
ChromLogD <sub>pH7.4</sub>	1.6
CLND solubility (μg/mL)	178
AMP (nm/s)	330

<sup>a</sup>LE = (1.37 × pIC<sub>50</sub>)/heavy atom count. <sup>b</sup>LLE = pIC<sub>50</sub> – ChromLogD. <sup>c</sup>Selectivity determined from the difference between potencies.

An X-ray of **18** bound to BRD9 enabled a better understanding of the interactions being made with the protein (Figure 5). Despite the pyridazinone core of **18** overlaying almost perfectly with that of compound **14** to make identical interactions with the protein, the more flexible benzylamine group shifts the phenyl ring of **18** ~1.6 Å closer to Ile53. This movement results in a dramatic shift of the attached piperazine ring ~3.7 Å away from the lipophilic Phe44 towards the more polar Tyr106 gatekeeper (Figure 5b). Presumably the more favorable dipole interactions of the weakly basic piperazine (pKa: 8.1) and Tyr106 phenol drives this shift. Additionally, the crystallography highlighted the piperazine methyl group as an exit vector from the protein to enable linkable analogue synthesis (Figure 5c). Confirming this hypothesis, linkable analogue **19** bearing a pendant amine retained activity against BRD9, together with 250-fold selectivity over BRD4(1) (Table 2). The identification and demonstration of a solvent exposed exit vector with compound **19** bearing a primary amine enables the development of

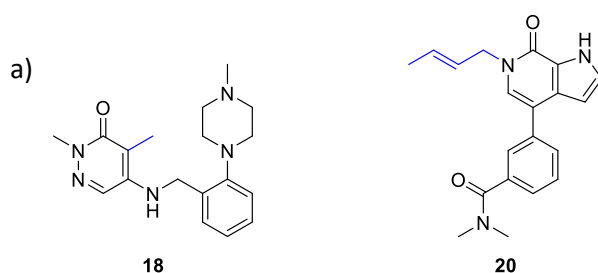
bifunctional tools such as PROTACs and attachment to a solid support for chemoproteomic experiments (vide infra).



**Figure 5.** X-ray crystallography of a) compound **18** (green) bound to BRD9 (grey, PDB: 6YQS); b) overlay of compound **18** (green, PDB: 6YQS) and compound **14** (yellow, PDB: 6YQR) bound to BRD9 (grey); c) compound **18** (green) bound to BRD9 (grey, 6YQS) highlighting the protein surface.

**Atypical KAc methyl mimetics as a path for selectivity.** With BROMOscan data demonstrating the potency of compound **18** at BRPF1, we sought to improve the selectivity against this bromodomain off-target. Attempts to deliver selectivity over BRPF1 through modification of the substituted benzyl group was unsuccessful with BRPF1 potency broadly tracking with BRD9. As an alternative approach, interactions with the conserved waters found in the bromodomain binding site was considered. The displacement of water molecules in small molecule binding sites is a commonly used method in medicinal chemistry to produce higher affinity ligands and impact target selectivity.<sup>39</sup> As mentioned previously, the bromodomain binding site contains four water molecules conserved across all bromodomains adjacent to the methyl group of the KAc and have been the subject of great interest in recent years (Figure 1 and 3a). The relative stabilities of these water networks vary between different bromodomains and offers a route to drastically impact the bromodomain selectivity profile of small molecules. Indeed, multiple groups have estimated the stability of each bromodomain

water network to help explain and predict such transformations.<sup>40,41</sup> The displacement of the bromodomain conserved water network to engender selectivity has been exploited in the development of chemical probes for ATAD2,<sup>42</sup> TAF1(2)<sup>43</sup> and the sub-family VIII bromodomains.<sup>44-46</sup> In direct contrast to water displacement, Crawford and co-workers at Genentech and Constellation Pharmaceuticals elegantly demonstrated that the stability of the conserved water network in the BRD9 and CECR2 bromodomains is such that hydrophobic pockets are preferentially induced by longer lipophilic KAc methyl mimetics to avoid displacing or clashing with the water network.<sup>35,47</sup> This fundamental observation which profoundly impacts the bromodomain selectivity of molecules incorporating larger lipophilic KAc methyl mimetics such as allyl and *E*-crotyl groups was central to Genentech and Constellation Pharmaceuticals development of chemical probes for CECR2 and BRD7/9.<sup>34,48</sup> Inspired by the selectivity profile of GNE-375 (**7**), attributable, in part, to the *E*-crotyl KAc methyl mimetic, it was hypothesised that atypical KAc methyl mimetics may offer a route to selectivity over BRPF1 for the pyridazinone template. Overlaying the crystal structures of **18** and **20** (an early derivative of **7**) revealed the pyridazinone C-Me group as a suitable vector for accessing the induced hydrophobic pocket (Figure 6).<sup>35</sup>



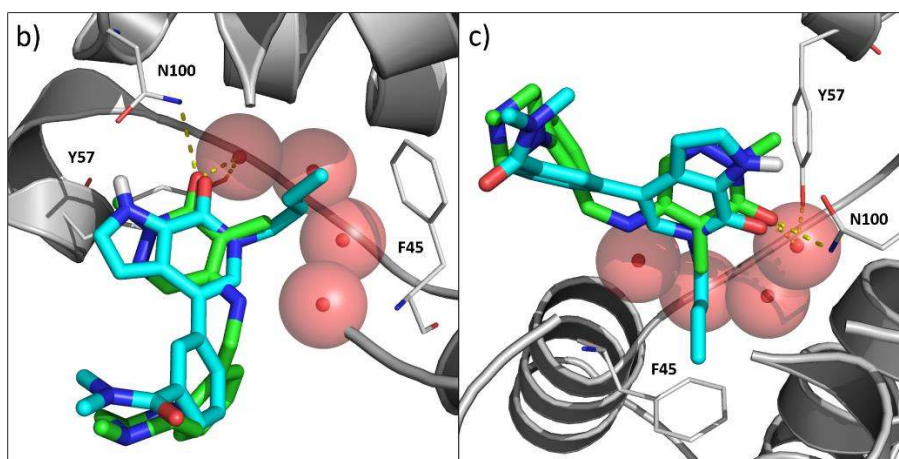
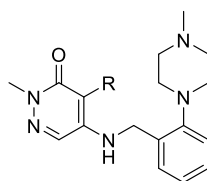


**Figure 6.** a) Structure of BRD9 inhibitors **18** and **20**, the methyl mimetic is coloured blue; b) and c) An overlay of the crystal structures of **18** (green, PDB: 6YQS) and **20** (cyan, PDB: 5I7Y) bound to BRD9 (grey, PDB: 5I7Y), highlighting the vector to access the induced pocket from different perspectives.

To test this design hypothesis, compound **22** bearing the same *E*-crotyl KAc methyl mimetic as compound **7** was accessed (Table 4). To rapidly generate data across several bromodomains, compounds were screened in the BROMOscan assay ( $pK_i$  values) as opposed to internal TR-FRET assays ( $pIC_{50}$  values) that had been used to guide the chemistry to this point.<sup>38</sup> Validating the scaffold-hopping approach outlined in Figure 6, a profound  $\geq 40$  fold reduction in BRPF1 potency was observed while retaining BRD9 activity with compound **22**. Interestingly, a six-fold rise in BRD4(1) potency was also observed with the *E*-crotyl KAc methyl mimetic. To further explore the potential of hydrophobic KAc methyl mimetics on the pyridazinone scaffold, a range of unsaturated groups were accessed (Table 4).

**Table 4.** Unsaturated and saturated alkyl chain KAc methyl mimetic BRD9, BRD4(1) and BRPF1 SAR table.  $pK_i$  values refer to potency within the DiscoverX BROMOscan assay.  $pIC_{50}$  values refer to potency within TR-FRET assays





Compound	R	BRD9 pK <sub>i</sub>	BRD9 LLE <sup>a</sup>	BRD4(1) pK <sub>i</sub> (selectivity) <sup>b</sup>	BRPF1 pK <sub>i</sub> (selectivity) <sup>b</sup>	Chrom LogD <sub>pH7.4</sub>
18	Me	7.4	5.8	4.6 (×630)	6.6 (×5)	1.6
21		7.0	4.5	<5.0 (>×100)	<5.0 (>×100)	2.5
22		7.4	4.3	5.4 (×100)	<5.0 (>×250)	3.1
23		6.6	3.6	<5.0 (>×40)	<5.0 (>×40)	3.0
24		<5	-	<5.0 (-)	<5.0 (-)	3.5
25		6.4	3.2	<5.0 (>×25)	<5.0 (>×25)	3.2
26 <sup>c</sup>		6.6	3.5	<5.0 (>×40)	<5.0 (>×40)	3.1
27 <sup>c</sup>		6.5	3.4	<5.0 (>×30)	<5.0 (>×30)	3.1
28		7.1	4.8	5.1 (×100)	5.2 (×80)	2.3
29		6.9	4.1	<5.0 (>×80)	<5.0 (>×80)	2.8
30		6.5	3.4	<5.0 (>×30)	5.1 (×25)	3.1
31		7.2	3.7	<4.5 (>×500)	<4.5 (>×500)	3.5
32		6.8	2.6	5.8 (×10)	<5.0 (>×63)	4.2
33	H	<4.3 (pIC <sub>50</sub> )	-	<4.3 (pIC <sub>50</sub> )	-	1.1

<sup>a</sup>LLE = pK<sub>i</sub> – ChromLogD. <sup>b</sup>Selectivity determined from the difference in measured biochemical potencies. <sup>c</sup>Single unassigned enantiomer.

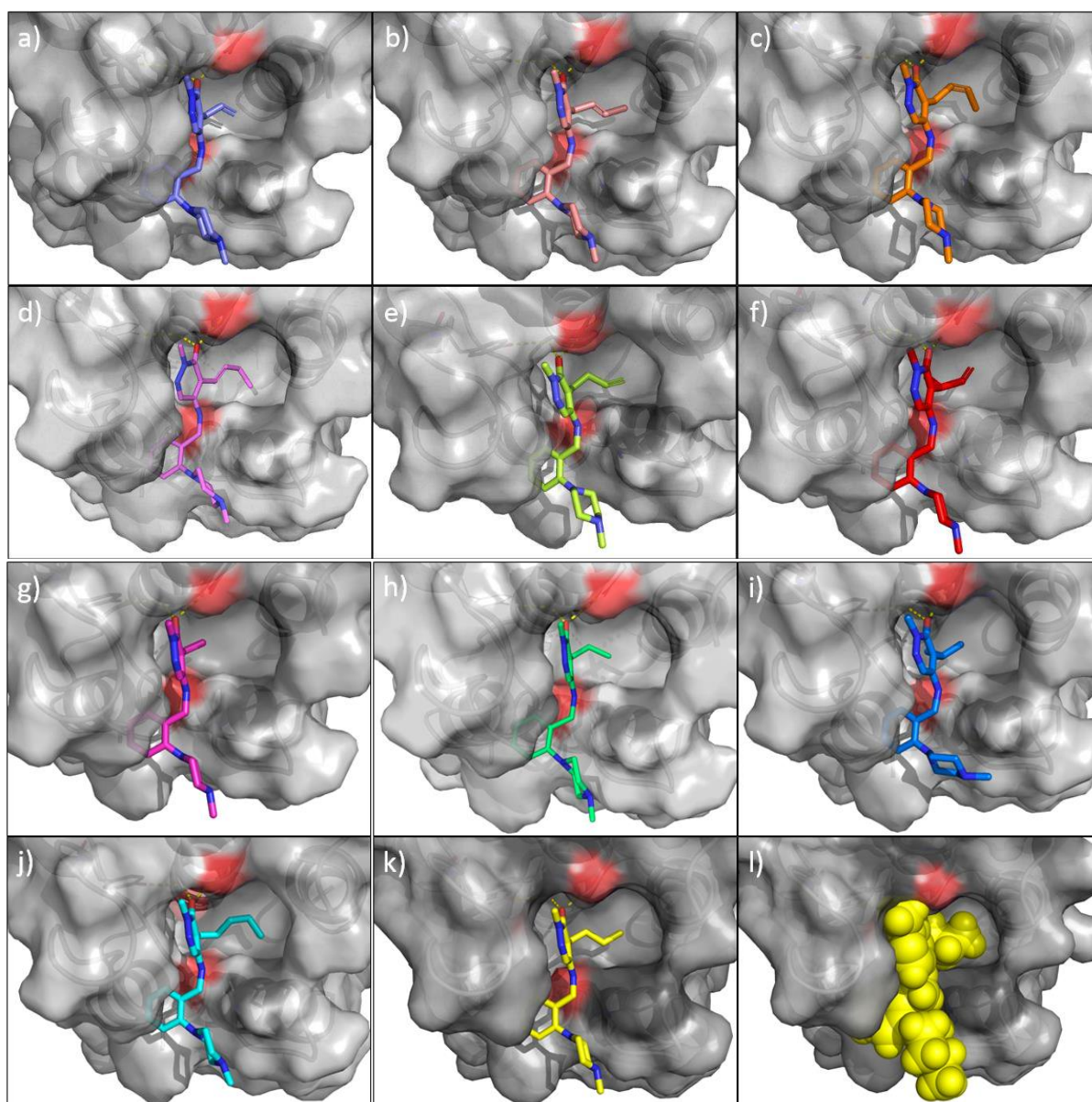
Truncation of the crotyl group to an allyl group with compound **21** maintained the reduced BRPF1 activity while also reducing BRD9 and BRD4(1) potency. Changing the crotyl group geometric isomer from *E* to *Z* resulted in a reduction in potency against both BRD9 and BRD4(1), suggesting the *Z* orientation cannot access the induced pocket as readily (compare compounds **22** and **23**). Moving the double bond into conjugation with the pyridazinone ring with **24** drastically reduced potency against BRD9, suggesting that the alkyl chain was no longer directed towards the induced pocket and was instead clashing with other residues within

the binding site. Butenyl **25** with a terminal alkene also showed a reduction in BRD9 potency. Methyl branching of the allyl group with enantiomers **26** and **27** revealed a reduction of BRD9 activity suggesting increased steric bulk was not tolerated at this position.

Although allyl **21** and *E*-crotyl **22** demonstrated an intriguing level of bromodomain selectivity, there was considerable concern around the risk of olefin isomerization into more thermodynamically stable conjugation with the pyridazinone ring. Such isomerization would likely lead to a large drop in BRD9 activity (compare non-conjugated **22** and **25** with conjugated **24**, Table 4). The potential for more flexible saturated analogues was considered to remove the isomerization risk while still accessing the induced BRD9 hydrophobic pocket.<sup>35</sup> Accordingly, saturated KAc methyl mimetic derivatives **28-32** were accessed and profiled. As also observed with the unsaturated KAc methyl mimetic studies (compounds **21-27**), at least a 25 fold reduction in BRPF1 potency was obtained across all saturated alkyl chains tested, highlighting the sensitivity of the BRPF1 bromodomain to substitution in this region (compare **18** with **28** and **29**, Table 4). Both ethyl **28** and propyl **29** profoundly reduced BRPF1 potency while showing a small decrease in BRD9 activity. Introduction of branching at the linker carbon in **30** remained detrimental to the BRD9 potency, confirming the poor tolerance for steric bulk at this position as seen with compounds **26** and **27**. Moving from a 3-carbon to a 4-carbon chain with *n*-butyl **31** showed an increase in BRD9 potency ( $pK_i = 7.2$ ), as observed for the unsaturated chains. Although **31** was more lipophilic than most other analogues, the compound remained inactive at BRD4(1) at the concentrations tested, maintaining high BET bromodomain selectivity ( $> \times 500$ ). Extending the chain further with *n*-pentyl **32** resulted in a drop in BRD9 potency, together with an unexpected rise of BRD4(1) activity suggesting 4-atom chains are optimal for occupying the induced BRD9 hydrophobic pocket. Complete removal of the *n*-butyl group with compound **33** ablated activity against BRD9 and BRD4(1)

providing further evidence of the critical importance of the KAc methyl mimetic to potency against these bromodomains.

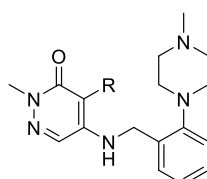
On the assumption that molecules with lipophilic KAc mimetics were inducing the same hydrophobic pocket in BRD9 as described by Crawford and co-workers,<sup>35</sup> compounds **21–32** were docked into a crystal structure of the BRD9 protein with the induced hydrophobic pocket derived from **20** bound to BRD9 (PDB: 5I7Y, Figure 7). Consistent with the biochemical data, the *E*-crotyl chain of **22** showed optimal occupancy of the induced pocket (Figure 7b), whereas reducing the carbon chain length resulted in partial occupancy of the pocket with **21** (Figure 7a). Alteration of the double bond geometry (compound **23**) and positioning (compounds **24** and **25**) appeared detrimental to binding, forcing the molecules to twist to accommodate the chain conformations (Figure 7c-e). Similarly, branching at the adjoining carbon with **27** caused a shift of the core to accommodate the additional steric demand (Figure 7f). Docking the saturated analogues revealed a similar pattern with the four-atom n-butyl chain **31** appearing optimal for occupying the induced pocket (Figure 7k and l). Shorter chains (**28** and **29**) again showed only partial occupancy of the induced pocket (Figure 7g and h) and branching with iso-propyl **30** appeared to cause the molecule to twist within the binding site (Figure 7i). The larger pentyl chain of **32** was also poorly accommodated as expected (Figure 7j).

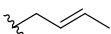
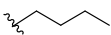


**Figure 7.** Docking of pyridazinone analogues bearing different KAc methyl mimetics a) allyl **21**; b) *E*-crotyl **22**; c) *Z*-crotyl **23**; d) 1,2-butenyl **24**; e) 3,4-butenyl **25**; f) *sec*-butenyl **27**; g) ethyl **28**; h) propyl **29**; i) isopropyl **30**; j) pentyl **32**; k) *n*-butyl **31**; l) *n*-butyl **31** space filled into the BRD9 bromodomain (grey) using Glide (Schrodinger Inc) 2018.3 with hydrogen-bonding constraints between docked ligands and both the W1 conserved water molecule and the carbonyl group of Phe44. Tyr106 has been removed from the visualisation to help show the induced pocket. PDB: 5I7Y was used for all dockings.

A comparison of matched molecular pair profiles of methyl, *E*-crotyl and n-butyl KAc methyl mimetics **18**, **22** and **31** highlighted some key differences (Table 5). As discussed above, **18** shows substantial activity for BRPF1 in the BROMOscan assay which is removed when moving to longer lipophilic chains **22** and **31**. The more flexible n-butyl chain drives reduced BRD4(1) potency and as a result, improved BRD4(1) selectivity compared to the *E*-crotyl chain. Additionally, inhibition of TAF1(2) was seen at 10  $\mu$ M for *E*-crotyl **22** which was ablated with n-butyl **31**. Although there is an expected increase in lipophilicity upon addition of the n-butyl chain, together with a concomitant decrease in LLE compared to the other KAc methyl mimetics profiled, the improvement in bromodomain selectivity warranted further profiling of compound **31**.

**Table 5.** Comparison of methyl mimetic SAR.  $pK_i$  and %I values refer to potency within the DiscoverX BROMOscan assay.



Compound	R	BRD9 $pK_i$	BRD9 LLE <sup>a</sup>	BRD4(1) $pK_i$ (selectivity) <sup>b</sup>	BRPF1 $pK_i$ (selectivity) <sup>b</sup>	TAF1(2) %I at 10 $\mu$ M	Chrom LogD <sub>pH7.4</sub>
<b>18</b>	Me	7.4	5.8	4.6 ( $\times 630$ )	6.6 ( $\times 5$ )	35	1.6
<b>22</b>		7.4	4.3	5.4 ( $\times 100$ )	<5.0 ( $>\times 250$ )	84	3.1
<b>31</b>		7.2	3.7	<4.5 ( $>\times 500$ )	<4.5 ( $>\times 500$ )	0	3.5

<sup>a</sup>LLE =  $pK_i$  - ChromLogD. <sup>b</sup>Selectivity determined from the difference in measured biochemical potencies.

The selectivity of **31** against the wider bromodomain family was determined using the DiscoverX BROMOscan panel (Figure 8 and Table S5).<sup>38</sup> Excluding high potency against the highly homologous BRD7 ( $pK_i$  = 6.3), excellent selectivity against the BET ( $>\times 500$ ) and non-BET bromodomains ( $\geq \times 285$ ) was observed. Compound **31** was also screened against an internal panel of 40 biological off-targets showing  $pXC_{50} \leq 5.0$  excluding G protein-coupled

receptor MrgX2 ( $pIC_{50} = 5.3$ ) and serotonin 1B ( $pIC_{50} = 5.7$ ) (Table S6). Compound **31** was soluble ( $\geq 228 \mu\text{g/mL}$ ) in a charged-aerosol detection (CAD) assay<sup>49</sup> and permeable (250 nm/s) in an artificial membrane permeability assay, indicating likely cell permeability by passive diffusion. Supporting this hypothesis, the concentration of compound **31** outside and inside HeLa cells was monitored using an intracellular concentration assay.<sup>50,51</sup> The cellular influx/efflux ratio was measured ( $p\Delta C = 0.54$ ) and demonstrated good cellular permeability with slight accumulation within the cell (Table 6).

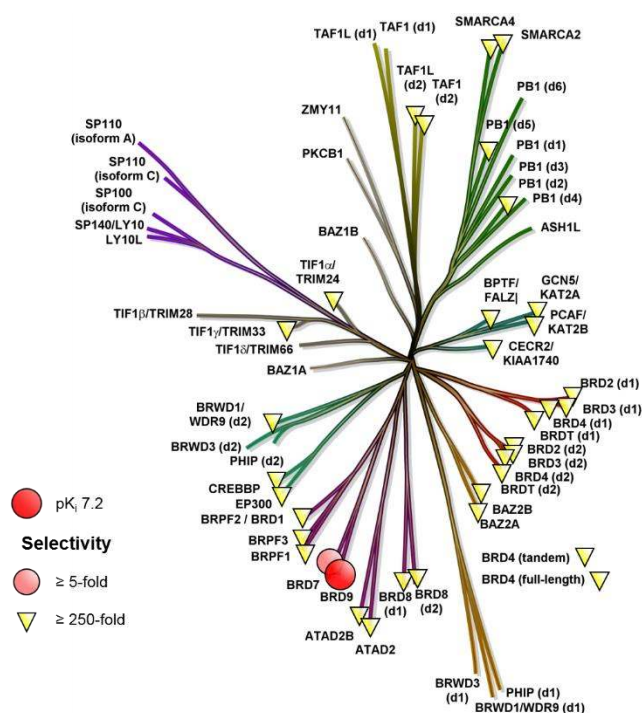
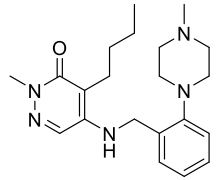


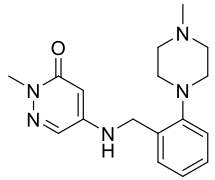
**Figure 8.** DiscoverX BROMOScan activity profile for compound **31** screened against 40 bromodomains.

The combination of **31** and **33** as inhibitor and negative control respectively represent two potential additions to the small molecule BRD7/9 target validation toolbox. However, assays to demonstrate cellular target engagement with compound **31** were not available within GSK and the data to support claiming compound **31** as a chemical probe for the BRD7/9 bromodomains is unavailable. It is of note that the profile outlined in Table 6 is consistent with a soluble, cell permeable compound, but the lack of BRD7/9 cellular target engagement data is an important caveat that should be acknowledged and considered before any use.

**Table 6.** Summary of properties for **31** and **33**. pIC<sub>50</sub> values refer to potency within a TR-FRET assays. pK<sub>i</sub> values refer to potency within the DiscoverX BROMOscan assay.



**31**  
(GSK6776)



**33**  
(GSK0951)

	<b>31</b>	<b>33</b>
BRD9 pK <sub>i</sub>	7.2	<4.3 (pIC <sub>50</sub> )
BRD9 LE <sup>a</sup> / LLE <sup>b</sup>	0.37 / 3.7	-
BRD4(1) pK <sub>i</sub>	<4.5	<4.3 (pIC <sub>50</sub> )
BRD7 pK <sub>i</sub>	6.3	-
BROMOscan selectivity <sup>a</sup>	BET >×500 All others ≥×285	-
ChromLogD <sub>pH7.4</sub> / cLogP	3.5 / 3.2	1.1 / 1.2
CAD solubility (μg/mL)	≥228	≥150
AMP (nm/s)	250	140
Intracellular influx:efflux ratio (pΔC)	0.52	-

<sup>a</sup>LE = (1.37 × pK<sub>i</sub>)/heavy atom count. <sup>b</sup>LLE = pIC<sub>50</sub> – ChromLogD. <sup>c</sup>Selectivity determined from the difference between potencies.

**Application of n-butyl KAc methyl mimetic across multiple chemotypes.** Having demonstrated the possibility of bromodomain selectivity through the use of an n-butyl KAc methyl mimetic in the development of **31**, the broader applicability of this group was considered. Three molecules from different scaffolds were selected to test the utility and translatability of this atypical KAc methyl mimetic: 1) compound **34**,<sup>36</sup> an unselective compound from the pyridazinone template; 2) iBRD9 (**2**),<sup>28</sup> a BRD9 selective compound with a pyridinone KAc mimetic; 3) bromosporine (**37**),<sup>52</sup> a pan-bromodomain inhibitor with a triazole KAc mimetic (Figure 9). Published X-ray crystallographic data was used to identify the KAc methyl mimetic and appropriate vector to introduce the n-butyl group.

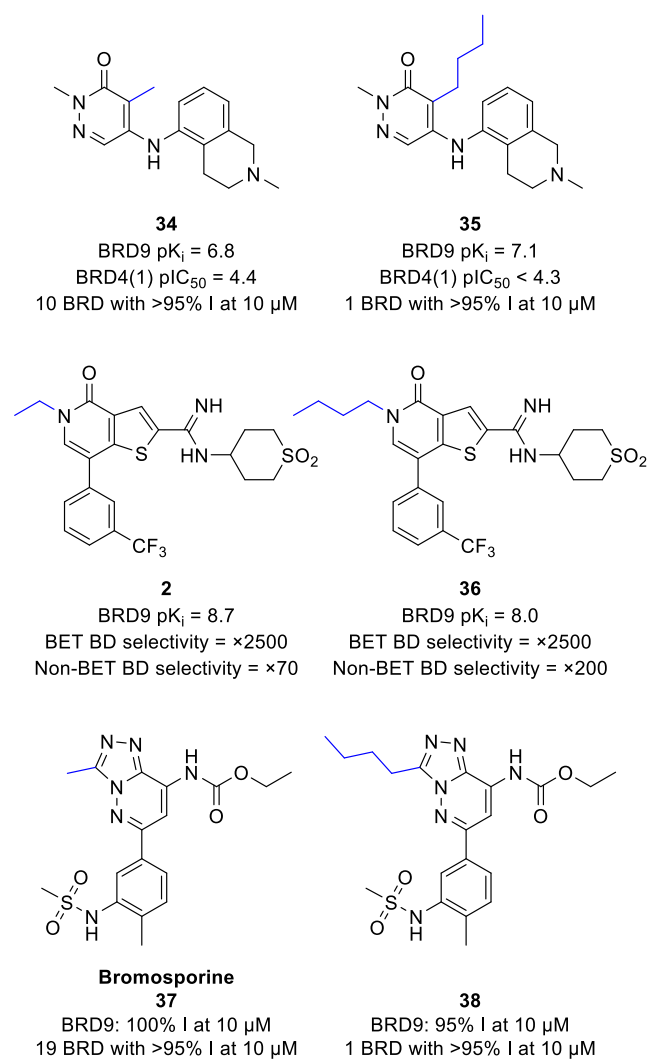


**Figure 9.** Three templates selected to test the broader applicability of the n-butyl KAc methyl mimetic methodology and their corresponding n-butyl derivatives. Full data shown in Table S8. Data for compound **2** can be found in reference 28.

Pyridiazinone **34** was identified during work developing PCAF/GCN5 inhibitors as a promiscuous pan-bromodomain inhibitor: screening at 10 μM concentration against 32 bromodomains revealed 10 bromodomains with >95% inhibition.<sup>36</sup> The n-butyl analogue **35** showed far improved selectivity for BRD7/9 at 10 μM across the same panel of 32 bromodomains and retained activity against BRD9 (pK<sub>i</sub> = 7.1) (Figure 10b and Table S7).<sup>38</sup> Similarly, **36**, the n-butyl derivative of iBRD9 (**2**), showed improved selectivity at 10 μM (Figure 10d and Table S7) and an overall increase in non-BET bromodomain selectivity (Table



S8). Interestingly, the CECR2 potency dropped upon moving from ethyl to n-butyl (CECR2 pK<sub>i</sub> **2**: 6.9 to **36**: 5.6), whereas the TAF1(2) potency increased (TAF1(2) pK<sub>i</sub> **2**: 5.1 to **36**: 5.7). However, the overall selectivity to the closest non-BET bromodomain increased from 70 to 200-fold. Bromosporine (**37**) is a highly promiscuous bromodomain inhibitor as demonstrated by 19 bromodomains showing ≥95% inhibition at 10 μM in the bromodomain panel (Figure 10e). In comparison, at 10 μM n-butyl analogue **38** only showed a single bromodomain (BRD9) at ≥95% inhibition (Figure 10f) highlighting the dramatic shift in selectivity profile possible across multiple chemotypes with different KAc mimetics.

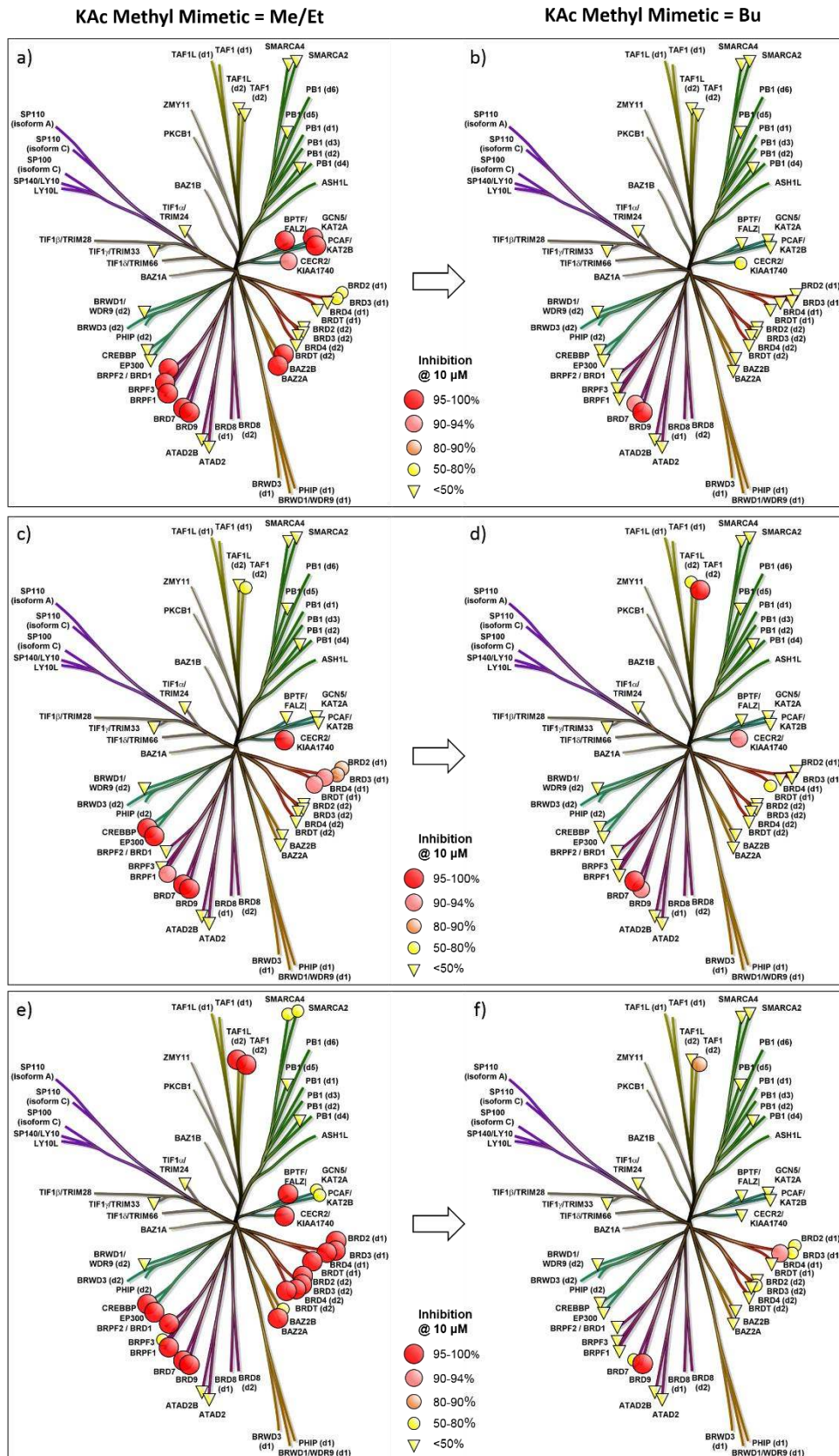


**Figure 10.** DiscoverX BROMOscan profiling at 10 μM for a) compound **34**; b) compound **35**; c) iBRD9 (**2**); d) compound **36**; e) bromosporine (**37**); f) compound **38**.

**Investigation of the PBAF and BAF complexes using chemoproteomics.** Affinity enrichment chemoproteomics is a powerful method to not only identify small molecule protein targets, but also to interrogate endogenous protein complexes.<sup>53</sup> Linkable pyridazinone analogue **19** bearing a solvent exposed primary amine facilitated such experiments and allowed interrogation of the endogenous BRD7 and BRD9 associated chromatin remodelling PBAF and BAF complexes which have been explored via proteomic and bioinformatic approaches previously. Nuclear and chromatin lysates from Hut-78 cells were incubated with sepharose immobilized **19** as an affinity resin and 10  $\mu$ M compound **18** as the binding competitor. Following washing, the residual proteins still bound on the affinity resin were eluted, identified and quantified by mass spectrometry (Figure 11, Table S10). The data was plotted as a Log<sub>2</sub> fold change (FC) versus the DMSO only control and those proteins specifically competed by compound **18** more than 60% in both replicates are labelled in Figure 11. Together with the expected BRD7 and BRD9 bromodomain containing proteins, seventeen other proteins were identified, all of which are reported members of the PBAF or BAF complexes.<sup>20</sup> Of note is the enrichment of BCL7A and BCL7B together with BRD9 which supports previous proteomic studies indicating these are dedicated, non-exchangeable subunits of the BAF complex.<sup>20</sup> Bromodomain containing proteins PBRM1, SMARCA2 and SMARCA4 were also identified as being specifically competed in this experiment. However, the low affinity of compound **18** to these bromodomain containing proteins as judged by BROMOScan (Table S3) further supports evidence that these proteins are enriched in the affinity-purification experiment because they are components of the PBAF and BAF complexes.

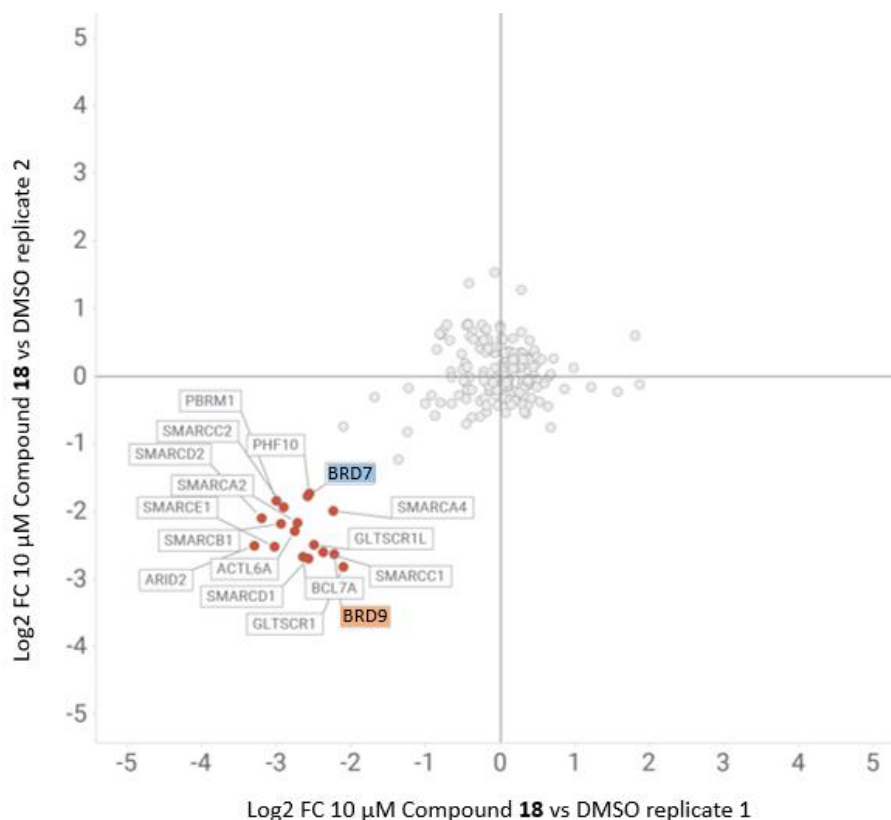
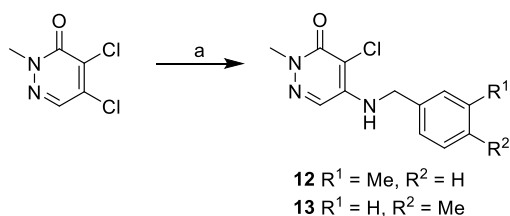


**Figure 11.** Affinity enrichment chemoproteomic experiments in Hut-78 nuclear and chromatin lysate.

**Chemistry: Synthesis of Compounds.** Pyridazinones **12** and **13** were synthesized from commercially available 4,5-dichloro-2-methylpyridazin-3(2H)-one (Scheme 1).<sup>36</sup>  $S_NAr$  with the corresponding amine occurred preferentially at the 5-position yielding compounds **12** and **13**.

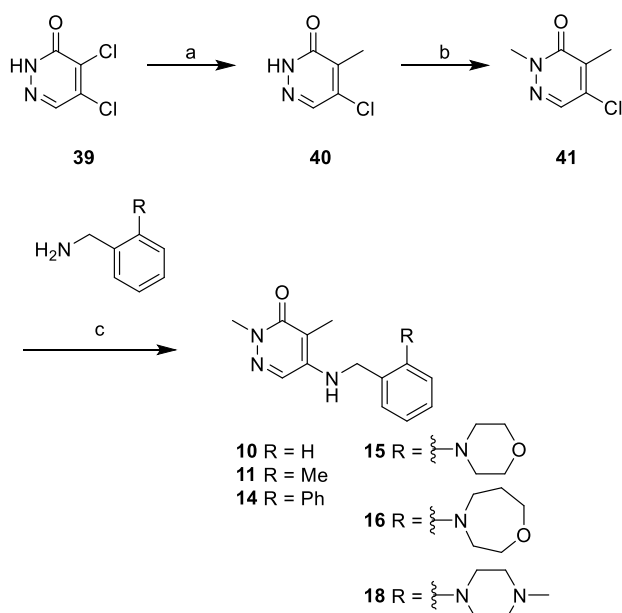
### Scheme 1



Reagents and conditions: (a) amine, DMSO, 120 °C, 1 h, 23-75%.

Compounds **10** and **11** were synthesized from commercially available **39** (Scheme 2). Deprotonation followed by S<sub>N</sub>Ar reaction with excess 3.4 M MeMgBr in THF gave 4-methyl pyridazinone **40**. Subsequent methylation with MeI gave key intermediate **41** which was reacted under a variety of Buchwald-Hartwig amination conditions using different Pd pre-catalysts and ligands with the requisite amine to give compounds **10**, **11**, **14-16** and **18**.

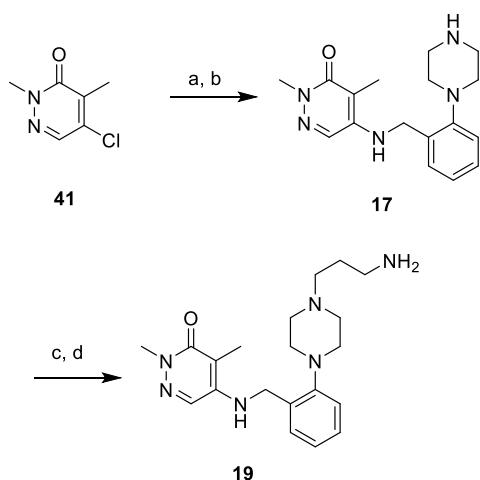
### Scheme 2



Reagents and conditions: (a) 3.4 M MeMgBr, THF, rt, 5.5 h, 81%; (b) MeI, TBAB, K<sub>2</sub>CO<sub>3</sub>, MeCN, rt-60 °C, 4 h, 55%; (c) Pd catalyzed Buchwald-Hartwig amination, NaO*t*-Bu or KO*t*-Bu, 1,4-dioxane, 100-120 °C, 30 min – 1 h, 13-61%.

Similarly, compound **17** was synthesized via a Buchwald-Hartwig amination followed by an acid mediated Boc deprotection to unveil the target compound. Cesium carbonate mediated alkylation of **17** was then followed by Boc deprotection to yield linkable analogue **19**.

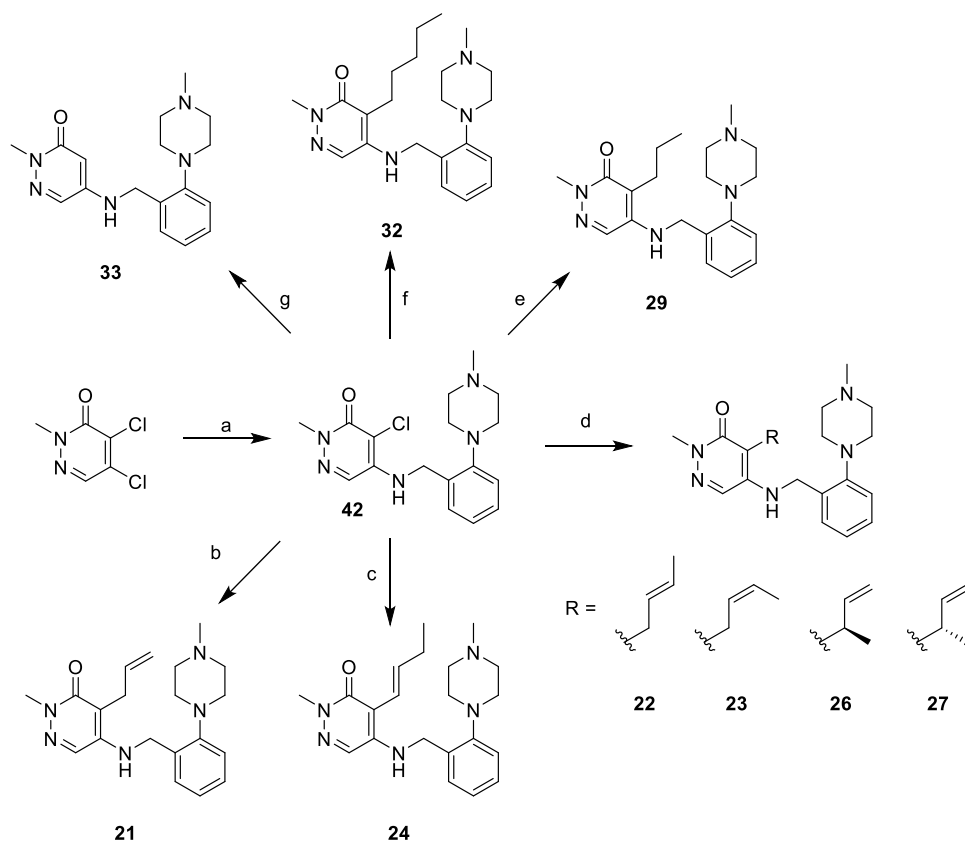
### Scheme 3



Reagents and conditions: (a) *tert*-butyl 4-(2-(aminomethyl)phenyl)piperazine-1-carboxylate, BrettPhos-Pd-G1, BrettPhos, NaO<sup>t</sup>Bu, 1,4-dioxane, microwave 120 °C, 30 min; (b) 4 M HCl 1,4-dioxane, DCM, rt, 18 h, 10% over two steps; (c) BocNHCH<sub>2</sub>CH<sub>2</sub>CH<sub>2</sub>Br, Cs<sub>2</sub>CO<sub>3</sub>, DMF, rt to 50 °C, 36 h, 20%; (d) HCl, 1,4-dioxane, rt, 18 h, 18%.

The synthesis of compounds **21-24**, **26**, **27**, **29**, **32** and **33** began from commercially available 4,5-dichloro-2-methylpyridazin-3(2H)-one (Scheme 4). S<sub>N</sub>Ar with (2-(4-methylpiperazin-1-yl)phenyl)methanamine occurred preferentially at the 5-position to yield pivotal intermediate **42**. Standard Suzuki cross-coupling introduced the desired alkenyl or alkyl chain to give **21**, **24**, **29** and **32**. Cross-coupling of **42** with (*E*)-2-(but-2-en-1-yl)-4,4,5,5-tetramethyl-1,3,2-dioxaborolane yielded a mixture of *Z* and *E* crotyl isomers (**22** and **23**) and sec-butenyl enantiomers **26** and **27** which were separated into a pair of unassigned enantiomers via chiral chromatography. Compound **33** was observed as the major by-product of the Suzuki reactions formed via proto-dechlorination of starting material **42**. This by product was particularly prevalent in the attempted Suzuki reaction with potassium butyltrifluoroborate and was isolated in 43% yield.

#### Scheme 4

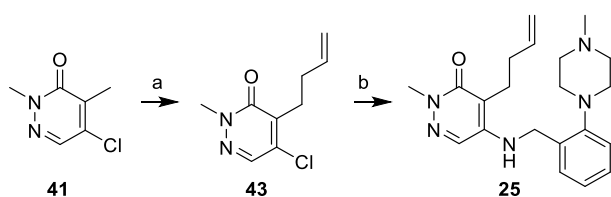


Reagents and conditions: (a) (2-(4-methylpiperazin-1-yl)phenyl)methanamine, DIPEA, DMSO, 120 °C, 1 h, 63%; (b) allyl-Bpin, RuPhos Pd G2, K<sub>2</sub>CO<sub>3</sub>, 1,4-dioxane/H<sub>2</sub>O, 100 °C, 1 h, 28%; (c) (*E*)-but-1-en-1-ylboronic acid, Pd(OAc)<sub>2</sub>, CataCXium A, K<sub>2</sub>CO<sub>3</sub>, 1,4-dioxane/H<sub>2</sub>O, 100 °C, 5 h, 47%; (d) (*E*)-2-(But-2-en-1-yl)-Bpin, Pd(OAc)<sub>2</sub>, CataCXium A, K<sub>2</sub>CO<sub>3</sub>, 1,4-dioxane/H<sub>2</sub>O, 100 °C, 1.5 h, 30% combined yield; (e) propylboronic acid, Pd(OAc)<sub>2</sub>, CataCXium A, K<sub>2</sub>CO<sub>3</sub>, 1,4-dioxane/H<sub>2</sub>O, 100 °C, 1 h, 29%; (f) pentylboronic acid, Pd(OAc)<sub>2</sub>, CataCXium A, K<sub>2</sub>CO<sub>3</sub>, 1,4-dioxane/H<sub>2</sub>O, 100 °C, 1 h, 25%; (g) potassium butyltrifluoroborate, Pd(OAc)<sub>2</sub>, CataCXium A, K<sub>2</sub>CO<sub>3</sub>, 1,4-dioxane/H<sub>2</sub>O, 100 °C, 1 h, 43%.

Terminal alkene **25** was synthesized from key intermediate **41** (Scheme 5).

Deprotonation of the ene-imine  $\gamma$ -proton with LiHMDS and alkylation with allyl bromine appended the butenyl chain to give **43**. A standard Buchwald-Hartwig amination with the substituted benzylamine gave target compound **25**.

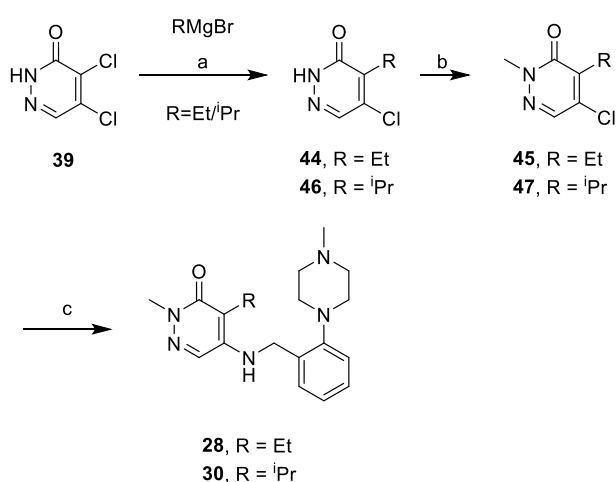
### Scheme 5



Reagents and conditions: (a) allylbromide, LiHMDS, THF, -78 °C, 45 min, 24%; (b) (2-(4-methylpiperazin-1-yl)phenyl)methanamine, Pd<sub>2</sub>(dba)<sub>3</sub>, BrettPhos, NaO<sup>t</sup>Bu, THF, 100 °C, 1 h, 20%.

Ethyl and isopropyl derivatives were synthesized from commercially available **39** in a similar manner to that described in Scheme 2. A chemoselective S<sub>N</sub>Ar with ethyl or isopropyl Grignard reagents yielded intermediates **44** and **46** respectively (Scheme 6). Straightforward alkylation with MeI of both intermediates was followed by a Buchwald-Hartwig reaction to give compounds **28** and **30**.

### Scheme 6

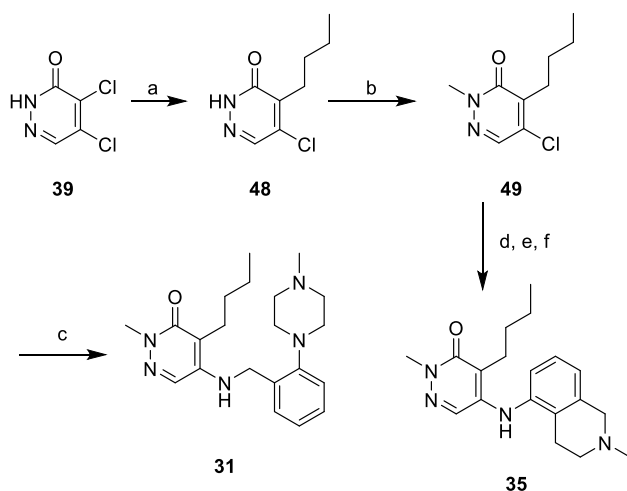


Reagents and conditions: (a) THF, 0 °C to rt, 1.5-3 h, 26-27%; (b) MeI, TBAB, K<sub>2</sub>CO<sub>3</sub>, MeCN, rt, 2.5-3 h, 19-63%; (c) (2-(4-methylpiperazin-1-yl)phenyl)methanamine, Pd<sub>2</sub>(dba)<sub>3</sub>, BrettPhos, NaO<sup>t</sup>Bu, THF, 100 °C, 1 h, 36-46%.

Butyl derivatives **31** and **35** were synthesized from commercially available **39** in a similar fashion (Scheme 7). A chemoselective S<sub>N</sub>Ar with 1.6 M n-BuLi in hexanes was followed by NH methylation under standard conditions to give intermediate **49**. A Buchwald-Hartwig reaction with the appropriate amine gave target **31**. Alternatively, Buchwald-Hartwig coupling with *tert*-butyl 5-amino-3,4-dihydroisoquinoline-2(1H)-carboxylate was then followed by Boc-deprotected under standard acidic conditions and then methylation via an Eschweiler-Clarke reaction to give **35**.

### Scheme 7

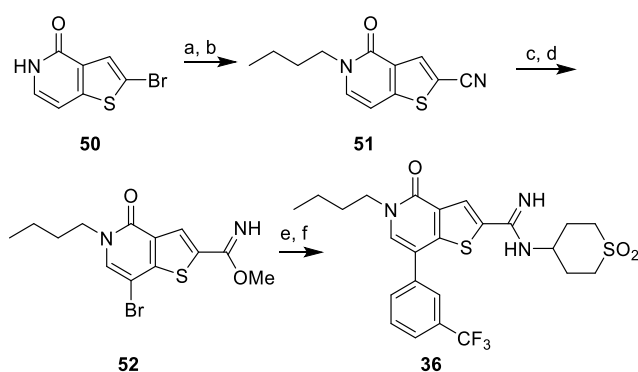




Reagents and conditions: (a) 1.6 M *n*-BuLi, THF, -78 °C, 15 min, 63%; (b) MeI, TBAB, K<sub>2</sub>CO<sub>3</sub>, MeCN, 60 °C, 5 h, 77%; (c) (2-(4-methylpiperazin-1-yl)phenyl)methanamine, Pd<sub>2</sub>(dba)<sub>3</sub>, BrettPhos, NaO<sup>t</sup>Bu, THF, 100 °C, 1 h, 22%; (d) *tert*-Butyl 5-amino-3,4-dihydroisoquinoline-2(1H)-carboxylate, Pd<sub>2</sub>(dba)<sub>3</sub>, BrettPhos, NaO<sup>t</sup>Bu, THF, microwave 100 °C, 1 h, 25%; (e) 4 M HCl, 1,4-dioxane, rt, 45 min, quant.; (f) 37 wt% formaldehyde, formic acid, 80 °C, 6 h, 59%.

Synthesis of **36** began from commercially available thienopyridinone **50** in a similar fashion to that described previously (Scheme 8).<sup>28</sup> Alkylation with 1-iodobutane followed by Negishi cross-coupling with zinc cyanide gave intermediate **51**. Bromination with NBS followed by a Pinner reaction produced intermediate **52**. Reaction with the required amine was followed by Suzuki cross-coupling to append the aryl ring and deliver target **36**.

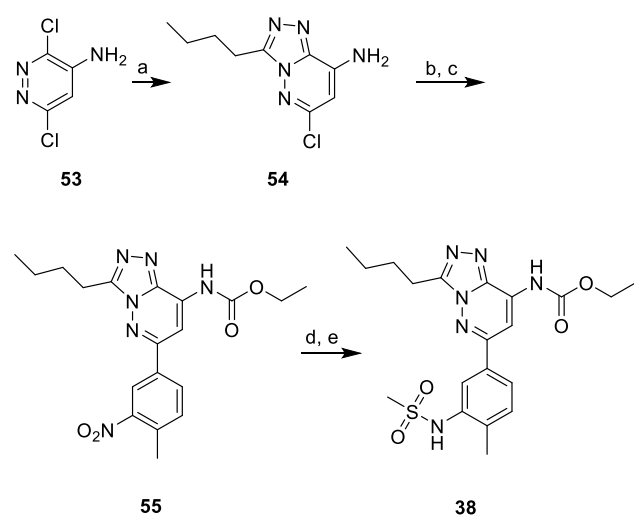
### Scheme 8



Reagents and conditions: (a) 1-Iodobutane, Cs<sub>2</sub>CO<sub>3</sub>, THF, 60 °C, 19 h, 71%; (b) Zn(CN)<sub>2</sub>, Pd(PPh<sub>3</sub>)<sub>4</sub>, DMF, 115 °C, 4.5 h, 61%; (c) NBS, THF, rt, 65 h, 86%; (d) 4-aminotetrahydro-2H-thiopyran 1,1-dioxide, 25 wt% NaOMe, MeOH, 75 °C, 26 h, 27%; (e) 4-aminotetrahydro-2H-thiopyran 1,1-dioxide, triethylamine, DMF, 120 °C, 17 h, 21%; (f) (3-(trifluoromethyl)phenyl)boronic acid, PEPPSI-<sup>i</sup>Pr, K<sub>2</sub>CO<sub>3</sub>, IPA/H<sub>2</sub>O, 120 °C, 30 mins, 52%.

Synthesis of compound **38** began from commercially available dichloro pyridazine **53** in a similar fashion to that reported elsewhere (Scheme 9).<sup>52</sup> S<sub>N</sub>Ar with hydrazine hydrate and subsequent cyclisation with pentanoic acid gave butyl intermediate **54**. Reaction with ethyl chloroformate was followed by a Suzuki-cross coupling to give intermediate **55**. Then reduction of the nitro group with powdered iron in acetic acid was followed by amine mesylation to deliver target compound **38**.

### Scheme 9



Reagents and conditions: (a) i) Hydrazine hydrate, 135 °C, 30 min; ii) pentanoic acid, 100 °C, 3 h, 43% over two steps; (b) ethylchloroformate, NMM, DCM, rt, 5 min, 67%; (c) (4-methyl-3-nitrophenyl)boronic acid, PdCl<sub>2</sub>(dppf), NaCO<sub>3</sub>, PhMe/EtOH, 100 °C, 5 h, 38%; (d) Fe, AcOH, EtOH/H<sub>2</sub>O, 80 °C, 2 h, 50%; (e) MsCl, pyridine, DCM, rt, 3 h, 74%.

### CONCLUSION

In conclusion, we report the development and utility of the atypical n-butyl KAc methyl mimetic as a straightforward approach to identifying selective BRD7/9 small molecule inhibitors. The n-butyl group was identified during structure guided optimisation efforts that began from an unselective pyridazinone template and enabled delivery of **31** as a soluble, permeable and selective BRD7/9 inhibitor. The atypical KAc methyl mimetic was then applied across three diverse chemotypes to enhance the bromodomain selectivity of an existing BRD9

inhibitor and to transform pan-bromodomain inhibitors into BRD7/9 selective compounds. Additionally, affinity enrichment chemoproteomic experiments enabled with linkable pyridazinone analogue **19** were used to interrogate the endogenous BRD7 and BRD9 protein complexes in Hut-78 cells. These experiments demonstrated specific enrichment of 19 proteins, all of which are reported to be members of the chromatin remodelling PBAF and BAF protein complexes.

## EXPERIMENTAL SECTION

**Physicochemical Properties.** Artificial membrane permeability, chromatographic  $\text{Log}D$  at pH 7.4, CLND and CAD aqueous solubility were measured using published protocols.<sup>54</sup>

**Chemistry methods.** All solvents were purchased from Sigma Aldrich (anhydrous solvents) and commercially available reagents were used as received. All reactions were followed by TLC analysis (TLC plates GF254, Merck) or LCMS (liquid chromatography mass spectrometry) using a Waters ZQ instrument. NMR spectra were recorded at ambient temperature unless otherwise stated using standard pulse methods on any of the following spectrometers and signal frequencies: Bruker AV-400 ( $^1\text{H} = 400 \text{ MHz}$ ,  $^{13}\text{C} = 100.6 \text{ MHz}$ ), Bruker AV-500 ( $^1\text{H} = 500 \text{ MHz}$ ,  $^{13}\text{C} = 125.8 \text{ MHz}$ ), Bruker AVII+ 600 ( $^1\text{H} = 600 \text{ MHz}$ ,  $^{13}\text{C} = 150.9 \text{ MHz}$ ). Chemical shifts are reported in ppm and are referenced to tetramethylsilane (TMS) or the following solvent peaks:  $\text{CDCl}_3$  ( $^1\text{H} = 7.27 \text{ ppm}$ ,  $^{13}\text{C} = 77.00 \text{ ppm}$ ),  $\text{DMSO-}d_6$  ( $^1\text{H} = 2.50 \text{ ppm}$ ,  $^{13}\text{C} = 39.51 \text{ ppm}$ ) and  $\text{CD}_3\text{OD}$  ( $^1\text{H} = 3.31 \text{ ppm}$ ,  $^{13}\text{C} = 49.15 \text{ ppm}$ ). Coupling constants are quoted to the nearest 0.1 Hz and multiplicities are given by the following abbreviations and combinations thereof: s (singlet), d (doublet), t (triplet), q (quartet), m (multiplet), br (broad). Column chromatography was performed on pre-packed silica gel columns using biotage SP4, Isolera One or Teledyne ISCO apparatus. High resolution mass

spectra (HRMS) were recorded on a Micromass Q-ToF Ultima hybrid quadrupole time-of-flight mass spectrometer, with analytes separated on an Agilent 1100 Liquid Chromatograph equipped with a Phenomenex Luna C18(2) reversed phase column (100 mm x 2.1 mm, 3  $\mu$ m packing diameter). LC conditions were 0.5 mL/min flow rate, 35 °C, injection volume 2 - 5  $\mu$ L. Gradient elution with (A) H<sub>2</sub>O containing 0.1% (v/v) formic acid and (B) acetonitrile containing 0.1% (v/v) formic acid. Gradient conditions were initially 5% B, increasing linearly to 100% B over 6 min, remaining at 100% B for 2.5 min then decreasing linearly to 5% B over 1 min followed by an equilibration period of 2.5 min prior to the next injection. LCMS analysis was carried out on a H<sub>2</sub>O Acquity UPLC instrument equipped with a BEH column (50 mm x 2.1 mm, 1.7  $\mu$ m packing diameter) and H<sub>2</sub>O micromass ZQ MS using alternate-scan positive and negative electrospray. Analytes were detected as a summed UV wavelength of 210 – 350 nm. Three liquid phase methods were used:

Formic acid – 40 °C, 1 mL/min flow rate. Gradient elution with the mobile phases as (A) H<sub>2</sub>O containing 0.1% volume/volume (v/v) formic acid and (B) acetonitrile containing 0.1% (v/v) formic acid. Gradient conditions were initially 1% B, increasing linearly to 97% B over 1.5 min, remaining at 97% B for 0.4 min then increasing to 100% B over 0.1 min.

High pH – 40 °C, 1 mL/min flow rate. Gradient elution with the mobile phases as (A) 10 mM aqueous ammonium bicarbonate solution, adjusted to pH 10 with 0.88 M aqueous ammonia and (B) acetonitrile. Gradient conditions were initially 1% B, increasing linearly to 97% B over 1.5 min, remaining at 97% B for 0.4 min then increasing to 100% B over 0.1 min.

TFA – 40 °C, 1 mL/min flow rate. Gradient elution with the mobile phases as (A) H<sub>2</sub>O containing 0.1% volume/volume (v/v) TFA and (B) acetonitrile containing 0.1% (v/v) TFA. Gradient conditions were initially 1% B, increasing linearly to 97% B over 1.5 min, remaining at 97% B for 0.4 min then increasing to 100% B over 0.1 min.

Mass-directed automatic purification (MDAP) was carried out using a H<sub>2</sub>O<sub>s</sub> ZQ MS using alternate-scan positive and negative electrospray and a summed UV wavelength of 210 – 350 nm. Two liquid phase methods were used:

Formic acid – Sunfire C18 column (100 mm x 19 mm, 5 µm packing diameter, 20 mL/min flow rate) or Sunfire C18 column (150 mm x 30 mm, 5 µm packing diameter, 40 mL/min flow rate). Gradient elution at ambient temperature with the mobile phases as (A) H<sub>2</sub>O containing 0.1% volume/volume (v/v) formic acid and (B) acetonitrile containing 0.1% (v/v) formic acid.

High pH – Xbridge C18 column (100 mm x 19 mm, 5 µm packing diameter, 20 mL/min flow rate) or Xbridge C18 column (150 mm x 30 mm, 5 µm packing diameter, 40 mL/min flow rate). Gradient elution at ambient temperature with the mobile phases as (A) 10 mM aqueous ammonium bicarbonate solution, adjusted to pH 10 with 0.88 M aqueous ammonia and (B) acetonitrile.

Melting point analysis was carried out using Buchi M-565 melting point apparatus. Melting points are uncorrected. IR spectra were obtained on a Perkin Elmer Spectrum 1 FTIR apparatus, with major peaks reported. The purity of all compounds tested was determined by LCMS and <sup>1</sup>H NMR to be >95%.

The synthesis of compounds **8** and **9** has been described previously.<sup>36</sup>

**4-Chloro-2-methyl-5-((3-methylbenzyl)amino)pyridazin-3(2H)-one (12). *m*-**

Tolylmethanamine (0.11 mL, 0.84 mmol) and 4,5-dichloro-2-methylpyridazin-3(2H)-one (100 mg, 0.56 mmol) were dissolved in DMSO (1.5 mL) at rt. The reaction mixture was then heated to 120 °C in a microwave reactor for 1 h. The reaction mixture was allowed to cool to rt before being diluted with DMSO (0.5 mL) and purified by MDAP (formic acid). The desired fractions were combined and concentrated *in vacuo* yielding 4-chloro-2-methyl-5-((3-

methylbenzyl)amino)pyridazin-3(2H)-one (34 mg, 0.13 mmol, 23%) as a white solid. <sup>1</sup>H NMR (400 MHz, CDCl<sub>3</sub>) δ ppm 7.53 (s, 1 H), 7.33-7.29 (m, 1 H), 7.16 (d, *J*=7.6 Hz, 1 H), 7.14-7.09 (m, 2 H), 4.52 (d, *J*=5.8 Hz, 2 H), 3.77 (s, 3 H), 2.39 (s, 3 H) (N.B. Exchangeable amine proton not visible); LC/MS (Formic acid): *R*<sub>t</sub> = 0.88 min (100%) [M+H]<sup>+</sup> = 264.

**4-Chloro-2-methyl-5-((4-methylbenzyl)amino)pyridazin-3(2H)-one (13).** *p*-Tolylmethanamine (0.18 mL, 1.40 mmol) and 4,5-dichloro-2-methylpyridazin-3(2H)-one (100 mg, 0.56 mmol) were dissolved in DMSO (1.5 mL) at rt. The reaction mixture was then heated to 120 °C in a microwave reactor for 1 h. The reaction mixture was allowed to cool to rt before being diluted with DMSO (0.5 mL) and purified by MDAP (formic acid). The desired fractions were combined and concentrated *in vacuo* yielding 4-chloro-2-methyl-5-((4-methylbenzyl)amino)pyridazin-3(2H)-one (110 mg, 0.42 mmol, 75%) as a white solid. <sup>1</sup>H NMR (400 MHz, DMSO-*d*<sub>6</sub>) δ ppm 7.67 (s, 1 H), 7.27 (t, *J*=6.6 Hz, 1 H), 7.21 (d, *J*=8.1 Hz, 2 H), 7.15 (d, *J*=8.1 Hz, 2 H), 4.52 (d, *J*=6.6 Hz, 2 H), 3.54 (s, 3 H), 2.27 (s, 3 H); LC/MS (Formic acid): *R*<sub>t</sub> = 0.89 min (100%) [M+H]<sup>+</sup> = 264.

**5-Chloro-4-methylpyridazin-3(2H)-one (40).** 3.4 M Methylmagnesium bromide in THF solution (13.40 mL, 45.50 mmol) was added dropwise to a stirred suspension of 4,5-dichloropyridazin-3(2H)-one (2.5 g, 15.15 mmol) in THF (50 mL) at 0 °C under nitrogen. The resultant solution was stirred at 0 °C for 10 min before being allowed to warm to rt and stirred for 5.5 hours. Saturated aq. NH<sub>4</sub>Cl solution (25 mL) was added dropwise. EtOAc (25 mL) and 2 M aq. HCl (25 mL) were added, the mixture shaken, and the organic layer removed. The aqueous layer was extracted further with EtOAc (25 mL). The organic layers were combined, washed with brine (25 mL), passed through a hydrophobic frit and concentrated *in vacuo*. The resulting solid was triturated and then sonicated in diethyl ether (75 mL). The solid was removed under reduced pressure and washed with Et<sub>2</sub>O. The filtrate was concentrated *in vacuo* yielding 5-chloro-4-methylpyridazin-3(2H)-one (1.785 g, 12.35 mmol, 81%) as a yellow solid.

m.p. 124–126 °C;  $\nu_{\max}$  (solid)/ $\text{cm}^{-1}$ : 2873, 1634 (C=O), 1376, 1177, 1024, 884, 564;  $^1\text{H}$  NMR (400 MHz,  $\text{CD}_3\text{OD}$ )  $\delta$  ppm 7.88 (s, 1 H), 2.24 (s, 3 H);  $^{13}\text{C}$  NMR (101 MHz,  $\text{CD}_3\text{OD}$ )  $\delta$  ppm 161.9, 137.6, 137.5, 136.9, 11.4; HRMS ( $\text{M}+\text{H}$ ) $^+$  calculated for  $\text{C}_5\text{H}_6\text{ClN}_2\text{O}$  145.0169; found 145.0168; LC/MS (formic acid):  $R_t = 0.53$  min (98%) [ $\text{M}+\text{H}$ ] $^+ = 145$ .

**5-Chloro-2,4-dimethylpyridazin-3(2H)-one (41).** Methyl iodide (1.14 mL, 18.16 mmol) was added to a stirred mixture of tetrabutylammonium bromide (6.630 g, 20.58 mmol), 5-chloro-4-methylpyridazin-3(2H)-one (1.750 g, 12.11 mmol) and potassium carbonate (3.35 g, 24.21 mmol) in MeCN (20 mL) at rt under nitrogen. The reaction mixture was stirred for 3 hours at rt before being heated to 60 °C and stirred for 1 hour. The resultant mixture was allowed to cool to rt before being filtered under reduced pressure and the filtrate concentrated *in vacuo*. The resultant solid was dissolved in EtOAc (60 mL) and washed with 2 M aq. HCl (40 mL). Methanol was added dropwise to dissolve a white precipitate. The organic layer was then washed with brine (40 mL), passed through a hydrophobic frit, and concentrated *in vacuo*. The resultant solid was dissolved in minimal DCM and purified by silica chromatography (0-50% EtOAc in cyclohexane). The desired fractions were concentrated *in vacuo* yielding 5-chloro-2,4-dimethylpyridazin-3(2H)-one (1.062 g, 6.70 mmol, 55%) as a white solid. m.p. 73–74 °C;  $\nu_{\max}$  (solid)/ $\text{cm}^{-1}$ : 3032, 1634 (C=O), 1591, 1016, 887, 501;  $^1\text{H}$  NMR (400 MHz,  $\text{CD}_3\text{OD}$ )  $\delta$  ppm 7.89 (s, 1 H), 3.76 (s, 3 H), 2.26 (s, 3 H);  $^{13}\text{C}$  NMR (101 MHz,  $\text{CD}_3\text{OD}$ )  $\delta$  ppm 160.7, 136.6, 136.0, 135.9, 39.4, 12.0; HRMS ( $\text{M}+\text{H}$ ) $^+$  calculated for  $\text{C}_6\text{H}_8\text{ClN}_2\text{O}$  159.0325; found 159.0325; LC/MS (TFA):  $R_t = 0.63$  min (100%) [ $\text{M}+\text{H}$ ] $^+ = 159$ .

**5-(Benzylamino)-2,4-dimethylpyridazin-3(2H)-one (10).** Phenylmethanamine (0.10 mL, 0.95 mmol), 5-chloro-2,4-dimethylpyridazin-3(2H)-one (151 mg, 0.95 mmol), BrettPhos-Pd-G1 (76 mg, 0.10 mmol), BrettPhos (51 mg, 0.10 mmol) and sodium *tert*-butoxide (137 mg, 1.43 mmol) were dissolved in 1,4-dioxane (5 mL) at rt under nitrogen. The reaction mixture was then heated to 120 °C in a microwave reactor for 30 mins. The reaction mixture was passed

through Celite and the Celite washed with EtOAc (3 × 10 mL). The resultant solution was then diluted with water (30 mL) and extracted with EtOAc (3 × 20 mL). The combined organic phases were passed through a hydrophobic frit and concentrated *in vacuo*. The resultant oil was then dissolved in 1:1 MeOH:DMSO, filtered and purified via MDAP (high pH). The desired fractions were combined and concentrated *in vacuo* yielding 5-(benzylamino)-2,4-dimethylpyridazin-3(2H)-one (108 mg, 0.47 mmol, 50%) as a white solid. <sup>1</sup>H NMR (400 MHz, CD<sub>3</sub>OD) δ ppm 7.57 (s, 1 H), 7.39-7.31 (m, 4 H), 7.30-7.23 (m, 1 H), 4.57 (s, 2 H), 3.66 (s, 3 H), 2.04 (s, 3 H); LC/MS (High pH): R<sub>t</sub> = 0.82 min (100%) [M+H]<sup>+</sup> = 230.

**2,4-Dimethyl-5-((2-methylbenzyl)amino)pyridazin-3(2H)-one (11).** *o*-Tolylmethanamine (24 mg, 0.20 mmol), 5-chloro-2,4-dimethylpyridazin-3(2H)-one (24 mg, 0.15 mmol), BrettPhos-Pd-G1 (12 mg, 0.02 mmol), BrettPhos (8 mg, 0.02 mmol) and sodium *tert*-butoxide (22 mg, 0.23 mmol) were dissolved in 1,4-dioxane (0.6 mL) and heated to 120 °C in a microwave reactor for 30 mins. The reaction mixture was loaded on to a preconditioned (MeCN × 2 mL) C18 SPE cartridge and eluted with 1:1 MeOH:DMSO. The resultant solution was concentrated under a positive pressure of nitrogen, redissolved in DMSO, and purified via MDAP (high pH). The desired fractions were combined and concentrated under a positive pressure of nitrogen yielding 2,4-dimethyl-5-((2-methylbenzyl)amino)pyridazin-3(2H)-one (9 mg, 0.04 mmol, 23%). <sup>1</sup>H NMR (600 MHz, DMSO-*d*<sub>6</sub>) δ ppm 7.42 (s, 1 H), 7.20-7.08 (m, 4 H), 6.51 (t, *J*=6.0 Hz, 1 H), 4.46 (d, *J*=6.0 Hz, 2 H), 3.50 (s, 3 H), 2.31 (s, 3 H), 1.94 (s, 3 H); LC/MS (Formic acid): R<sub>t</sub> = 0.85 min (100%) [M+H]<sup>+</sup> = 244.

**5-(((1,1'-Biphenyl)-2-ylmethyl)amino)-2,4-dimethylpyridazin-3(2H)-one (14).** [1,1'-Biphenyl]-2-ylmethanamine (0.08 mL, 0.47 mmol), 5-chloro-2,4-dimethylpyridazin-3(2H)-one (50 mg, 0.32 mmol), BrettPhos (17 mg, 0.03 mmol), Brettphos-Pd-G1 (25 mg, 0.03 mmol) and sodium *tert*-butoxide (35 mg, 0.36 mmol) were dissolved in 1,4-dioxane (1 mL). The reaction mixture was heated to 100 °C in a microwave reactor for 30 min. The reaction mixture



was allowed to cool to rt, before being diluted with sat. sodium bicarbonate solution (15 mL) and the aqueous phase extracted with DCM (3 × 15mL). The organic layers were combined, passed through a hydrophobic frit and concentrated *in vacuo*. The resultant residue was dissolved in DMSO (2 mL) and purified by MDAP (formic acid). The desired fractions were combined and concentrated *in vacuo* yielding 5-(([1,1'-biphenyl]-2-ylmethyl)amino)-2,4-dimethylpyridazin-3(2H)-one (58 mg, 0.19 mmol, 61%) as a beige solid. <sup>1</sup>H NMR (400 MHz, DMSO-*d*<sub>6</sub>) δ ppm 7.51-7.46 (m, 2 H), 7.44-7.39 (m, 3 H), 7.38-7.32 (m, 3 H), 7.27-7.23 (m, 1 H), 7.15 (s, 1 H), 6.46 (t, *J*=6.1 Hz, 1 H), 4.40 (d, *J*=6.1 Hz, 2 H), 3.47 (s, 3 H), 1.84 (s, 3 H); LC/MS (Formic acid): R<sub>t</sub> = 1.01 min (100%) [M+H]<sup>+</sup> = 306.

**2,4-Dimethyl-5-((2-morpholinobenzyl)amino)pyridazin-3(2H)-one (15).** (2-Morpholinophenyl)methanamine (145 mg, 0.76 mmol), 5-chloro-2,4-dimethylpyridazin-3(2H)-one (50 mg, 0.32 mmol), XPhos-Pd-G1 (47 mg, 0.06 mmol), XPhos (30 mg, 0.06 mmol) and potassium *tert*-butoxide (35 mg, 0.36 mmol) were dissolved in 1,4-dioxane (4 mL). The reaction mixture was heated to 110 °C in a microwave reactor for 1 h. The reaction mixture was allowed to cool to rt before being diluted with EtOAc and washed with water and brine. The organic layer was passed through a hydrophobic frit and concentrated *in vacuo*. The resultant residue was dissolved in 1:1 MeOH:DMSO and purified via MDAP (high pH). The desired fractions were combined and concentrated *in vacuo* yielding 2,4-dimethyl-5-((2-morpholinobenzyl)amino)pyridazin-3(2H)-one (33 mg, 0.10 mmol, 16%) as a white solid. <sup>1</sup>H NMR (400 MHz, CDCl<sub>3</sub>) δ ppm 7.51 (s, 1 H), 7.36-7.29 (m, 2 H), 7.20 (d, *J*=7.8 Hz, 1 H), 7.17-7.10 (m, 1 H), 4.84-4.74 (m, 1 H), 4.56 (d, *J*=5.6 Hz, 2 H), 3.91-3.85 (m, 4 H), 3.73-3.66 (m, 3 H), 2.98-2.92 (m, 4 H), 2.02 (s, 3 H); LC/MS (High pH): R<sub>t</sub> = 0.82 min (100%) [M+H]<sup>+</sup> = 315.

**5-((2-(1,4-oxazepan-4-yl)benzyl)amino)-2,4-dimethylpyridazin-3(2H)-one, hydrochloride (16).** (2-(1,4-Oxazepan-4-yl)phenyl)methanamine (400 mg, 1.94 mmol), 5-chloro-2,4-

dimethylpyridazin-3(2H)-one (369 mg, 2.33 mmol), RuPhos (277 mg, 0.58 mmol), Pd<sub>2</sub>(dba)<sub>3</sub> (178 mg, 0.19 mmol) and sodium *tert*-butoxide (559 mg, 5.82 mmol) were dissolved in 1,4-dioxane (2 mL) at 20 °C under nitrogen. The system was then sparged with nitrogen for 5 min. The reaction mixture was then heated to 110 °C in a microwave reactor for 1 h. The reaction mixture was allowed to cool to rt, filtered, and the filtrate concentrated *in vacuo*. The resultant residue was purified via prep-HPLC (high pH). The desired fractions were combined along with a drop of 2 M HCl and concentrated *in vacuo* yielding 5-((2-(1,4-oxazepan-4-yl)benzyl)amino)-2,4-dimethylpyridazin-3(2H)-one, hydrochloride (90 mg, 0.25 mmol, 13%) as a white solid. <sup>1</sup>H NMR (400 MHz, DMSO-*d*<sub>6</sub>) δ ppm 7.43 (s, 1 H), 7.29-7.14 (m, 3 H), 7.08-6.99 (m, 1 H), 6.72 (t, *J*=6.4 Hz, 1 H), 4.49 (d, *J*=6.4 Hz, 2 H), 3.85 (t, *J*=6.0 Hz, 2 H), 3.82-3.74 (m, 2 H), 3.48 (s, 3 H), 3.17-3.07 (m, 4 H), 1.99 (quin, *J*=5.8 Hz, 2 H), 1.91 (s, 3 H); LC/MS (Formic acid): R<sub>t</sub> = 0.82 min (100%) [M+H]<sup>+</sup> = 328.

**2,4-Dimethyl-5-((2-(piperazin-1-yl)benzyl)amino)pyridazin-3(2H)-one (17).** *tert*-Butyl 4-(2-(aminomethyl)phenyl)piperazine-1-carboxylate (58 mg, 0.2 mmol), 5-chloro-2,4-dimethylpyridazin-3(2H)-one (24 mg, 0.15 mmol), BrettPhos-Pd-G1 (12 mg, 0.02 mmol), BrettPhos (8 mg, 0.02 mmol) and sodium *tert*-butoxide (22 mg, 0.23 mmol) were dissolved in 1,4-dioxane and heated to 120 °C in a microwave reactor for 30 mins. The reaction mixture was loaded on to a preconditioned (MeCN × 2 mL) C18 SPE cartridge and eluted with 1:1 MeOH:DMSO. The resultant solution was concentrated under a positive pressure of nitrogen, redissolved in DMSO, and purified via MDAP (high pH). The desired fractions were combined and concentrated under a positive pressure of nitrogen. The resultant residue was dissolved in DCM (0.5 mL) at rt and 4 M HCl in 1,4-dioxane added (0.5 mL). The reaction mixture was stood at rt for 18 h before being concentrated *in vacuo*. The residue was dissolved in DMSO (0.6 mL) and purified via MDAP (high pH). The desired fractions were combined and concentrated *in vacuo* yielding 2,4-dimethyl-5-((2-(piperazin-1-yl)benzyl)amino)pyridazin-

3(2H)-one (5 mg, 0.02 mmol, 10%). <sup>1</sup>H NMR (400 MHz, CD<sub>3</sub>OD) δ ppm 7.59 (s, 1 H), 7.34 (dd, *J*=7.6, 1.3 Hz, 1 H), 7.30-7.24 (m, 1 H), 7.22-7.17 (m, 1 H), 7.09 (td, *J*=7.6, 1.3 Hz, 1 H), 4.58 (s, 2 H), 3.64 (s, 3 H), 3.07-3.01 (m, 4 H), 2.96-2.89 (m, 4 H), 2.02 (s, 3 H); LC/MS (Formic acid): R<sub>t</sub> = 0.49 min (100%) [M+H]<sup>+</sup> = 314.

**2,4-Dimethyl-5-((2-(4-methylpiperazin-1-yl)benzyl)amino)pyridazin-3(2H)-one (18).** (2-(4-Methylpiperazin-1-yl)phenyl)methanamine (200 mg, 0.97 mmol), 5-chloro-2,4-dimethylpyridazin-3(2H)-one (103 mg, 0.65 mmol), XPhos (31 mg, 0.07 mmol), XPhos-Pd-G1 (48 mg, 0.07 mmol) and sodium *tert*-butoxide (75 mg, 0.78 mmol) were dissolved in 1,4-dioxane (4 mL) at rt. The reaction mixture was heated to 100 °C in a microwave reactor for 30 mins. The reaction mixture was allowed to cool to rt before being diluted with water (10 mL) and extracted with EtOAc (3 × 10 mL). The combined organic phases were passed through a hydrophobic frit and concentrated *in vacuo*. The resultant oil was dissolved in 1:1 MeOH:DMSO purified via MDAP (high pH). The desired fractions were combined and concentrated *in vacuo*. The colourless oil was dissolved in MeOH (10 mL) and loaded onto a preconditioned (MeOH × 10 mL) amino propyl (2 g) column. The product was eluted with MeOH (10 mL) and the desired fractions combined and concentrated *in vacuo* yielding 2,4-dimethyl-5-((2-(4-methylpiperazin-1-yl)benzyl)amino)pyridazin-3(2H)-one (118 mg, 0.36 mmol, 56%) as a white solid. <sup>1</sup>H NMR (400 MHz, DMSO-*d*<sub>6</sub>) δ ppm 7.43 (s, 1 H), 7.29 (dd, *J*=7.6, 1.5 Hz, 1 H), 7.25-7.18 (m, 1 H), 7.15-7.10 (m, 1 H), 7.05 (td, *J*=7.4, 1.1 Hz, 1 H), 6.71 (t, *J*=6.4 Hz, 1 H), 4.44 (d, *J*=6.4 Hz, 2 H), 3.47 (s, 3 H), 2.92-2.83 (m, 4 H), 2.26 (s, 3 H), 1.89 (s, 3 H) (N.B. Signal obscured by DMSO solvent peak); LC/MS (High pH): R<sub>t</sub> = 0.77 min (98%) [M+H]<sup>+</sup> = 328.

***tert*-Butyl (3-(4-(2-(((1,5-dimethyl-6-oxo-1,6-dihydropyridazin-4-yl)amino)methyl)phenyl)piperazin-1-yl)propyl)carbamate.** *tert*-Butyl (3-

bromopropyl)carbamate (449 mg, 1.886 mmol) was added to a solution of 2,4-dimethyl-5-((2-

(piperazin-1-yl)benzyl)amino)pyridazin-3(2H)-one hydrochloride (600 mg, 1.715 mmol) and cesium carbonate (2235 mg, 6.860 mmol) in DMF (13 mL). The reaction mixture was stirred at rt for 18 hours before being heated to 50 °C and stirred for an additional 18 hours. The reaction mixture was concentrated *in vacuo* and the resultant residue dissolved in EtOAc (50 mL) and washed with water (50 mL). The layers were separated, and the aqueous layer extracted further with EtOAc (3 × 50 mL). The organic layers were combined, washed with brine (50 mL), passed through a hydrophobic frit and concentrated *in vacuo*. The resulting residue was purified by silica chromatography (0-10% 2 M NH<sub>3</sub> in MeOH in DCM). The desired fractions were combined and concentrated *in vacuo* yielding *tert*-butyl (3-(4-(2-(((1,5-dimethyl-6-oxo-1,6-dihydropyridazin-4-yl)amino)methyl)phenyl)piperazin-1-yl)propyl)carbamate (236 mg, 501 μmol, 20%) as a yellow oil. <sup>1</sup>H NMR (400 MHz, CDCl<sub>3</sub>) δ ppm 7.54 (s, 1 H), 7.36-7.29 (m, 2 H), 7.22-7.08 (m, 2 H), 4.90-4.84 (m, 1 H), 4.54 (m, 2 H), 3.71 (s, 3 H), 3.28-3.19 (m, 2 H), 2.99 (t, *J*=4.6 Hz, 4 H), 2.65 (br. s, 4 H), 2.51 (t, *J*=6.7 Hz, 2 H), 2.01 (s, 3 H), 1.72 (quin., *J*=6.7 Hz, 2 H), 1.47 (s, 9 H) (N.B. exchangeable amine proton not visible); LC/MS (formic acid): R<sub>t</sub> = 0.70 min (72%) [M+H]<sup>+</sup> = 471.

**5-((2-(4-(3-Aminopropyl)piperazin-1-yl)benzyl)amino)-2,4-dimethylpyridazin-3(2H)-one**

**(19).** *tert*-Butyl (3-(4-(2-(((1,5-dimethyl-6-oxo-1,6-dihydropyridazin-4-yl)amino)methyl)phenyl)piperazin-1-yl)propyl)carbamate (236 mg, 0.501 mmol) was dissolved in 4 M HCl in 1,4-dioxane (5 mL, 20.00 mmol) and left to stir at rt for 18 hours. The reaction mixture was concentrated *in vacuo* and the resultant residue was suspended in diethyl ether (30 mL), filtered under reduced pressure, rinsed with diethyl ether (20 mL) and collected. The residue was purified by MDAP (high pH). The desired fractions were combined and concentrated *in vacuo* yielding 5-((2-(4-(3-aminopropyl)piperazin-1-yl)benzyl)amino)-2,4-dimethylpyridazin-3(2H)-one (33 mg, 0.089 mmol, 18%) as a pale-yellow solid. <sup>1</sup>H NMR (400 MHz, CD<sub>3</sub>OD) δ ppm 7.58 (s, 1 H), 7.35 (d, *J*=7.6 Hz, 1 H), 7.30-7.24 (m, 1 H), 7.21 (d, *J* =

7.8 Hz, 1 H), 7.12-7.06 (m, 1 H), 4.57 (s, 2 H), 3.63 (s, 3 H), 3.02 (t,  $J=4.6$  Hz, 4 H), 2.93 (t,  $J=7.0$  Hz, 2 H), 2.74 (br. s, 4 H), 2.59 (t,  $J=7.0$  Hz, 2 H), 2.01 (s, 3 H), 1.84 (quin.,  $J=7.0$  Hz, 2 H) (N.B. Exchangeable amine protons not visible); LC/MS (high pH):  $R_t = 0.65$  min (100%)  $[M+H]^+ = 371$ .

**4-Chloro-2-methyl-5-((2-(4-methylpiperazin-1-yl)benzyl)amino)pyridazin-3(2H)-one (42).** DIPEA (0.73 mL, 4.19 mmol) was added to a stirred solution of 4,5-dichloro-2-methylpyridazin-3(2H)-one (500 mg, 2.79 mmol) and (2-(4-methylpiperazin-1-yl)phenyl)methanamine (0.66 mL, 3.41 mmol) in DMSO (10 mL) at rt. The resultant solution was heated to 120 °C and stirred for 1 hour in a microwave reactor. The resultant solution was diluted with saturated aq.  $NH_4Cl$  solution (15 mL) and EtOAc (15 mL) and the layers separated. The aqueous layer was then extracted further with EtOAc (5 mL  $\times$  2). The organic fractions were combined and washed with brine before being passed through a hydrophobic frit and concentrated *in vacuo*. The resultant residue was dissolved in minimal DCM and purification by silica chromatography attempted (0-20% 2 M  $NH_3$  in MeOH in DCM). The desired fractions were combined and concentrated *in vacuo*. The resultant solid was dissolved in 1:1 DMSO and MeOH and purified by MDAP (high pH). The desired fractions were combined yielding 4-chloro-2-methyl-5-((2-(4-methylpiperazin-1-yl)benzyl)amino)pyridazin-3(2H)-one (607 mg, 1.75 mmol, 63%) as a cream solid.  $\nu_{max}$  (solid)/ $cm^{-1}$ : 3322 (N-H), 1609 (C=O), 1201, 1118, 720;  $^1H$  NMR (400 MHz,  $CD_3OD$ )  $\delta$  ppm 7.63 (s, 1 H), 7.41-7.31 (m, 2 H), 7.30-7.26 (m, 1 H), 7.19 (td,  $J=7.4, 1.3$  Hz, 1 H), 4.71-4.63 (m, 2 H), 3.68 (s, 3 H), 3.39 (app. br. s, 4 H), 3.20 (t,  $J=4.9$  Hz, 4 H), 2.91 (s, 3 H) (N.B. exchangeable amine proton not visible);  $^{13}C$  NMR (101 MHz,  $CD_3OD$ )  $\delta$  ppm 158.5, 149.3, 145.2, 133.2, 128.5, 128.2, 127.0, 125.4, 120.2, 105.9, 54.2, 50.3, 42.8, 41.3, 39.1; LC/MS (formic acid):  $R_t = 0.44$  min (99%)  $[M+H]^+ = 348$ .

**4-Allyl-2-methyl-5-((2-(4-methylpiperazin-1-yl)benzyl)amino)pyridazin-3(2H)-one (21).**

The solvent system was sparged with nitrogen for 30 min prior to use. 2-Allyl-4,4,5,5-

tetramethyl-1,3,2-dioxaborolane (0.05 mL, 0.29 mmol) was added to a stirred solution of 4-chloro-2-methyl-5-((2-(4-methylpiperazin-1-yl)benzyl)amino)pyridazin-3(2H)-one (50 mg, 0.14 mmol), potassium carbonate (50 mg, 0.36 mmol) and RuPhos-Pd-G2 (17 mg, 0.02 mmol) in 1,4-dioxane (2 mL) and water (1 mL) under nitrogen at rt. The resultant mixture was heated to 100 °C and stirred for 1 hour. The resultant solution was diluted with EtOAc and filtered through Celite before being concentrated *in vacuo*. The resultant residue was dissolved in EtOAc (10 mL) and washed with water (10 mL). The organic layer was passed through a hydrophobic frit and concentrated *in vacuo*. The resultant residue was dissolved in 1:1 MeOH:DMSO and purified by MDAP (High pH: extended). The desired fractions were combined and concentrated *in vacuo* yielding 4-allyl-2-methyl-5-((2-(4-methylpiperazin-1-yl)benzyl)amino)pyridazin-3(2H)-one (14 mg, 0.04 mmol, 28%) as a colourless oil. <sup>1</sup>H NMR (400 MHz, CD<sub>3</sub>OD) δ ppm 7.59 (s, 1 H), 7.34-7.30 (m, 1 H), 7.26 (td, *J*=7.6, 1.2 Hz, 1 H), 7.20 (dd, *J*=7.6, 1.2 Hz, 1 H), 7.08 (td, *J*=7.6, 1.2 Hz, 1 H), 5.87 (ddt, *J*=17.1, 10.3, 5.7 Hz, 1 H), 5.11-5.01 (m, 2 H), 4.56 (s, 2 H), 3.63 (s, 3 H), 3.00 (t, *J*=4.8 Hz, 4 H), 2.70 (app. br. s, 4 H), 2.40 (s, 3 H) (N.B. amine proton not visible and CH<sub>2</sub> allyl proton signal obscured by MeOH solvent peak); <sup>13</sup>C NMR (101 MHz, CD<sub>3</sub>OD) δ ppm 161.7, 150.5, 146.1, 133.3, 132.9, 128.3, 128.1, 128.0, 124.1, 119.5, 114.4, 109.1, 55.1, 52.1, 44.8, 40.9, 38.9, 26.6; HRMS (M+H)<sup>+</sup> calculated for C<sub>20</sub>H<sub>28</sub>N<sub>5</sub>O 354.2294; found 354.2299; LC/MS (high pH): R<sub>t</sub> = 0.90 min (100%) [M+H]<sup>+</sup> = 354.

**(*E*)-4-(But-1-en-1-yl)-2-methyl-5-((2-(4-methylpiperazin-1-yl)benzyl)amino)pyridazin-3(2H)-one (24).** The solvent system was sparged with nitrogen for 20 min prior to use. (*E*)-But-1-en-1-ylboronic acid (15 mg, 0.15 mmol), 4-chloro-2-methyl-5-((2-(4-methylpiperazin-1-yl)benzyl)amino)pyridazin-3(2H)-one (24 mg, 0.07 mmol), potassium carbonate (24 mg, 0.17 mmol), Pd(OAc)<sub>2</sub> (2 mg, 0.01 mmol) and butyldi-1-adamantylphosphine (4 mg, 0.01 mmol) were dissolved in 1,4-dioxane (2 mL) and water (1 mL) under nitrogen at rt. The

resultant mixture was heated to 100 °C and stirred for 1 hour in a microwave reactor. A further portion of (*E*)-but-1-en-1-ylboronic acid (15 mg, 0.15 mmol), potassium carbonate (24 mg, 0.17 mmol), Pd(OAc)<sub>2</sub> (2 mg, 0.01 mmol) and butyldi-1-adamantylphosphine (4 mg, 0.01 mmol) were added under nitrogen and the reaction stirred at 100 °C for 2 hours in a microwave reactor. A further portion of (*E*)-but-1-en-1-ylboronic acid (15 mg, 0.15 mmol), potassium carbonate (24 mg, 0.17 mmol), Pd(OAc)<sub>2</sub> (2 mg, 0.01 mmol) and butyldi-1-adamantylphosphine (4 mg, 0.01 mmol) were added under nitrogen and the reaction stirred at 100 °C for 2 hours. The solution was allowed to cool to rt before being diluted with EtOAc (10 mL), filtered through Celite, and concentrated *in vacuo*. The resultant residue was dissolved in EtOAc (5 mL) and washed sequentially with water (5 mL) and brine (5 mL) before being passed through a hydrophobic frit and concentrated *in vacuo*. The resultant residue was dissolved in 1:1 MeOH:DMSO and purified by MDAP (high pH). the desired fractions were combined yielding (*E*)-4-(but-1-en-1-yl)-2-methyl-5-((2-(4-methylpiperazin-1-yl)benzyl)amino)pyridazin-3(2H)-one (12 mg, 0.03 mmol, 47%) as a colourless oil. <sup>1</sup>H NMR (400 MHz, CD<sub>3</sub>OD) δ ppm 7.60 (s, 1 H), 7.34 (dd, *J*=7.6, 1.2 Hz, 1 H), 7.31-7.25 (m, 1 H), 7.24-7.19 (m, 1 H), 7.10 (td, *J*=7.6, 1.2 Hz, 1 H), 6.77 (dt, *J*=16.0, 6.6 Hz, 1 H), 6.30 (dt, *J*=16.0, 1.7 Hz, 1 H), 4.57 (s, 2 H), 3.63 (s, 3 H), 3.00 (t, *J*=4.8 Hz, 4 H), 2.70 (app. br. s, 4 H), 2.39 (s, 3 H), 2.36-2.27 (m, 2 H), 1.14 (t, *J*=7.5 Hz, 3 H) (N.B. Amine proton not visible); <sup>13</sup>C NMR (101 MHz, CD<sub>3</sub>OD) δ ppm 160.8, 150.6, 144.6, 139.3, 133.2, 128.4, 128.2, 128.1, 124.3, 119.7, 118.1, 108.5, 55.2, 52.1, 44.8, 41.6, 38.8, 27.0, 12.6; HRMS (M+H)<sup>+</sup> calculated for C<sub>21</sub>H<sub>30</sub>N<sub>5</sub>O 368.2450; found 368.2461; LC/MS (high pH): R<sub>t</sub> = 1.01 min (98%) [M+H]<sup>+</sup> = 368.

**(*E*)-4-(But-2-en-1-yl)-2-methyl-5-((2-(4-methylpiperazin-1-yl)benzyl)amino)pyridazin-3(2H)-one (22), (*Z*)-4-(But-2-en-1-yl)-2-methyl-5-((2-(4-methylpiperazin-1-yl)benzyl)amino)pyridazin-3(2H)-one (23), Single unknown enantiomer (*R*)-4-(But-3-en-2-yl)-2-methyl-5-((2-(4-methylpiperazin-1-yl)benzyl)amino)pyridazin-3(2H)-one (26)**

**and Single unknown enantiomer (S)-4-(But-3-en-2-yl)-2-methyl-5-((2-(4-methylpiperazin-1-yl)benzyl)amino)pyridazin-3(2H)-one (27).** The solvent system was sparged with nitrogen for 2 hours prior to use. (*E*)-2-(But-2-en-1-yl)-4,4,5,5-tetramethyl-1,3,2-dioxaborolane (0.34 mL, 1.67 mmol) was added to a stirred solution of 4-chloro-2-methyl-5-((2-(4-methylpiperazin-1-yl)benzyl)amino)pyridazin-3(2H)-one (290 mg, 0.834 mmol), potassium carbonate (288 mg, 2.08 mmol), Pd(OAc)<sub>2</sub> (37 mg, 0.17 mmol) and butyldi-1-adamantylphosphine (60 mg, 0.17 mmol) in 1,4-dioxane (1 mL) and water (0.5 mL) under nitrogen at rt. The resultant mixture was heated to 100 °C and stirred for 1.5 hours in a microwave reactor. The resultant solution was diluted with EtOAc (3 mL) and passed through Celite before being concentrated *in vacuo*. The resultant residue was dissolved in EtOAc (3 mL) and washed with H<sub>2</sub>O (3 mL) before being concentrated *in vacuo*, dissolved in 1:1 MeOH:DMSO and purified by MDAP (high pH). MDAP failed to separate the isomers. The desired fractions were combined and concentrated *in vacuo* yielding a mixture of 4-(but-3-en-2-yl)-2-methyl-5-((2-(4-methylpiperazin-1-yl)benzyl)amino)pyridazin-3(2H)-one, (*E*)-4-(but-2-en-1-yl)-2-methyl-5-((2-(4-methylpiperazin-1-yl)benzyl)amino)pyridazin-3(2H)-one and (*Z*)-4-(but-2-en-1-yl)-2-methyl-5-((2-(4-methylpiperazin-1-yl)benzyl)amino)pyridazin-3(2H)-one as a combined off-white gum. The gum was dissolved in EtOH (4.5 mL) and purified via chiral chromatography: Chiralpak AD-H column, 30 mm × 25 cm, 10%EtOH (+0.2% isopropylamine)/heptane (+0.2 %isopropylamine), 30 mL/min. The desired fractions were combined and concentrated *in vacuo* yielding the four products:

(*E*)-4-(but-2-en-1-yl)-2-methyl-5-((2-(4-methylpiperazin-1-yl)benzyl)amino)pyridazin-3(2H)-one (**22**) as a white solid (26 mg, 0.07 mmol, 8%) as a colourless oil. <sup>1</sup>H NMR (400 MHz, CD<sub>3</sub>OD) δ ppm 7.60 (s, 1 H), 7.33-7.24 (m, 2 H), 7.21 (dd, *J*=7.2, 1.2 Hz, 1 H), 7.09 (td, *J*=7.2, 1.2 Hz, 1 H), 5.49 (dqt, *J*=16.0, 6.0, 1.0 Hz, 1 H), 5.45 (dtq, *J*=16.0, 6.0, 1.0 Hz, 1 H), 4.56 (s, 2 H), 3.63 (s, 3 H), 3.26-3.20 (m, 2 H), 3.00 (t, *J*=4.8 Hz, 4 H), 2.71 (app. br. s, 4 H),



2.40 (s, 3 H), 1.70-1.63 (m, 3 H);  $^{13}\text{C}$  NMR (101 MHz,  $\text{CD}_3\text{OD}$ )  $\delta$  ppm 161.8, 150.6, 145.9, 133.3, 128.4, 128.1, 128.0, 125.6, 125.3, 124.1, 119.6, 110.1, 55.1, 52.1, 44.8, 40.9, 38.9, 25.4, 16.6; HRMS ( $\text{M}+\text{H}$ ) $^+$  calculated for  $\text{C}_{21}\text{H}_{30}\text{N}_5\text{O}$  368.2450; found 368.2447; LC/MS (high pH):  $R_t = 0.96$  min (100%) [ $\text{M}+\text{H}$ ] $^+ = 368$ .

(*Z*)-4-(but-2-en-1-yl)-2-methyl-5-((2-(4-methylpiperazin-1-yl)benzyl)amino)pyridazin-3(2H)-one (**23**) (15 mg, 0.04 mmol, 5%) as a colourless oil.  $^1\text{H}$  NMR (400 MHz,  $\text{CD}_3\text{OD}$ )  $\delta$  ppm 7.61 (s, 1 H), 7.37-7.24 (m, 2 H), 7.24-7.19 (m, 1 H), 7.13-7.07 (m, 1 H), 5.59 (dqt,  $J=10.5, 6.8, 2.0$  Hz, 1 H), 5.34 (dtq,  $J=10.5, 6.8, 1.8$  Hz, 1 H), 4.57 (s, 2 H), 3.64 (s, 3 H), 3.04-2.96 (m, 4 H), 2.70 (app. br. s, 4 H), 2.40 (s, 3 H), 1.77-1.73 (m, 3 H);  $^{13}\text{C}$  NMR (101 MHz,  $\text{CD}_3\text{OD}$ )  $\delta$  ppm 161.7, 150.6, 145.8, 133.2, 128.4, 128.2, 128.1, 125.8, 125.3, 124.7, 119.6, 111.1, 55.1, 52.1, 44.7, 41.2, 38.9, 20.7, 11.9; HRMS ( $\text{M}+\text{H}$ ) $^+$  calculated for  $\text{C}_{21}\text{H}_{30}\text{N}_5\text{O}$  368.2450; found 368.2444; LC/MS (high pH):  $R_t = 0.97$  min (100%) [ $\text{M}+\text{H}$ ] $^+ = 368$ .

Single unknown enantiomer (*R*)-4-(but-3-en-2-yl)-2-methyl-5-((2-(4-methylpiperazin-1-yl)benzyl)amino)pyridazin-3(2H)-one (**26**) (27 mg, 0.07 mmol, 9%) as a colourless oil. HPLC (Chiralpak AD-H column, 4.6 mm  $\times$  25 cm, 10%EtOH(+0.2% isopropylamine)/heptane, 1 mL/min): 10.5 min (major enantiomer) 11.6 (minor enantiomer) 97% ee;  $[\alpha_D]^{23}$  ( $c = 10$  mg/mL, MeOH):  $+21^\circ$ ;  $^1\text{H}$  NMR (400 MHz,  $\text{CD}_3\text{OD}$ )  $\delta$  ppm 7.59 (s, 1 H), 7.35-7.24 (m, 2 H), 7.23-7.18 (m, 1 H), 7.10 (td,  $J=7.6, 1.2$  Hz, 1 H), 6.18 (ddd,  $J=17.4, 10.5, 5.1$  Hz, 1 H), 5.17 (dt,  $J=17.4, 1.8$  Hz, 1 H), 5.13 (dt,  $J=10.5, 1.8$  Hz, 1 H) 4.59-4.49 (m, 2 H), 4.05-3.97 (m, 1 H), 3.62 (s, 3 H), 3.05-2.95 (m, 4 H), 2.80-2.63 (m, 4 H), 2.40 (s, 3 H), 1.38 (d,  $J=7.3$  Hz, 3 H);  $^{13}\text{C}$  NMR (101 MHz,  $\text{CD}_3\text{OD}$ )  $\delta$  ppm 161.3, 150.5, 145.4, 139.8, 133.2, 128.7, 128.2, 128.1, 124.2, 119.6, 113.8, 113.4, 55.1, 52.2, 44.7, 41.0, 38.9, 32.6, 14.1; HRMS ( $\text{M}+\text{H}$ ) $^+$  calculated for  $\text{C}_{21}\text{H}_{30}\text{N}_5\text{O}$  368.2450; found 368.2444; LC/MS (high pH):  $R_t = 0.98$  min (100%) [ $\text{M}+\text{H}$ ] $^+ = 368$ .

Single unknown enantiomer (*S*)-4-(but-3-en-2-yl)-2-methyl-5-((2-(4-methylpiperazin-1-yl)benzyl)amino)pyridazin-3(2H)-one (**27**) (23 mg, 0.06 mmol, 8%) as a colourless oil. Analytical data as **26** above except; HPLC (Chiralpak AD-H column, 4.6 mm × 25 cm, 10%EtOH(+0.2% isopropylamine)/heptane, 1 mL/min): 11.3 (major enantiomer), 10.4 (minor enantiomer) 95% ee [ $\alpha_D$ ]<sup>23</sup> (c = 10 mg/mL, MeOH): -21°.

**4-(But-3-en-1-yl)-5-chloro-2-methylpyridazin-3(2H)-one (43).** 5-Chloro-2,4-dimethylpyridazin-3(2H)-one (500 mg, 3.15 mmol) was dissolved in THF (10 mL) at rt under nitrogen. The solution was cooled to -78 °C and LiHMDS (1 M in THF, 4.73 mL, 4.73 mmol) and 3-bromoprop-1-ene (0.36 mL, 4.10 mmol) added under nitrogen. The resultant solution was stirred at -78 °C under nitrogen for 45 min before being diluted with MeOH (5 mL), allowed to warm to rt, and concentrated *in vacuo*. The resultant residue was dissolved in EtOAc (10 mL) and washed with water. The aqueous layer was separated and extracted further with EtOAc (10 mL × 2). The organic layers were combined, washed with brine (15 mL), passed through a hydrophobic frit before being concentrated *in vacuo*. The resultant residue was dissolved in minimal DCM and purified by silica chromatography (0-50% EtOAc in cyclohexane). The desired fractions were combined yielding 4-(but-3-en-1-yl)-5-chloro-2-methylpyridazin-3(2H)-one (150 mg, 0.76 mmol, 24%) as a colourless oil. <sup>1</sup>H NMR (400 MHz, CD<sub>3</sub>OD)  $\delta$  ppm 7.89 (s, 1 H), 5.89 (ddt, *J*=17.0, 10.2, 6.8 Hz, 1 H), 5.04 (app. dq, *J*=17.1, 1.8 Hz, 1 H), 4.98 (ddt, *J*=10.1, 1.8, 1.1 Hz, 1 H) 3.75 (s, 3 H), 2.84 (t, *J*=7.3 Hz, 2 H), 2.39-2.30 (m, 2 H); <sup>13</sup>C NMR (101 MHz, CD<sub>3</sub>OD)  $\delta$  ppm 160.3, 138.9, 136.7, 136.6, 114.7, 39.4, 30.5, 26.7 (N.B. One sp<sup>2</sup> carbon signal missing, 136.7 broad and intense possible overlap of two signals); HRMS (M+H)<sup>+</sup> calculated for C<sub>9</sub>H<sub>12</sub>ClN<sub>2</sub>O 199.0638; found 199.0638; LC/MS (formic acid): R<sub>t</sub> = 0.96 min (91%) [M+H]<sup>+</sup> = 199.

**4-(But-3-en-1-yl)-2-methyl-5-((2-(4-methylpiperazin-1-yl)benzyl)amino)pyridazin-3(2H)-one (25).** (2-(4-Methylpiperazin-1-yl)phenyl)methanamine (0.17 mL, 0.88 mmol), 4-

(but-3-en-1-yl)-5-chloro-2-methylpyridazin-3(2H)-one (145 mg, 0.73 mmol), sodium *tert*-butoxide (140 mg, 1.46 mmol), Pd<sub>2</sub>(dba)<sub>3</sub> (54 mg, 0.07 mmol) and BrettPhos (78 mg, 0.15 mmol) were dissolved in THF (0.5 mL). The resultant solution was stirred at 100 °C for 1 hour in a microwave reactor. The reaction was allowed to cool to rt before being concentrated *in vacuo*. The resultant residue was dissolved in 1:1 MeOH:DMSO and purified by MDAP (high pH). The desired fractions were combined yielding 4-(but-3-en-1-yl)-2-methyl-5-((2-(4-methylpiperazin-1-yl)benzyl)amino)pyridazin-3(2H)-one (54 mg, 0.15 mmol, 20%) as a white solid. <sup>1</sup>H NMR (400 MHz, CD<sub>3</sub>OD) δ ppm 7.56 (s, 1 H), 7.35 (dd, *J*=7.5, 1.2 Hz, 1 H), 7.30-7.24 (m, 1 H), 7.20 (dd, *J*=7.5, 1.2 Hz, 1 H), 7.09 (td, *J*=7.5, 1.2 Hz, 1 H), 5.93 (ddt, *J*=17.0, 10.2, 6.8 Hz, 1 H), 5.09-5.01 (m, 1 H), 4.99-4.94 (m, 1 H), 4.55 (s, 2 H), 3.62 (s, 3 H), 3.01 (t, *J*=4.8 Hz, 4 H), 2.78-2.60 (m, 6 H), 2.40 (s, 3 H), 2.27 (app. q, *J*=7.4 Hz, 2 H) (N.B. exchangeable amine proton not visible); <sup>13</sup>C NMR (101 MHz, CD<sub>3</sub>OD) δ ppm 161.9, 150.5, 145.9, 137.7, 133.4, 128.4, 128.1, 128.0, 124.1, 119.5, 114.2, 111.6, 55.2, 52.1, 44.8, 40.9, 38.8, 30.6, 22.4; HRMS (M+H)<sup>+</sup> calculated for C<sub>21</sub>H<sub>30</sub>N<sub>5</sub>O 368.2450; found 368.2451; LC/MS (high pH): R<sub>t</sub> = 0.93 min (100%) [M+H]<sup>+</sup> = 368.

**5-Chloro-4-ethylpyridazin-3(2H)-one (44).** 3 M Ethylmagnesium bromide in Et<sub>2</sub>O solution (15.15 mL, 45.50 mmol) was added dropwise to a stirred suspension of 4,5-dichloropyridazin-3(2H)-one (2.500 g, 15.15 mmol) in THF (50 mL) at 0 °C under nitrogen. The resultant solution was stirred at 0 °C for 10 min before being allowed to warm to rt and stirred for 3 hours. Saturated aq. NH<sub>4</sub>Cl solution (25 mL) was added slowly over 10 min. EtOAc (50 mL) and 2 M aqueous HCl (50 mL) were added, the mixture shaken, and the organic layer removed. The aqueous layer was extracted further with EtOAc (25 mL). The organic layers were combined, washed with brine (25 mL), passed through a hydrophobic frit and concentrated *in vacuo*. The resultant oil was dissolved in minimal DCM and purified by silica chromatography (0-40% EtOAc in cyclohexane). The desired fractions were combined yielding 5-chloro-4-

ethylpyridazin-3(2H)-one (625 mg, 3.94 mmol, 26%) as a white solid. m.p. 135–138 °C;  $\nu_{\max}$  (solid)/ $\text{cm}^{-1}$ : 2864, 1638 (C=O), 1177, 914, 575;  $^1\text{H}$  NMR (400 MHz,  $\text{CD}_3\text{OD}$ )  $\delta$  ppm 7.88 (s, 1 H), 2.75 (q,  $J=7.6$  Hz, 2 H), 1.17 (t,  $J=7.6$  Hz, 3 H) (N.B. exchangeable lactam proton not visible);  $^{13}\text{C}$  NMR (101 MHz,  $\text{CD}_3\text{OD}$ )  $\delta$  ppm 161.4, 141.7, 137.9, 137.0, 20.0, 10.0; HRMS ( $\text{M}+\text{H}$ ) $^+$  calculated for  $\text{C}_6\text{H}_8\text{ClN}_2\text{O}$  159.0325; found 159.0325; LC/MS (formic acid):  $R_t$  = 0.66 min (98%) [ $\text{M}+\text{H}$ ] $^+$  = 159.

**5-Chloro-4-ethyl-2-methylpyridazin-3(2H)-one (45).** Methyl iodide (0.20 mL, 3.15 mmol) was added to a stirred mixture of tetrabutylammonium bromide (1.118 g, 3.47 mmol), 5-chloro-4-ethylpyridazin-3(2H)-one (250 mg, 1.58 mmol) and potassium carbonate (436 mg, 3.15 mmol) in MeCN (5 mL) at rt. The resultant mixture was stirred under nitrogen for 3 hours at rt. The resultant mixture was filtered under reduced pressure and the filtrate concentrated *in vacuo*. The resultant solid was dissolved in EtOAc (50 mL) and washed with 2 M aq. HCl (30 mL). MeOH was added dropwise to dissolve a white precipitate. The organic layer was then washed with brine (30 mL), passed through a hydrophobic frit, and concentrated *in vacuo*. The resultant solid was dissolved in minimal DCM and purified by silica chromatography (0-50% EtOAc in cyclohexane). The desired fractions were concentrated *in vacuo* yielding 5-chloro-4-ethyl-2-methylpyridazin-3(2H)-one (170 mg, 0.99 mmol, 63%) as a colourless oil.  $^1\text{H}$  NMR (400 MHz,  $\text{CD}_3\text{OD}$ )  $\delta$  ppm 7.89 (s, 1 H), 3.75 (s, 3 H), 2.76 (q,  $J=7.6$  Hz, 2 H), 1.16 (t,  $J=7.6$  Hz, 3 H);  $^{13}\text{C}$  NMR (101 MHz,  $\text{CD}_3\text{OD}$ )  $\delta$  ppm 160.2, 140.9, 136.8, 136.0, 39.4, 20.6, 9.9; HRMS ( $\text{M}+\text{H}$ ) $^+$  calculated for  $\text{C}_7\text{H}_{10}\text{ClN}_2\text{O}$  173.0482; found 173.0478; LC/MS (formic acid):  $R_t$  = 0.80 min (99%) [ $\text{M}+\text{H}$ ] $^+$  = 173.

**4-Ethyl-2-methyl-5-((2-(4-methylpiperazin-1-yl)benzyl)amino)pyridazin-3(2H)-one (28).** (2-(4-Methylpiperazin-1-yl)phenyl)methanamine (0.13 mL, 0.70 mmol), 5-chloro-4-ethyl-2-methylpyridazin-3(2H)-one (100 mg, 0.58 mmol), sodium *tert*-butoxide (111 mg, 1.16 mmol),  $\text{Pd}_2(\text{dba})_3$  (53 mg, 0.058 mmol) and BrettPhos (62 mg, 0.12 mmol) were dissolved in THF (0.5

mL) and heated to 100 °C in a microwave reactor. The reaction mixture was stirred at 100 °C for 1 hour. The resultant solution was allowed to cool to rt, diluted with EtOAc (10 mL), filtered through Celite and concentrated *in vacuo*. The resultant residue was dissolved in EtOAc (10 mL) and washed sequentially with water (10 mL) and brine (10 mL). The organic layer was passed through a hydrophobic frit and concentrated *in vacuo*. The resultant residue was dissolved in 1:1 MeOH:DMSO and purified by MDAP (high pH). The desired fractions were combined and concentrated *in vacuo* yielding 4-ethyl-2-methyl-5-((2-(4-methylpiperazin-1-yl)benzyl)amino)pyridazin-3(2H)-one (91 mg, 0.27 mmol, 46%) as a white solid. m.p. 148–149 °C;  $\nu_{\max}$  (solid)/ $\text{cm}^{-1}$ : 3344, 2796, 1595 (C=O), 1225, 769;  $^1\text{H}$  NMR (400 MHz,  $\text{CD}_3\text{OD}$ )  $\delta$  ppm 7.56 (s, 1 H), 7.37-7.31 (m, 1 H), 7.30-7.23 (m, 1 H), 7.21 (dd,  $J=7.4, 1.3$  Hz, 1 H), 7.09 (td,  $J=7.4, 1.3$  Hz, 1 H), 4.56 (s, 2 H), 3.62 (s, 3 H), 3.01 (t,  $J=4.8$  Hz, 4 H), 2.71 (app. br. s, 4 H), 2.57 (q,  $J=7.5$  Hz, 2 H), 2.40 (s, 3 H), 1.10 (t,  $J=7.5$  Hz, 3 H) (N.B. exchangeable amine proton not visible);  $^{13}\text{C}$  NMR (101 MHz,  $\text{CD}_3\text{OD}$ )  $\delta$  ppm 161.7, 150.5, 145.5, 133.4, 128.5, 128.0, 127.9, 124.1, 119.5, 113.8, 55.2, 52.2, 44.8, 40.8, 38.8, 16.0, 10.1; HRMS ( $\text{M}+\text{H}$ ) $^+$  calculated for  $\text{C}_{19}\text{H}_{28}\text{N}_5\text{O}$  342.2294; found 342.2292; LC/MS (high pH):  $R_t = 0.84$  min (100%) [ $\text{M}+\text{H}$ ] $^+ = 342$ .

**5-Chloro-4-isopropylpyridazin-3(2H)-one (46).** 2.9 M Isopropylmagnesium bromide in 2-methyl THF solution (3.14 mL, 9.09 mmol) was added dropwise to a stirred suspension of 4,5-dichloropyridazin-3(2H)-one (500 mg, 3.03 mmol) in THF (10 mL) at 0 °C under nitrogen. The resultant solution was stirred at 0 °C for 10 min before being allowed to warm to rt and stirred for 1.5 hours. Saturated aq.  $\text{NH}_4\text{Cl}$  solution (5 mL) was added dropwise. EtOAc (5 mL) and 2 M aq. HCl (5 mL) were added, the mixture shaken, and the organic layer removed. The aqueous layer was extracted further with EtOAc (25 mL). The organic layers were combined, washed with brine (25 mL), passed through a hydrophobic frit and concentrated *in vacuo*. The resultant oil was dissolved in minimal DCM and purified by silica chromatography (0-40%

EtOAc in cyclohexane). The desired fractions were combined and concentrated *in vacuo* yielding 5-chloro-4-isopropylpyridazin-3(2H)-one (140 mg, 0.81 mmol, 27%) as an off-white solid. m.p. 98–102 °C;  $\nu_{\text{max}}$  (solid)/ $\text{cm}^{-1}$ : 2966, 2876, 1645 (C=O), 1180, 1055, 918, 593;  $^1\text{H}$  NMR (400 MHz,  $\text{CD}_3\text{OD}$ )  $\delta$  ppm 7.84 (s, 1 H), 3.50 (sept.,  $J=7.1$  Hz, 1 H), 1.36 (d,  $J=7.1$  Hz, 6 H);  $^{13}\text{C}$  NMR (101 MHz,  $\text{CD}_3\text{OD}$ )  $\delta$  ppm 160.9, 143.8, 138.0, 136.2, 28.9, 17.4; HRMS ( $\text{M}+\text{H}$ ) $^+$  calculated for  $\text{C}_7\text{H}_{10}\text{ClN}_2\text{O}$  173.0482; found 173.0477; LC/MS (formic acid):  $R_t = 0.81$  min (85%) [ $\text{M}+\text{H}$ ] $^+ = 173$ .

**5-Chloro-4-isopropyl-2-methylpyridazin-3(2H)-one (47).** Methyl iodide (0.07 mL, 1.11 mmol) was added to a stirred mixture of tetrabutylammonium bromide (406 mg, 1.26 mmol), 5-chloro-4-isopropylpyridazin-3(2H)-one (128 mg, 0.74 mmol) and potassium carbonate (205 mg, 1.48 mmol) in MeCN (5 mL) at rt. The resultant mixture was stirred under nitrogen for 2.5 hours at rt. The reaction mixture was filtered under reduced pressure and the filtrate concentrated *in vacuo*. The resultant solid was dissolved in EtOAc (10 mL) and washed with 2 M aq. HCl (10 mL). MeOH was added dropwise to dissolve a white precipitate. The organic layer was then washed with brine (10 mL), passed through a hydrophobic frit, and concentrated *in vacuo*. The resultant solid was dissolved in minimal DCM and purified by silica chromatography (0-50% EtOAc in cyclohexane). The desired fractions were concentrated *in vacuo* yielding 5-chloro-4-isopropyl-2-methylpyridazin-3(2H)-one (26 mg, 0.139 mmol, 19%) as a colourless oil.  $^1\text{H}$  NMR (400 MHz,  $\text{DMSO}-d_6$ )  $\delta$  ppm 7.94 (s, 1 H), 3.63 (s, 3 H), 3.38 (sept.,  $J=7.1$  Hz, 1 H), 1.28 (d,  $J=7.1$  Hz, 6 H);  $^{13}\text{C}$  NMR (101 MHz,  $\text{DMSO}-d_6$ )  $\delta$  ppm 158.9, 142.8, 136.8, 134.7, 29.3, 18.7 (N.B. one  $\text{sp}^3$  carbon signal obscured by solvent peak at 40.2 ppm); HRMS ( $\text{M}+\text{H}$ ) $^+$  calculated for  $\text{C}_8\text{H}_{12}\text{ClN}_2\text{O}$  187.0638; found 187.0638 LC/MS (formic acid):  $R_t = 0.97$  min (100%) [ $\text{M}+\text{H}$ ] $^+ = 187$ .

**4-Isopropyl-2-methyl-5-((2-(4-methylpiperazin-1-yl)benzyl)amino)pyridazin-3(2H)-one (30).** (2-(4-Methylpiperazin-1-yl)phenyl)methanamine (0.09 mL, 0.48 mmol), 5-chloro-4-

isopropyl-2-methylpyridazin-3(2H)-one (75 mg, 0.40 mmol), sodium *tert*-butoxide (77 mg, 0.80 mmol), Pd<sub>2</sub>(dba)<sub>3</sub> (37 mg, 0.04 mmol) and BrettPhos (43 mg, 0.08 mmol) were dissolved in THF (4 mL). The reaction mixture was stirred at 100 °C for 1 hour in a microwave reactor. The resultant solution was allowed to cool to rt, diluted with EtOAc (10 mL), filtered through Celite and concentrated *in vacuo*. The resultant residue was dissolved in EtOAc (10 mL) and washed sequentially with water (15 mL) and brine (15 mL). The organic layer was passed through a hydrophobic frit and concentrated *in vacuo*. The resultant residue was dissolved in 1:1 MeOH:DMSO and purified by MDAP (high pH). The desired fractions were combined and concentrated *in vacuo* yielding 4-isopropyl-2-methyl-5-((2-(4-methylpiperazin-1-yl)benzyl)amino)pyridazin-3(2H)-one (51 mg, 0.14 mmol, 36%) as a white solid. m.p. 163–165 °C;  $\nu_{\text{max}}$  (solid) /cm<sup>-1</sup>: 3308, 2794, 1591 (C=O), 1450, 1141, 772; <sup>1</sup>H NMR (400 MHz, CD<sub>3</sub>OD)  $\delta$  ppm 7.52 (s, 1 H), 7.33 (dd, *J*=7.7, 1.1 Hz, 1 H), 7.29-7.23 (m, 1 H), 7.23-7.19 (dd, *J*=7.3, 1.2 Hz, 1 H), 7.10 (td, *J*=7.3, 1.2 Hz, 1 H), 4.55 (s, 2 H), 3.58 (s, 3 H), 3.23-3.14 (m, 1 H), 3.01 (t, *J*=4.8 Hz, 4 H), 2.69 (app. br. s, 4 H), 2.40 (s, 3 H), 1.35 (d, *J*=7.1 Hz, 6 H) (N.B. exchangeable amine proton not visible); <sup>13</sup>C NMR (101 MHz, CD<sub>3</sub>OD)  $\delta$  ppm 161.3, 150.5, 145.2, 133.4, 128.6, 128.1, 128.0, 124.2, 119.5, 116.6, 55.1, 52.1, 44.8, 41.1, 38.7, 24.6, 17.8; HRMS (M+H)<sup>+</sup> calculated for C<sub>20</sub>H<sub>30</sub>N<sub>5</sub>O 356.2450; found 356.2449.; LC/MS (high pH): R<sub>t</sub> = 0.92 min (98%) [M+H]<sup>+</sup> = 356.

**4-Butyl-5-chloropyridazin-3(2H)-one (48).** 4,5-Dichloropyridazin-3(2H)-one (1000 mg, 6.06 mmol) was dissolved in THF (30 mL) at rt under nitrogen. The solution was allowed to cool to -78 °C before 1.6 M BuLi in hexanes (8.90 mL, 14.24 mmol) was added dropwise over 10 min. The resultant solution was stirred at -78 °C for 15 min. The solution was diluted with IPA (20 mL) and allowed to warm to rt before being concentrated *in vacuo*. The resultant residue was dissolved in EtOAc (40 mL) and washed with water (40 mL). The layers were separated and the aqueous extracted further with EtOAc (30 mL). The combined organic

fractions were washed with brine (30 mL) and passed through a hydrophobic frit before being concentrated *in vacuo*. The resultant residue was dissolved in minimal DCM and purified by silica chromatography (0-30% EtOAc in cyclohexane). The desired fractions were combined yielding 4-butyl-5-chloropyridazin-3(2H)-one (715 mg, 3.83 mmol, 63%) as an off white solid. <sup>1</sup>H NMR (400 MHz, CDCl<sub>3</sub>) δ ppm 11.88 (br. s, 1 H), 7.76 (s, 1 H), 2.80-2.69 (m, 2 H), 1.64-1.54 (m, 2 H), 1.50-1.38 (m, 2 H), 0.97 (t, *J*=7.2 Hz, 3 H); <sup>13</sup>C NMR (101 MHz, CDCl<sub>3</sub>) δ ppm 161.8, 141.6, 138.1, 137.3, 28.9, 27.0, 22.8, 13.8; HRMS (M+H)<sup>+</sup> calculated for C<sub>8</sub>H<sub>12</sub>ClN<sub>2</sub>O 187.0638; found 187.0644; LC/MS (formic acid): R<sub>t</sub> = 0.90 min (100%) [M+H]<sup>+</sup> = 187.

**4-Butyl-5-chloro-2-methylpyridazin-3(2H)-one (49).** Methyl iodide (0.36 mL, 5.75 mmol) was added to a stirred mixture of tetrabutylammonium bromide (2.099 g, 6.51 mmol), 4-butyl-5-chloropyridazin-3(2H)-one (715 mg, 3.83 mmol) and potassium carbonate (1.059 g, 7.66 mmol) in MeCN (8 mL) at rt. The resultant solution was heated to 60 °C and stirred for 5 hours. The resultant mixture was allowed to cool to rt before being filtered under reduced pressure and the filtrate concentrated *in vacuo*. The resultant solid was dissolved in EtOAc (30 mL) and washed with 1 M aq. HCl (30 mL). The organic layer was then washed with brine (20 mL), passed through a hydrophobic frit, and concentrated *in vacuo*. The resultant solid was dissolved in minimal DCM and purified by silica chromatography (0-25% EtOAc in cyclohexane). The desired fractions were concentrated *in vacuo* yielding 4-butyl-5-chloro-2-methylpyridazin-3(2H)-one (593 mg, 2.96 mmol, 77%) as a yellow oil. <sup>1</sup>H NMR (400 MHz, CDCl<sub>3</sub>) δ ppm 7.68 (s, 1 H), 3.77 (s, 3 H), 2.79-2.68 (m, 2 H), 1.60-1.52 (m, 2 H), 1.49-1.37 (m, 2 H), 0.97 (t, *J*=7.3 Hz, 3 H); <sup>13</sup>C NMR (101 MHz, CDCl<sub>3</sub>) δ ppm 160.2, 140.6, 136.3, 135.9, 40.2, 28.9, 27.5, 22.8, 13.8; HRMS (M+H)<sup>+</sup> calculated for C<sub>9</sub>H<sub>14</sub>ClN<sub>2</sub>O 201.0795; found 201.0802; LC/MS (formic acid): R<sub>t</sub> = 1.07 min (95%) [M+H]<sup>+</sup> = 201.

**4-Butyl-2-methyl-5-((2-(4-methylpiperazin-1-yl)benzyl)amino)pyridazin-3(2H)-one (31).** (2-(4-Methylpiperazin-1-yl)phenyl)methanamine (0.06 mL, 0.30 mmol), 4-butyl-5-chloro-2-



methylpyridazin-3(2H)-one (50 mg, 0.25 mmol), sodium *tert*-butoxide (48 mg, 0.50 mmol), Pd<sub>2</sub>(dba)<sub>3</sub> (23 mg, 0.03 mmol) and BrettPhos (27 mg, 0.05 mmol) were dissolved in THF (0.5 mL). The reaction mixture was heated to 100 °C in a microwave reactor and stirred for 1 hour. The resultant solution was allowed to cool to rt, diluted with EtOAc (10 mL), filtered through Celite and concentrated *in vacuo*. The resultant residue was dissolved in EtOAc (10 mL) and washed sequentially with water (10 mL) and brine (10 mL). The organic layer was passed through a hydrophobic frit and concentrated *in vacuo*. The resultant residue was dissolved in 1:1 MeOH:DMSO and purified by MDAP (high pH). The desired fractions were combined and concentrated *in vacuo* yielding 4-butyl-2-methyl-5-((2-(4-methylpiperazin-1-yl)benzyl)amino)pyridazin-3(2H)-one (20 mg, 0.05 mmol, 22%) as an orange oil. <sup>1</sup>H NMR (400 MHz, CD<sub>3</sub>OD) δ ppm 7.55 (s, 1 H), 7.36-7.31 (m, 1 H), 7.30-7.24 (m, 1 H), 7.21 (dd, *J*=7.3, 1.2 Hz, 1 H), 7.09 (td, *J*=7.3, 1.2 Hz, 1 H), 4.56 (s, 2 H), 3.62 (s, 3 H), 3.02 (t, *J*=4.9 Hz, 4 H), 2.73 (app. br. s, 4 H), 2.55 (t, *J*=7.2 Hz, 2 H), 2.42 (s, 3 H), 1.56-1.38 (m, 4 H), 0.98 (t, *J*=7.2 Hz, 3 H) (N.B. exchangeable amine proton not visible); <sup>13</sup>C NMR (101 MHz, CD<sub>3</sub>OD) δ ppm 161.9, 150.5, 145.8, 133.4, 128.4, 128.0, 127.9, 124.1, 119.5, 112.6, 55.2, 52.1, 44.8, 40.9, 38.8, 28.8, 26.6, 22.5, 13.1; HRMS (M+H)<sup>+</sup> calculated for C<sub>21</sub>H<sub>32</sub>N<sub>5</sub>O 370.2607; found 370.2607; LC/MS (high pH): R<sub>t</sub> = 1.01 min (100%) [M+H]<sup>+</sup> = 370.

### **2-Methyl-5-((2-(4-methylpiperazin-1-yl)benzyl)amino)-4-propylpyridazin-3(2H)-one**

(**29**). The solvent system was sparged with nitrogen for 1 hour prior to use. 4-Chloro-2-methyl-5-((2-(4-methylpiperazin-1-yl)benzyl)amino)pyridazin-3(2H)-one (100 mg, 0.29 mmol), propylboronic acid (100 mg, 1.14 mmol), potassium carbonate (99 mg, 0.72 mmol), Pd(OAc)<sub>2</sub> (26 mg, 0.12 mmol) and butyldi-1-adamantylphosphine (52 mg, 0.14 mmol) were dissolved in 1,4-dioxane (1.65 mL) and water (0.83 mL) under nitrogen at rt. The resultant mixture was heated to 100 °C and stirred for 1 hour in a microwave reactor. The resultant solution was diluted with EtOAc (10 mL) and filtered through Celite before being concentrated *in vacuo*.

The resultant residue was dissolved in 1:1 MeOH:DMSO and purified by MDAP (high pH). The desired fractions were combined yielding 2-methyl-5-((2-(4-methylpiperazin-1-yl)benzyl)amino)-4-propylpyridazin-3(2H)-one (30 mg, 0.08 mmol, 29%) as an off white solid. <sup>1</sup>H NMR (400 MHz, CD<sub>3</sub>OD) δ ppm 7.55 (s, 1 H), 7.37-7.31 (m, 1 H), 7.29-7.24 (m, 1 H), 7.23-7.17 (m, 1 H), 7.09 (td, *J*=7.5, 1.2 Hz, 1 H), 4.55 (s, 2 H), 3.62 (s, 3 H), 3.01 (t, *J*=4.8 Hz, 4 H), 2.71 (app. br. s, 4 H), 2.57-2.48 (m, 2 H), 2.40 (s, 3 H), 1.61-1.46 (m, 2 H), 1.02 (t, *J*=7.3 Hz, 3 H). (N.B. exchangeable amine proton not visible); <sup>13</sup>C NMR (101 MHz, CD<sub>3</sub>OD) δ ppm 162.0, 150.5, 145.9, 133.4, 128.4, 128.0, 127.9, 124.1, 119.5, 112.4, 55.1, 52.1, 44.8, 40.8, 38.8, 24.8, 19.7, 13.0; HRMS (M+H)<sup>+</sup> calculated for C<sub>20</sub>H<sub>30</sub>N<sub>5</sub>O 356.2450; found 356.2442; LC/MS (high pH): R<sub>t</sub> = 0.92 min (100%) [M+H]<sup>+</sup> = 356.

### **2-Methyl-5-((2-(4-methylpiperazin-1-yl)benzyl)amino)-4-pentylpyridazin-3(2H)-one**

**(32).** The solvent system sparged with nitrogen for 1 hour prior to use. 4-Chloro-2-methyl-5-((2-(4-methylpiperazin-1-yl)benzyl)amino)pyridazin-3(2H)-one (100 mg, 0.29 mmol), pentylboronic acid (100 mg, 0.86 mmol), potassium carbonate (99 mg, 0.72 mmol), Pd(OAc)<sub>2</sub> (26 mg, 0.12 mmol) and butyldi-1-adamantylphosphine (52 mg, 0.14 mmol) were dissolved in 1,4-dioxane (1.65 mL) and water (0.83 mL) under nitrogen at rt. The reaction mixture was heated to 100 °C and stirred for 1 hour in a microwave reactor. The resultant solution was diluted with EtOAc (5 mL) and filtered through Celite before being concentrated *in vacuo*. The resultant residue was dissolved in 1:1 MeOH:DMSO and purified by MDAP (high pH). The desired fractions were combined yielding 2-methyl-5-((2-(4-methylpiperazin-1-yl)benzyl)amino)-4-pentylpyridazin-3(2H)-one (28 mg, 0.07 mmol, 25%) as an off white solid. <sup>1</sup>H NMR (400 MHz, CD<sub>3</sub>OD) δ ppm 7.56 (s, 1 H), 7.36-7.31 (m, 1 H), 7.30-7.24 (m, 1 H), 7.20 (dd, *J*=7.5, 1.2 Hz, 1 H), 7.09 (td, *J*=7.5, 1.2 Hz, 1 H), 4.55 (s, 2 H), 3.62 (s, 3 H), 3.01 (t, *J*=4.8 Hz, 4 H), 2.71 (app. br. s, 4 H), 2.58-2.49 (m, 2 H), 2.40 (s, 3 H), 1.57-1.46 (m, 2 H), 1.44-1.34 (m, 4 H), 0.97-0.91 (m, 3 H); <sup>13</sup>C NMR (101 MHz, CD<sub>3</sub>OD) δ ppm 162.0, 150.5, 145.8, 133.4,

128.4, 128.0, 127.9, 124.1, 119.5, 112.7, 55.2, 52.2, 44.8, 40.9, 38.8, 31.6, 26.3, 22.9, 22.4, 13.0; HRMS (M+H)<sup>+</sup> calculated for C<sub>22</sub>H<sub>34</sub>N<sub>5</sub>O 384.2763; found 384.2756; LC/MS (high pH): R<sub>t</sub> = 1.08 min (96%) [M+H]<sup>+</sup> = 384.

**2-Methyl-5-((2-(4-methylpiperazin-1-yl)benzyl)amino)pyridazin-3(2H)-one (33).** The solvent system sparged with nitrogen for 20 min prior to use. 4-Chloro-2-methyl-5-((2-(4-methylpiperazin-1-yl)benzyl)amino)pyridazin-3(2H)-one (100 mg, 0.29 mmol), butyltrifluoroborate, potassium salt (94 mg, 0.58 mmol), potassium carbonate (99 mg, 0.72 mmol), Pd(OAc)<sub>2</sub> (13 mg, 0.06 mmol) and butyldi-1-adamantylphosphine (22 mg, 0.06 mmol) were dissolved in 1,4-dioxane (3 mL) and water (1.5 mL) under nitrogen at rt. The resultant mixture was heated to 100 °C and stirred for 1 hour in a microwave reactor. The resultant solution was diluted with EtOAc (5 mL) and filtered through Celite before being concentrated *in vacuo*. The resultant residue was dissolved in EtOAc (10 mL) and washed sequentially with water (10 mL) and brine (10 mL). The organic layer was then passed through a hydrophobic frit and concentrated *in vacuo*. The resultant residue was dissolved in 1:1 MeOH:DMSO and purified by MDAP (high pH). The desired fractions were combined yielding 2-methyl-5-((2-(4-methylpiperazin-1-yl)benzyl)amino)pyridazin-3(2H)-one (39 mg, 0.12 mmol, 43%) as a white solid. m.p. 190–192 °C;  $\nu_{\max}$  (solid) /cm<sup>-1</sup>: 3245, 2941, 2790, 1591 (C=O), 1450, 761; <sup>1</sup>H NMR (400 MHz, CD<sub>3</sub>OD)  $\delta$  ppm 7.57 (d, *J*=2.7 Hz, 1 H), 7.37-7.32 (m, 1 H), 7.31-7.25 (m, 1 H), 7.22 (dd, *J*=7.5, 1.2 Hz, 1 H), 7.11 (td, *J*=7.5, 1.2 Hz, 1 H), 5.62 (d, *J*=2.7 Hz, 1 H), 4.39 (s, 2 H), 3.61 (s, 3 H), 2.99 (t, *J*=4.8 Hz, 4 H), 2.68 (app. br. s, 4 H), 2.38 (s, 3 H); HRMS (M+H)<sup>+</sup> calculated for C<sub>17</sub>H<sub>24</sub>N<sub>5</sub>O 314.1981; found 314.1986; LC/MS (High pH): R<sub>t</sub> = 0.76 min (100%) [M+H]<sup>+</sup> = 314.

***tert*-Butyl 5-((5-butyl-1-methyl-6-oxo-1,6-dihydropyridazin-4-yl)amino)-3,4-dihydroisoquinoline-2(1H)-carboxylate (50).** *tert*-Butyl 5-amino-3,4-dihydroisoquinoline-2(1H)-carboxylate (515 mg, 2.07 mmol), 4-butyl-5-chloro-2-methylpyridazin-3(2H)-one (320

mg, 1.60 mmol), sodium *tert*-butoxide (307 mg, 3.19 mmol), Pd<sub>2</sub>(dba)<sub>3</sub> (118 mg, 0.16 mmol) and BrettPhos (171 mg, 0.32 mmol) were dissolved in THF (10 mL). The reaction mixture was stirred at 100 °C for 1 hour in a microwave reactor. The resultant solution was allowed to cool to rt, diluted with EtOAc (25 mL), filtered through Celite and concentrated *in vacuo*. The resultant residue was dissolved in EtOAc (30 mL) and washed sequentially with water (30 mL) and brine (20 mL). The organic layer was passed through a hydrophobic frit and concentrated *in vacuo*. The resultant residue was dissolved in minimal DCM and purified by silica chromatography (0-50% EtOAc in cyclohexane). The desired fractions were combined yielding *tert*-butyl 5-((5-butyl-1-methyl-6-oxo-1,6-dihydropyridazin-4-yl)amino)-3,4-dihydroisoquinoline-2(1H)-carboxylate (167 mg, 0.41 mmol, 25%) as a pale orange solid; m.p. 60-65 °C;  $\nu_{\text{max}}$  (solid)/cm<sup>-1</sup>: 3295, 2930, 1694 (C=O), 1584 (C=O), 1395, 1163, 769; <sup>1</sup>H NMR (400 MHz, CD<sub>3</sub>OD)  $\delta$  ppm 7.29 (t, *J*=7.6 Hz, 1 H), 7.22 (s, 1 H), 7.15 (d, *J*=7.6 Hz, 1 H), 7.09 (d, *J*=7.6 Hz, 1 H), 4.62 (s, 2 H), 3.68 (s, 3 H), 3.64 (t, *J*=5.9 Hz, 2 H), 2.74 (t, *J*=5.9 Hz, 2 H), 2.68-2.61 (m, 2 H), 1.61-1.40 (m, 13 H), 0.98 (t, *J*=7.2 Hz, 3 H) (N.B. exchangeable amine proton not visible); <sup>13</sup>C NMR (101 MHz, CD<sub>3</sub>OD)  $\delta$  ppm 162.2, 155.1, 144.6, 137.4, 135.5, 131.9, 129.3, 126.9, 124.9, 124.6, 115.1, 80.1, 38.9, 28.9, 27.3, 26.6, 24.4, 22.9, 22.4, 13.1 (N.B. one sp<sup>3</sup> carbon missing); HRMS (M+H)<sup>+</sup> calculated for C<sub>23</sub>H<sub>33</sub>N<sub>4</sub>O<sub>3</sub> 413.2555; found 413.2557; LC/MS (formic acid): R<sub>t</sub> = 1.24 min (98%) [M+H]<sup>+</sup> = 413.

#### **4-Butyl-2-methyl-5-((1,2,3,4-tetrahydroisoquinolin-5-yl)amino)pyridazin-3(2H)-one**

**(51).** *tert*-Butyl 5-((5-butyl-1-methyl-6-oxo-1,6-dihydropyridazin-4-yl)amino)-3,4-dihydroisoquinoline-2(1H)-carboxylate (150 mg, 0.36 mmol) was dissolved in 4 M HCl in 1,4-dioxane (3.00 mL, 12.00 mmol) at rt and stirred for 45 min. The reaction mixture was concentrated *in vacuo*. The resultant residue was dissolved in MeOH and passed through a preconditioned (MeOH) amino propyl column (1 g) and eluted with MeOH (10 mL). The desired fractions were concentrated *in vacuo* yielding 4-butyl-2-methyl-5-((1,2,3,4-

tetrahydroisoquinolin-5-yl)amino)pyridazin-3(2H)-one (114 mg, 0.36 mmol, 100%) as a yellow solid.  $^1\text{H}$  NMR (400 MHz,  $\text{CD}_3\text{OD}$ )  $\delta$  ppm 7.28 (t,  $J=7.6$  Hz, 1 H), 7.23 (s, 1 H), 7.14-7.08 (m, 2 H), 4.14 (s, 2 H), 3.68 (s, 3 H), 3.22 (t,  $J=6.1$  Hz, 2 H), 2.79 (t,  $J=6.1$  Hz, 2 H), 2.69-2.61 (m, 2 H), 1.61-1.51 (m, 2 H), 1.51-1.41 (m, 2 H), 0.98 (t,  $J=7.2$  Hz, 3 H) (N.B. exchangeable amine protons not visible);  $^{13}\text{C}$  NMR (101 MHz,  $\text{CD}_3\text{OD}$ )  $\delta$  ppm 162.2, 144.6, 137.7, 135.0, 131.2, 129.3, 126.8, 125.3, 124.9, 115.2, 46.4, 42.3, 39.0, 29.0, 23.5, 23.0, 22.4, 13.1; HRMS ( $\text{M}+\text{H}$ ) $^+$  calculated for  $\text{C}_{18}\text{H}_{25}\text{N}_4\text{O}$  313.2028; found 313.2033; LC/MS (formic acid):  $R_t = 0.48$  min (100%) [ $\text{M}+\text{H}$ ] $^+ = 313$ .

**4-Butyl-2-methyl-5-((2-methyl-1,2,3,4-tetrahydroisoquinolin-5-yl)amino)pyridazin-3(2H)-one (35).** 37% Formaldehyde in water with 10-15 % MeOH (0.25 mL, 3.36 mmol) and formic acid (1 mL, 26.10 mmol) were added to 4-butyl-2-methyl-5-((1,2,3,4-tetrahydroisoquinolin-5-yl)amino)pyridazin-3(2H)-one (105 mg, 0.34 mmol) in a sealed tube and heated to 80 °C for 6 hours. The Reaction mixture was allowed to cool to rt and concentrated *in vacuo*. The resultant residue was dissolved in minimal DCM and purified by silica chromatography (0-10% MeOH in DCM). The desired fractions were combined and concentrated *in vacuo*. The resultant solid was dissolved in MeOH (1.5 mL) and loaded on to an SCX (1 g) column, eluting with 2 M ammonia in MeOH solution (4 mL). The desired fractions were combined yielding 4-butyl-2-methyl-5-((2-methyl-1,2,3,4-tetrahydroisoquinolin-5-yl)amino)pyridazin-3(2H)-one (65 mg, 0.20 mmol, 59%) as a white solid.  $^1\text{H}$  NMR (400 MHz,  $\text{CDCl}_3$ )  $\delta$  ppm 7.44 (s, 1 H), 7.18 (t,  $J=7.8$  Hz, 1 H), 7.00 (d,  $J=7.8$  Hz, 1 H), 6.95 (d,  $J=7.8$  Hz, 1 H), 5.41 (s, 1 H), 3.73 (s, 3 H), 3.62 (s, 2 H), 2.79-2.71 (m, 4 H), 2.66-2.59 (m, 2 H), 2.49 (s, 3 H), 1.63-1.54 (m, 2 H), 1.52-1.45 (m, 2 H), 0.99 (t,  $J=7.3$  Hz, 3 H);  $^{13}\text{C}$  NMR (101 MHz,  $\text{CDCl}_3$ )  $\delta$  ppm 161.5, 142.4, 137.2, 137.1, 128.9, 128.7, 126.6, 124.0, 121.9, 117.7, 58.0, 52.5, 45.9, 39.8, 29.2, 25.5, 23.6, 23.0, 14.0; HRMS ( $\text{M}+\text{H}$ ) $^+$  calculated for

C<sub>19</sub>H<sub>27</sub>N<sub>4</sub>O 327.2185; found 327.2189; LC/MS (formic acid): R<sub>t</sub> = 0.49 min (100%) [M+H]<sup>+</sup> = 327.

**2-Bromo-5-butylthieno[3,2-c]pyridin-4(5H)-one.** To a solution of 2-bromothieno[3,2-c]pyridin-4(5H)-one (**50**) (1 g, 4.35 mmol) and cesium carbonate (4.25 g, 13.04 mmol) in THF (25 mL), 1-iodobutane (0.72 mL, 6.52 mmol) was added in a single portion and the mixture heated to 60 °C for 19 hours. The reaction mixture was allowed to cool to room temperature and concentrated in vacuo. The resultant solid was suspended in water (15 mL) and filtered under reduced pressure. The solid was washed with water (10 mL), collected and dried under vacuum at 40 °C yielding 2-bromo-5-butylthieno[3,2-c]pyridin-4(5H)-one (884 mg, 3.09 mmol, 71%) as a brown solid. <sup>1</sup>H NMR (400 MHz, CDCl<sub>3</sub>) δ ppm 7.63 (s, 1 H), 7.13 (d, *J*=7.1 Hz, 1 H), 6.56 (d, *J*=7.1 Hz, 1 H), 4.01 (t, *J*=7.4 Hz, 2 H), 1.83-1.70 (m, 2 H), 1.41 (s, *J*=7.4 Hz, 2 H), 0.98 (t, *J*=7.4 Hz, 3 H); <sup>13</sup>C NMR (101 MHz, CDCl<sub>3</sub>) δ ppm 157.6, 148.4, 132.6, 131.3, 127.7, 112.2, 100.8, 49.2, 31.6, 19.9, 13.7; HRMS (M+H)<sup>+</sup> calculated for C<sub>11</sub>H<sub>13</sub>BrNOS 285.9901; found 285.9910; LC/MS (formic acid): R<sub>t</sub> = 1.13 min (97%) [M+H]<sup>+</sup> = 286.

**5-Butyl-4-oxo-4,5-dihydrothieno[3,2-c]pyridine-2-carbonitrile (51).** Two batches of 2-bromo-5-butylthieno[3,2-c]pyridin-4(5H)-one (1 g, 3.50 mmol), Zn(CN)<sub>2</sub> (821 mg, 6.99 mmol) and Pd(PPh<sub>3</sub>)<sub>4</sub> (404 mg, 0.35 mmol) in DMF (5 mL) were heated to 115 °C in a microwave reactor for 4.5 hours. The batches were diluted with EtOAc (50 mL each), combined, filtered through Celite and concentrated in vacuo. The resulting residue was diluted with DCM, filtered under reduced pressure, and the filtrate concentrated *in vacuo*. The resultant residue was dissolved in minimal DCM and purified by silica gel chromatography (0-40% EtOAc in cyclohexane). The desired fractions were combined and concentrated *in vacuo* yielding 5-butyl-4-oxo-4,5-dihydrothieno[3,2-c]pyridine-2-carbonitrile (984 mg, 4.24 mmol, 61%) as a white solid. m.p. 95–99 °C; ν<sub>max</sub> (solid)/cm<sup>-1</sup>: 3103, 2960, 2871, 2209 (C≡N), 1631 (C=O), 1588, 769; <sup>1</sup>H NMR (400 MHz, CDCl<sub>3</sub>) δ ppm 8.15 (s, 1 H), 7.32 (d, *J*=7.1 Hz, 1 H),

6.65 (d,  $J=7.1$  Hz, 1 H), 4.06-3.99 (m, 2 H), 1.82-1.72 (m, 2 H), 1.41 (sxt.,  $J=7.3$  Hz, 2 H), 0.99 (t,  $J=7.3$  Hz, 3 H);  $^{13}\text{C}$  NMR (101 MHz,  $\text{CDCl}_3$ )  $\delta$  ppm 158.1, 150.6, 136.3, 135.9, 130.0, 113.8, 107.6, 100.6, 49.2, 31.5, 19.9, 13.7; HRMS ( $\text{M}+\text{H}$ ) $^+$  calculated for  $\text{C}_{12}\text{H}_{13}\text{N}_2\text{OS}$  233.0749; found 233.0754; LC/MS (formic acid):  $R_t = 0.98$  min (93%) [ $\text{M}+\text{H}$ ] $^+ = 233$ .

**7-Bromo-5-butyl-4-oxo-4,5-dihydrothieno[3,2-c]pyridine-2-carbonitrile.** To a stirred solution of 5-butyl-4-oxo-4,5-dihydrothieno[3,2-c]pyridine-2-carbonitrile (984 mg, 4.24 mmol) in THF (20 mL) was added 1-bromopyrrolidine-2,5-dione (1131 mg, 6.35 mmol) at rt. The resultant solution was stirred at rt for 65 hours before being concentrated *in vacuo*. The resultant solid was triturated with diethyl ether (15 mL) and filtered under reduced pressure. The collected solid was washed sequentially with diethyl ether (10 mL) and water (20 mL) before being dried yielding 7-bromo-5-butyl-4-oxo-4,5-dihydrothieno[3,2-c]pyridine-2-carbonitrile (816 mg, 2.62 mmol, 62%) as a cream solid. The filtrate was diluted with EtOAc (25 mL) and washed sequentially with water (20 mL) and brine (20 mL). The organic layer was passed through a hydrophobic frit and concentrated *in vacuo*. The resultant solid was dissolved in minimal DCM and purified by silica chromatography (0-30% EtOAc in cyclohexane). The desired fractions were combined and concentrated *in vacuo* yielding 7-bromo-5-butyl-4-oxo-4,5-dihydrothieno[3,2-c]pyridine-2-carbonitrile (313 mg, 1.006 mmol, 24%) as a cream solid. Both solids were combined yielding 7-bromo-5-butyl-4-oxo-4,5-dihydrothieno[3,2-c]pyridine-2-carbonitrile (1129 mg, 3.63 mmol, 86%) as a cream solid. m.p. 115–116 °C;  $\nu_{\text{max}}$  (solid)/ $\text{cm}^{-1}$ : 3043, 2957, 2872, 2212 ( $\text{C}\equiv\text{N}$ ), 1651 ( $\text{C}=\text{O}$ ), 1582, 764;  $^1\text{H}$  NMR (400 MHz,  $\text{CDCl}_3$ )  $\delta$  ppm 8.23 (s, 1 H), 7.45 (s, 1 H), 4.02 (t,  $J=7.3$  Hz, 2 H), 1.83-1.72 (m, 2 H), 1.42 (sxt.,  $J=7.3$  Hz, 2 H), 1.00 (t,  $J=7.3$  Hz, 3 H);  $^{13}\text{C}$  NMR (101 MHz,  $\text{CDCl}_3$ )  $\delta$  ppm 160.8, 156.3, 140.8, 139.5, 133.2, 117.2, 112.6, 95.6, 53.3, 35.3, 23.6, 17.4; HRMS ( $\text{M}+\text{H}$ ) $^+$  calculated for  $\text{C}_{12}\text{H}_{12}\text{BrN}_2\text{OS}$  310.9854; found 310.9855; LC/MS (formic acid):  $R_t = 1.18$  min (95%) [ $\text{M}+\text{H}$ ] $^+ = 312$ .

**Methyl 7-bromo-5-butyl-4-oxo-4,5-dihydrothieno[3,2-c]pyridine-2-carbimidate (52).** To a suspension of 7-bromo-5-butyl-4-oxo-4,5-dihydrothieno[3,2-c]pyridine-2-carbonitrile (1106 mg, 3.55 mmol) in MeOH (35 mL) was added sodium methoxide (25 wt% in MeOH) solution (0.813 mL, 3.55 mmol). The reaction mixture was heated to 75 °C when solvation was achieved. After 15 minutes 4-aminotetrahydro-2H-thiopyran 1,1-dioxide (499 mg, 3.34 mmol) was added and the solution was heated for a further 18 hours. A further equivalent of sodium methoxide (25% by weight solution in MeOH) (0.813 mL, 3.55 mmol) was added at rt before the reaction was heated to 85 °C and stirred for 3 hours. No product observed. Reaction was cooled to 75 °C and a portion of 4-aminotetrahydro-2H-thiopyran 1,1-dioxide, hydrochloride (125 mg, 0.67 mmol) was added. The reaction was stirred at 75 °C for 5 hours. The solution was allowed to cool to rt before being concentrated *in vacuo*. The resultant residue was dry loaded and purified by silica chromatography (0-75% EtOAc in cyclohexane). The desired fractions were combined yielding methyl 7-bromo-5-butyl-4-oxo-4,5-dihydrothieno[3,2-c]pyridine-2-carbimidate (326 mg, 0.95 mmol, 27%) as a white solid. m.p. 152-154 °C;  $\nu_{\max}$  (solid)/ $\text{cm}^{-1}$ : 3295, 3077, 2953, 1648 (C=O), 1578, 1314, 1129, 702;  $^1\text{H}$  NMR (400 MHz,  $\text{CD}_3\text{OD}$ )  $\delta$  ppm 8.23 (s, 1 H), 7.84 (s, 1 H), 4.07 (t,  $J=7.5$  Hz, 2 H), 3.97-3.87 (m, 3 H), 1.82-1.71 (m, 2 H), 1.41 (sxt.,  $J=7.3$  Hz, 2 H), 1.00 (t,  $J=7.3$  Hz, 3 H);  $^{13}\text{C}$  NMR (176 MHz,  $\text{CD}_3\text{OD}$ )  $\delta$  ppm 163.4, 159.8, 152.7, 136.5, 136.4, 135.7, 130.9, 128.7, 94.5, 50.6, 32.7, 21.0, 14.2; HRMS ( $\text{M}+\text{H}$ ) $^+$  calculated for  $\text{C}_{13}\text{H}_{16}\text{BrN}_2\text{O}_2\text{S}$  343.0116; found 343.0119; LC/MS (formic acid):  $R_t = 0.92$  min (97%) [ $\text{M}+\text{H}$ ] $^+ = 343$ .

**7-Bromo-5-butyl-N-(1,1-dioxidotetrahydro-2H-thiopyran-4-yl)-4-oxo-4,5-dihydrothieno[3,2-c]pyridine-2-carboximidamide.** Triethylamine (0.18 mL, 1.30 mmol) was added to a stirred solution 4-aminotetrahydro-2H-thiopyran 1,1-dioxide (168 mg, 1.13 mmol) and methyl 7-bromo-5-butyl-4-oxo-4,5-dihydrothieno[3,2-c]pyridine-2-carbimidate (297 mg, 0.87 mmol) in DMF (5 mL). The resultant solution was heated to 120 °C and stirred



for 17 hours. The resultant solution was allowed to cool to rt before being diluted with water (35 mL). The resultant precipitate was collected under reduced pressure, dissolved in minimal DCM and purified by silica chromatography (0-50% 25% MeOH in DCM in cyclohexane). The desired fractions were combined and concentrated *in vacuo* yielding 7-bromo-5-butyl-*N*-(1,1-dioxidotetrahydro-2H-thiopyran-4-yl)-4-oxo-4,5-dihydrothieno[3,2-*c*]pyridine-2-carboximidamide (83 mg, 0.18 mmol, 21%) as a pale orange solid. <sup>1</sup>H NMR (400 MHz, CDCl<sub>3</sub>) δ ppm 7.91 (s, 1 H), 7.33 (s, 1 H), 5.01 (br. s, 1 H), 4.01 (t, *J*=7.3 Hz, 2 H), 3.77-3.53 (m, 2 H), 3.05-2.88 (m, 2 H), 2.49-2.33 (m, 2 H), 2.26-2.12 (m, 2 H), 1.80-1.72 (quint., *J*=7.3 Hz, 2 H), 1.49-1.36 (m, 2 H), 0.99 (t, *J*=7.3 Hz, 3 H) (N.B. exchangeable amidine protons not visible); HRMS (M+H)<sup>+</sup> calculated for C<sub>17</sub>H<sub>23</sub>BrN<sub>3</sub>O<sub>3</sub>S<sub>2</sub> 460.0364; found 460.0368; LC/MS (formic acid): R<sub>t</sub> = 0.56 min (91%) [M+H]<sup>+</sup> = 460.

**5-Butyl-*N*-(1,1-dioxidotetrahydro-2H-thiopyran-4-yl)-4-oxo-7-(3-**

**(trifluoromethyl)phenyl)-4,5-dihydrothieno[3,2-*c*]pyridine-2-carboximidamide (36).** 7-

Bromo-5-butyl-*N*-(1,1-dioxidotetrahydro-2H-thiopyran-4-yl)-4-oxo-4,5-dihydrothieno[3,2-*c*]pyridine-2-carboximidamide (73 mg, 0.16 mmol), (3-(trifluoromethyl)phenyl)boronic acid (36 mg, 0.19 mmol), potassium carbonate (53 mg, 0.38 mmol) and PEPPSI-<sup>i</sup>Pr (10 mg, 0.01 mmol) were dissolved in water (0.13 mL) and IPA (0.38 mL). The resultant mixture was heated to 120 °C and stirred for 30 minutes in a microwave reactor. The reaction mixture was allowed to cool to rt before being diluted with EtOAc (10 mL), filtered through Celite and concentrated *in vacuo*. The resultant residue was dissolved in 1:1 MeOH:DMSO and purified by MDAP (high pH). The desired fractions were combined yielding 5-butyl-*N*-(1,1-dioxidotetrahydro-2H-thiopyran-4-yl)-4-oxo-7-(3-(trifluoromethyl)phenyl)-4,5-dihydrothieno[3,2-*c*]pyridine-2-carboximidamide (43 mg, 0.08 mmol, 52%) as a white solid. m.p. 121-124 °C; ν<sub>max</sub> (solid)/cm<sup>-1</sup>: 3296, 2957, 1651 (C=O), 1583, 1118; <sup>1</sup>H NMR (400 MHz, CDCl<sub>3</sub>) δ ppm 7.97 (s, 1 H), 7.88-7.78 (m, 1 H), 7.76-7.60 (m, 3 H), 7.24 (s, 1 H), 4.09 (t, *J*=7.3 Hz, 2 H), 3.76 (br. s, 1 H), 3.57-

3.45 (m, 2 H), 3.01-2.86 (m, 2 H), 2.49-2.29 (m, 2 H), 2.26-2.13 (m, 2 H), 1.82 (quin.,  $J=7.3$  Hz, 2 H), 1.44 (sxt.,  $J=7.3$  Hz, 2 H), 1.00 (t,  $J=7.3$  Hz, 3 H) (N.B. exchangeable amidine protons not visible);  $^{19}\text{F}$  NMR (376 MHz,  $\text{CDCl}_3$ )  $\delta$  ppm -62.64 (s); HRMS ( $\text{M}+\text{H}$ ) $^+$  calculated for  $\text{C}_{24}\text{H}_{27}\text{F}_3\text{N}_3\text{O}_3\text{S}_2$  526.1446; found 526.1448; LC/MS (high pH):  $R_t = 1.20$  min (100%) [ $\text{M}+\text{H}$ ] $^+ = 526$ .

**3-Butyl-6-chloro-[1,2,4]triazolo[4,3-b]pyridazin-8-amine (54).** 3,6-Dichloropyridazin-4-amine (**53**) (3000 mg, 18.29 mmol) was dissolved in hydrazine hydrate (22.25 mL, 274 mmol) at rt under nitrogen. The resultant mixture was heated to 135 °C and stirred under nitrogen for 30 min. The solution was allowed to cool to rt before being diluted with crushed ice. The precipitate was collected under reduced pressure, washed with ice-cold water and dried under vacuum at 40 °C yielding a pale brown solid. The solid was dissolved in pentanoic acid (7.85 mL, 71.40 mmol) at rt under nitrogen. The resultant solution was heated to 100 °C and stirred for 3 hours. The resultant solution was allowed to cool to rt before being diluted with water (75 mL) and EtOAc (75 mL). The layers were separated, and the aqueous layer extracted with EtOAc (50 mL). The combined organic fractions were washed with brine (75 mL), passed through a hydrophobic frit, and concentrated *in vacuo*. The resultant residue was loaded on to silica and purified by silica chromatography (0-50% 3:1 EtOAc:EtOH in cyclohexane). The desired fractions were combined yielding 3-butyl-6-chloro-[1,2,4]triazolo[4,3-b]pyridazin-8-amine (1.754 g, 7.77 mmol, 43%) as a yellow solid.  $^1\text{H}$  NMR (400 MHz,  $\text{DMSO}-d_6$ )  $\delta$  ppm 7.86 (s, 2 H), 6.12 (s, 1 H), 2.99 (t,  $J=7.6$  Hz, 2 H), 1.77 (quint.,  $J=7.6$  Hz, 2 H), 1.38 (sxt.,  $J=7.6$  Hz, 2 H), 0.92 (t,  $J=7.6$  Hz, 3 H);  $^{13}\text{C}$  NMR (101 MHz,  $\text{DMSO}-d_6$ )  $\delta$  ppm 150.3, 149.8, 144.4, 139.8, 94.1, 28.5, 23.7, 22.2, 14.0; HRMS ( $\text{M}+\text{H}$ ) $^+$  calculated for  $\text{C}_9\text{H}_{13}\text{ClN}_5$  226.0859; found 226.0866; LC/MS (formic acid):  $R_t = 0.89$  min (100%) [ $\text{M}+\text{H}$ ] $^+ = 226$ .

**Ethyl (3-butyl-6-chloro-[1,2,4]triazolo[4,3-b]pyridazin-8-yl)carbamate.** 4-Methylmorpholine (3.35 mL, 30.50 mmol) and ethyl chloroformate (1.83 mL, 19.06 mmol)

were added to a stirred solution of 3-butyl-6-chloro-[1,2,4]triazolo[4,3-b]pyridazin-8-amine (1721 mg, 7.63 mmol) in DCM (15 mL) at 0 °C. The resultant solution was allowed to warm to rt and stirred for 5 min. The resultant solution was diluted with DCM (50 mL) and washed with water (2 × 50 mL). The organic layer was separated, washed with brine (50 mL), passed through a hydrophobic frit and concentrated *in vacuo*. The resultant residue was dissolved in minimal DCM and purified by silica chromatography (0-80% EtOAc in cyclohexane). The desired fractions were combined yielding ethyl (3-butyl-6-chloro-[1,2,4]triazolo[4,3-b]pyridazin-8-yl)carbamate (1.523 g, 5.12 mmol, 67%) as an orange oil. <sup>1</sup>H NMR (400 MHz, DMSO-*d*<sub>6</sub>) δ ppm 11.17 (br. s, 1 H), 7.64 (s, 1 H), 4.26 (q, *J*=7.1 Hz, 2 H), 3.05 (t, *J*=7.3 Hz, 2 H), 1.85-1.75 (m, 2 H), 1.45-1.35 (m, 2 H), 1.29 (t, *J*=7.1 Hz, 3 H), 0.93 (t, *J*=7.3 Hz, 3 H); <sup>13</sup>C NMR (101 MHz, DMSO-*d*<sub>6</sub>) δ ppm 154.0, 150.8, 149.9, 138.9, 136.7, 103.5, 62.5, 28.4, 23.6, 22.2, 14.7, 14.0; HRMS (M+H)<sup>+</sup> calculated for C<sub>12</sub>H<sub>17</sub>ClN<sub>5</sub>O<sub>2</sub> 298.1071; found 298.1076; LC/MS (formic acid): R<sub>t</sub> = 1.14 min (86%) [M+H]<sup>+</sup> = 298.

**Ethyl (3-butyl-6-(4-methyl-3-nitrophenyl)-[1,2,4]triazolo[4,3-b]pyridazin-8-yl)carbamate (55).** Solvent system was sparged with nitrogen for 1 hour prior to use. Ethyl (3-butyl-6-chloro-[1,2,4]triazolo[4,3-b]pyridazin-8-yl)carbamate (480 mg, 1.61 mmol), (4-methyl-3-nitrophenyl)boronic acid (438 mg, 2.42 mmol), PdCl<sub>2</sub>(dppf) (590 mg, 0.81 mmol) and sodium carbonate (1709 mg, 16.12 mmol) were dissolved in toluene (15 mL) and EtOH (15 mL) under nitrogen at rt. The resultant solution was heated to 100 °C and stirred for 5 hours under nitrogen before being allowed to cool to rt and concentrated *in vacuo*. The resultant residue was dissolved in EtOAc (35 mL) and washed sequentially with water (35 mL) and brine (35 mL). The organic layer was passed through a hydrophobic frit and concentrated *in vacuo*. The resultant residue was dissolved in minimal DCM and purified by silica chromatography (0-100% EtOAc in cyclohexane). The desired fractions were combined yielding ethyl (3-butyl-6-(4-methyl-3-nitrophenyl)-[1,2,4]triazolo[4,3-b]pyridazin-8-yl)carbamate (243 mg, 0.61

mmol, 38%) as an orange gum. m.p. 135-140 °C;  $\nu_{\max}$  (solid)/ $\text{cm}^{-1}$ : 3295, 2959, 2211, 1738, 1529 (N-O), 1220;  $^1\text{H}$  NMR (400 MHz,  $\text{DMSO-}d_6$ )  $\delta$  ppm 10.91 (s, 1 H), 8.50 (d,  $J=2.0$  Hz, 1 H), 8.18 (dd,  $J=8.1, 2.0$  Hz, 1 H), 8.13 (s, 1 H), 7.70 (d,  $J=8.1$  Hz, 1 H), 4.28 (q,  $J=7.1$  Hz, 2 H), 3.17 (t,  $J=7.5$  Hz, 2 H), 2.60 (s, 3 H), 1.94-1.81 (m, 2 H), 1.51-1.37 (m, 2 H), 1.32 (t,  $J=7.1$  Hz, 3 H), 0.96 (t,  $J=7.5$  Hz, 3 H);  $^{13}\text{C}$  NMR (101 MHz,  $\text{DMSO-}d_6$ )  $\delta$  ppm 154.1, 152.4, 149.8, 139.2, 135.9, 135.5, 134.6, 134.3, 131.7, 123.0, 101.0, 62.2, 28.6, 23.7, 22.2, 19.9, 14.7, 14.0 (N.B. one  $\text{sp}^2$  carbon signal not visible); HRMS ( $\text{M}+\text{H}$ ) $^+$  calculated for  $\text{C}_{19}\text{H}_{23}\text{N}_6\text{O}_4$  399.1781; found 399.1778; LC/MS (formic acid):  $R_t = 1.30$  min (92%) [ $\text{M}+\text{H}$ ] $^+ = 399$ .

**Ethyl (6-(3-amino-4-methylphenyl)-3-butyl-[1,2,4]triazolo[4,3-b]pyridazin-8-yl)carbamate.** Powdered iron (142 mg, 2.55 mmol) was added to a stirred solution of ethyl (3-butyl-6-(4-methyl-3-nitrophenyl)-[1,2,4]triazolo[4,3-b]pyridazin-8-yl)carbamate (203 mg, 0.51 mmol) and acetic acid (0.18 mL, 3.06 mmol) in EtOH (15 mL) and water (5 mL). The reaction mixture was then heated to 80 °C and stirred for 2 hours. The resultant solution was allowed to cool to rt before being concentrated *in vacuo*. The resultant residue was dissolved in saturated aq.  $\text{NaHCO}_3$  (15 mL) and extracted with EtOAc (3  $\times$  20 mL). The organic fractions were combined, washed with brine (20 mL), passed through a hydrophobic frit and concentrated *in vacuo*. The resultant residue was dissolved in minimal DCM and purified by silica chromatography (30-100% EtOAc in cyclohexane). The desired fractions were combined yielding ethyl (6-(3-amino-4-methylphenyl)-3-butyl-[1,2,4]triazolo[4,3-b]pyridazin-8-yl)carbamate (93 mg, 0.25 mmol, 50%) as a pale brown solid. m.p. 79-83 °C;  $\nu_{\max}$  (solid)/ $\text{cm}^{-1}$ : 2959, 1738, 1561, 1530, 1220;  $^1\text{H}$  NMR (400 MHz,  $\text{DMSO-}d_6$ )  $\delta$  ppm 10.71 (br. s, 1 H), 8.08 (s, 1 H), 7.25 (d,  $J=1.5$  Hz, 1 H), 7.15-7.04 (m, 2 H), 5.16 (br. s, 2 H), 4.26 (q,  $J=7.1$  Hz, 2 H), 3.15 (t,  $J=7.5$  Hz, 2 H), 2.13 (s, 3 H), 1.86 (quint.,  $J=7.5$  Hz, 2 H), 1.41 (s, 2 H), 1.30 (t,  $J=7.1$  Hz, 3 H), 0.95 (t,  $J=7.5$  Hz, 3 H);  $^{13}\text{C}$  NMR (101 MHz,  $\text{DMSO-}d_6$ )  $\delta$  ppm 155.2, 154.2, 150.9, 147.7, 139.4, 135.0, 133.8, 131.0, 124.4, 115.2, 112.4, 101.6, 62.1, 28.6,

23.8, 22.2, 17.8, 14.8, 14.0; HRMS (M+H)<sup>+</sup> calculated for C<sub>19</sub>H<sub>25</sub>N<sub>6</sub>O<sub>2</sub> 369.2039; found 369.2036; LC/MS (formic acid): R<sub>t</sub> = 1.11 min (94%) [M+H]<sup>+</sup> = 369.

**Ethyl (3-butyl-6-(4-methyl-3-(methylsulfonamido)phenyl)-[1,2,4]triazolo[4,3-b]pyridazin-8-yl)carbamate (38).** Mesyl-Cl (0.17 mL, 2.17 mmol) was added to a stirred solution of ethyl (6-(3-amino-4-methylphenyl)-3-butyl-[1,2,4]triazolo[4,3-b]pyridazin-8-yl)carbamate (80 mg, 0.22 mmol) and pyridine (0.06 mL, 0.76 mmol) in DCM (3 mL) and the resultant solution stirred at rt for 3 hours before being concentrated *in vacuo*. The resultant residue was dissolved in 1:1 MeOH:DMSO and purified by MDAP (high pH). The desired fractions were concentrated *in vacuo* yielding ethyl (3-butyl-6-(4-methyl-3-(methylsulfonamido)phenyl)-[1,2,4]triazolo[4,3-b]pyridazin-8-yl)carbamate (72 mg, 0.16 mmol, 74%) as a white solid. m.p. 199-204 °C;  $\nu_{\max}$  (solid)/cm<sup>-1</sup>: 3228, 2959, 1727, 1564, 1533, 1223; <sup>1</sup>H NMR (400 MHz, DMSO-*d*<sub>6</sub>)  $\delta$  ppm 8.11 (s, 1 H), 7.91 (d, *J*=1.8 Hz, 1 H), 7.75 (dd, *J*=8.0, 1.8 Hz, 1 H), 7.47 (d, *J*=8.0 Hz, 1 H), 4.27 (q, *J*=7.1 Hz, 2 H), 3.16 (t, *J*=7.5 Hz, 2 H), 3.03 (s, 3 H), 2.40 (s, 3 H), 1.86 (quint., *J*=7.5 Hz, 2 H), 1.42 (s, *J*=7.5 Hz, 2 H), 1.31 (t, *J*=7.1 Hz, 3 H), 0.95 (t, *J*=7.5 Hz, 3 H) (N.B. exchangeable sulfonamide and carbamate protons not visible); <sup>13</sup>C NMR (101 MHz, DMSO-*d*<sub>6</sub>)  $\delta$  ppm 154.2, 154.0, 151.1, 139.3, 137.1, 136.9, 135.5, 134.0, 132.1, 124.8, 124.7, 101.3, 62.2, 40.6, 28.6, 23.8, 22.2, 18.6, 14.8, 14.0. (N.B. peak at 40.6 is obscured by DMSO solvent peak but clearly visible); HRMS (M+H)<sup>+</sup> calculated for C<sub>20</sub>H<sub>27</sub>N<sub>6</sub>O<sub>4</sub>S 447.1814; found 447.1809; LC/MS (formic acid): R<sub>t</sub> = 1.07 min (99%) [M+H]<sup>+</sup> = 447.

#### ASSOCIATED CONTENT

**Supporting Information.** Additional text describing all methods and results, all screening statistics, representative LCMS traces of target compounds, full BROMOscan and selectivity

data and X-ray data collection and refinement statistics. This material is available free of charge via the Internet <http://pubs.acs.org>.

Accession Codes: Coordinates have been deposited with the Protein Data Bank under accession codes 6YQW (BRD9/8 complex), 6YQR (BRD9/14 complex), 6YQZ (BRD4(1)/14 complex), 6YQS (BRD9/18 complex). Authors will release atomic coordinates and experimental data upon article publication.

## AUTHOR INFORMATION

### **Corresponding Author**

\*E-mail: philip.g.humphreys@gsk.com. Phone: +44 (0)1438 764252.

### **Present Addresses**

M.A.C.: MSD, Francis Crick Institute, 1 Midland Road, London, NW1 1AT, U. K.

M.L.: Respiratory, Inflammation and Autoimmune (RIA) BioPharmaceuticals R&D, AstraZeneca, SE-431 83, Mölndal, Sweden.

J.M.: Mission Therapeutics Ltd, McClintock Building, Granta Park, Great Abington, Cambridge, CB21 6GP, U. K.

N.H.T: The University of Manchester, Oxford Road, Manchester, M13 9PL, U.K.

### **Author Contributions**

The manuscript was written through contributions of all authors. All authors have given approval to the final version of the manuscript.

### **Notes**

The authors declare the following competing financial interest(s): All authors except M.A.C and N.C.O.T, are current or former employees of GlaxoSmithKline.

## ACKNOWLEDGMENT

M.A.C. and N.H.T. are grateful to GlaxoSmithKline R&D, Stevenage and the University of Strathclyde for Ph.D. studentship and we thank the EPSRC for funding via Prosperity Partnership EP/S035990/1. We also thank Heather Barnett for array support; Sean Lynn and Richard Upton for assistance with NMR; Steve Jackson and Eric Hortense for chiral HPLC; and Tony Cook for high resolution mass spectrometry. We appreciate helpful discussions with Emmanuel Demont during the course of this work.

## ABBREVIATIONS

AMP, artificial membrane permeability; ATAD2A, ATPase family, AAA domain containing 2A; ATAD2B, ATPase family, AAA domain containing 2B; BAF, BRG1/BRM-associated factor; BAZ2A, bromodomain adjacent to zinc finger domain 2A; BAZ2B, bromodomain adjacent to zinc finger domain 2B; BCP, bromodomain containing protein; BD, bromodomain; BET, bromodomain and extra terminal domain; BRD1, bromodomain containing protein 1; BRD2, bromodomain containing protein 2; BRD3, bromodomain containing protein 3; BRD4, bromodomain containing protein 4; BRD7, bromodomain containing protein 7; BRD8, bromodomain containing protein 8; BRD9, bromodomain containing protein 9; BRDT, bromodomain containing protein, testis-specific; BRPF1, bromodomain and PHD finger-containing protein 1; BRPF3, bromodomain and PHD finger-containing protein 3; CAD, charged aerosol detection; CECR2, cat eye syndrome chromosome region candidate 2; CLND, chemiluminescent nitrogen detection; CREBBP, CREB binding protein; EP300, E1A-associated protein p300; FALZ, bromodomain PHD finger transcription factor; GCN5L2, general control non-depressible 5; KAc, acetylated lysine; LCMS, liquid chromatography mass spectrometry; LE, ligand efficiency; LLE, lipophilic ligand efficiency; PBAF, polybromo-associated BAF; PBRM1, polybromo 1; PCAF, P300/CREBBP associated factor; PEPPSI, pyridine-enhanced precatalyst preparation stabilization and initiation; PHD, plant

homeodomain; pIC<sub>50</sub>, -log<sub>10</sub> (IC<sub>50</sub>); SMARCA2, SWI/SNF related, matrix associated, actin dependent regulator of chromatin subfamily A, member 2; SMARCA4, SWI/SNF related, matrix associated, actin dependent regulator of chromatin, subfamily A, member 4; TRIM24, tripartite motif containing 24; TRIM33, tripartite motif containing 33; WDR9, WD repeat-containing protein 9.

## REFERENCES

(1) Smith, S. G.; Zhou, M.-M. The Bromodomain: A New Target in Emerging Epigenetic Medicine. *ACS Chem. Biol.* **2016**, *11*, 598–608.

(2) Filippakopoulos, P.; Knapp, S. Targeting Bromodomains: Epigenetic Readers of Lysine Acetylation. *Nat. Rev. Drug Discov.* **2014**, *13*, 337–356.

(3) Filippakopoulos, P.; Picaud, S.; Mangos, M.; Keates, T.; Lambert, J. P.; Barsyte-Lovejoy, D.; Felletar, I.; Volkmer, R.; Müller, S.; Pawson, T.; Gingras, A. C.; Arrowsmith, C. H.; Knapp, S. Histone Recognition and Large-scale Structural Analysis of the Human Bromodomain Family. *Cell* **2012**, *149*, 214–231.

(4) Muller, S.; Filippakopoulos, P.; Knapp, S. Bromodomains as Therapeutic Targets. *Expert Rev. Mol. Med.* **2011**, *13*, e29.

(5) Jain, A. K.; Barton, M. C. Bromodomain Histone Readers and Cancer. *J. Mol. Biol.* **2017**, *429*, 2003–2010.

(6) Noguchi-Yachide, T. BET Bromodomain as a Target of Epigenetic Therapy. *Chem. Pharm. Bull. (Tokyo)*. **2016**, *64*, 540–547.



(7) Padmanabhan, B.; Mathur, S.; Manjula, R.; Tripathi, S. Bromodomain and Extra-Terminal (BET) Family Proteins: New Therapeutic Targets in Major Diseases. *J. Biosci.* **2016**, *41*, 295–311.

(8) Zhang, F.; Ma, S. Disrupting Acetyl-Lysine Interactions: Recent Advance in the Development of BET Inhibitors. *Curr. Drug Targets* **2018**, *19*, 1148–1165.

(9) CCS14 Scientific Posters <https://www.cellcentric.com/ccs1477/Publications/> (accessed Sep 30, 2019).

(10) NCT03568656 - Study to Evaluate CCS1477 in Advanced Tumours <https://clinicaltrials.gov/ct2/show/NCT03568656?term=CCS1477&rank=1> (accessed Sep 30, 2019).

(11) Zaware, N.; Zhou, M.-M. Bromodomain Biology and Drug Discovery. *Nat. Struct. Mol. Biol.* **2019**, *26*, 870–879.

(12) Schiedel, M.; Moroglu, M.; Ascough, D. M. H.; Chamberlain, A. E. R.; Kamps, J. J. A. G.; Sekirnik, A. R.; Conway, S. J. Chemical Epigenetics: The Impact of Chemical and Chemical Biology Techniques on Bromodomain Target Validation. *Angew. Chem. Int. Ed.* **2019**, *58*, 17930–17952.

(13) Oprea, T. I.; Bologa, C. G.; Boyer, S.; Curpan, R. F.; Glen, R. C.; Hopkins, A. L.; Lipinski, C. A.; Marshall, G. R.; Martin, Y. C.; Ostopovici-Halip, L.; Rishton, G.; Ursu, O.; Vaz, R. J.; Waller, C.; Waldmann, H.; Sklar, L. A. A Crowdsourcing Evaluation of the NIH Chemical Probes. *Nat. Chem. Biol.* **2009**, *5*, 441–447.

(14) Frye, S. V. The Art of the Chemical Probe. *Nat. Chem. Biol.* **2010**, *6*, 159–161.

(15) Bunnage, M. E.; Piatnitski Chekler, E. L.; Jones, L. H. Target Validation Using Chemical Probes. *Nat. Chem. Biol.* **2013**, *9*, 195–199.

(16) Bassi, Z. I.; Fillmore, M. C.; Miah, A. H.; Chapman, T. D.; Maller, C.; Roberts, E. J.; Davis, L. C.; Lewis, D. E.; Galwey, N. W.; Waddington, K. E.; Parravicini, V.; MacMillan-Jones, A. L.; Gongora, C.; Humphreys, P. G.; Churcher, I.; Prinjha, R. K.; Tough, D. F. Modulating PCAF/GCN5 Immune Cell Function Through a PROTAC Approach. *ACS Chem. Biol.* **2018**, *13*, 2862–2867.

(17) Clegg, M. A.; Tomkinson, N. C. O.; Prinjha, R. K.; Humphreys, P. G. Advancements in the Development of Non-BET Bromodomain Chemical Probes. *ChemMedChem* **2019**, *14*, 362–385.

(18) Shain, A. H.; Pollack, J. R. The Spectrum of SWI/SNF Mutations, Ubiquitous in Human Cancers. *PLoS One* **2013**, *8*, e55119.

(19) Kadoch, C.; Hargreaves, D. C.; Hodges, C.; Elias, L.; Ho, L.; Ranish, J.; Crabtree, G. R. Proteomic and Bioinformatic Analysis of Mammalian SWI/SNF Complexes Identifies Extensive Roles in Human Malignancy. *Nat. Genet.* **2013**, *45*, 592–601.

(20) Hodges, C.; Kirkland, J. G.; Crabtree, G. R. The Many Roles of BAF (MSWI/SNF) and PBAF Complexes in Cancer. *Cold Spring Harb. Perspect. Med.* **2016**, *6*, 1–24.

(21) Cleary, S. P.; Jeck, W. R.; Zhao, X.; Chen, K.; Selitsky, S. R.; Savich, G. L.; Tan, T.-X.; Wu, M. C.; Getz, G.; Lawrence, M. S.; Parker, J. S.; Li, J.; Powers, S.; Kim, H.; Fischer, S.; Guindi, M.; Ghanekar, A.; Chiang, D. Y. Identification of Driver Genes in Hepatocellular Carcinoma by Exome Sequencing. *Hepatology* **2013**, *58*, 1693–1702.

(22) Wang, X.; Wang, S.; Troisi, E. C.; Howard, T. P.; Haswell, J. R.; Wolf, B. K.; Hawk, W. H.; Ramos, P.; Oberlick, E. M.; Tzvetkov, E. P.; Vazquez, F.; Hahn, W. C.; Park, P. J.; Roberts, C. W. M. BRD9 Defines a SWI/SNF Sub-Complex and Constitutes a Specific Vulnerability in Malignant Rhabdoid Tumors. *Nat. Commun.* **2019**, *10*, 1–11.

(23) Liu, Y.; Zhao, R.; Wang, H.; Luo, Y.; Wang, X.; Niu, W.; Zhou, Y.; Wen, Q.; Fan, S.; Li, X.; Xiong, W.; Ma, J.; Li, X.; Tan, M.; Li, G.; Zhou, M. MiR-141 Is Involved in BRD7-Mediated Cell Proliferation and Tumor Formation Through Suppression of the PTEN/AKT Pathway in Nasopharyngeal Carcinoma. *Cell Death Dis.* **2016**, *7*, e2156.

(24) Yu, X.; Li, Z.; Shen, J. BRD7: A Novel Tumor Suppressor Gene in Different Cancers. *Am. J. Transl. Res.* **2016**, *8*, 742–748.

(25) Drost, J.; Mantovani, F.; Tocco, F.; Elkon, R.; Comel, A.; Holstege, H.; Kerkhoven, R.; Jonkers, J.; Voorhoeve, P. M.; Agami, R.; Del Sal, G. BRD7 Is a Candidate Tumour Suppressor Gene Required for P53 Function. *Nat. Cell Biol.* **2010**, *12*, 380–389.

(26) Ma, J.; Niu, W.; Wang, X.; Zhou, Y.; Wang, H.; Liu, F.; Liu, Y.; Guo, J.; Xiong, W.; Zeng, Z.; Fan, S.; Li, X.; Nie, X.; Li, G.; Gui, R.; Luo, Y.; Zhou, M. Bromodomain-containing Protein 7 Sensitizes Breast Cancer Cells to Paclitaxel by Activating Bcl2-antagonist/Killer Protein. *Oncol. Rep.* **2019**, *41*, 1487–1496.

(27) Clark, P. G. K.; Vieira, L. C. C.; Tallant, C.; Fedorova, O.; Singleton, D. C.; Rogers, C. M.; Monteiro, O. P.; Bennet, J. M.; Baronio, R.; Müller, S.; Daniels, D. L.; Méndez, J.; Knapp, S.; Brennan, P. E.; Dixon, D. J. LP99: Discovery and Synthesis of the First Selective BRD7/9 Bromodomain Inhibitor. *Angew. Chem. Int. Ed.* **2015**, *54*, 6217–6221

(28) Theodoulou, N. H.; Bamborough, P.; Bannister, A. J.; Becher, I.; Bit, R. A.; Che, K. H.; Chung, C.; Dittmann, A.; Drewes, G.; Drewry, D. H.; Gordon, L.; Grandi, P.; Leveridge, M.; Lindon, M.; Michon, A.-M.; Molnar, J.; Robson, S. C.; Tomkinson, N. C. O.; Kouzarides, T.; Prinjha, R. K.; Humphreys, P. G. Discovery of I-BRD9, a Selective Cell Active Chemical Probe for Bromodomain Containing Protein 9 Inhibition. *J. Med. Chem.* **2016**, *59*, 1425–1439.

(29) SGC | TP-472 <http://www.thesgc.org/chemical-probes/TP-472> (accessed Oct 3, 2019).

(30) For alternative molecules from the same series, see: Hay, D. A.; Rogers, C. M.; Fedorov, O.; Tallant, C.; Martin, S.; Monteiro, O. P.; Müller, S.; Knapp, S.; Schofield, C. J.; Brennan, P. E. Design and Synthesis of Potent and Selective Inhibitors of BRD7 and BRD9 Bromodomains. *Med. Chem. Commun.* **2015**, *6*, 1381–1386.

(31) Martin, L. J.; Koegl, M.; Bader, G.; Cockcroft, X.-L.; Fedorov, O.; Fiegen, D.; Gerstberger, T.; Hofmann, M. H.; Hohmann, A. F.; Kessler, D.; Knapp, S.; Knesl, P.; Kornigg, S.; Müller, S.; Nar, H.; Rogers, C.; Rumpel, K.; Schaaf, O.; Steurer, S.; Tallant, C.; Vakoc, C. R.; Zeeb, M.; Zoephel, A.; Pearson, M.; Boehmelt, G.; McConnell, D. Structure-Based Design of an in Vivo Active Selective BRD9 Inhibitor. *J. Med. Chem.* **2016**, *59*, 4462–4475.

(32) Remillard, D.; Buckley, D. L.; Paulk, J.; Brien, G. L.; Sonnett, M.; Seo, H.-S.; Dastjerdi, S.; Wühr, M.; Dhe-Paganon, S.; Armstrong, S. A.; Bradner, J. E. Degradation of the BAF Complex Factor BRD9 by Heterobifunctional Ligands. *Angew. Chem. Int. Ed.* **2017**, *56*, 5738–5743.

(33) Brien, G. L.; Remillard, D.; Shi, J.; Hemming, M. L.; Chabon, J.; Wynne, K.; Dillon, E. T.; Cagney, G.; Van Mierlo, G.; Baltissen, M. P.; Vermeulen, M.; Qi, J.; Fröhling, S.; Gray,

N. S.; Bradner, J. E.; Vakoc, C. R.; Armstrong, S. A. Targeted Degradation of BRD9 Reverses Oncogenic Gene Expression in Synovial Sarcoma. *eLife* **2018**, *7*, e41305.

(34) Crawford, T. D.; Vartanian, S.; Côté, A.; Bellon, S.; Duplessis, M.; Flynn, E. M.; Hewitt, M.; Huang, H.-R.; Kiefer, J. R.; Murray, J.; Nasveschuk, C. G.; Pardo, E.; Romero, F. A.; Sandy, P.; Tang, Y.; Taylor, A. M.; Tsui, V.; Wang, J.; Wang, S.; Zawadzke, L.; Albrecht, B. K.; Magnuson, S. R.; Cochran, A. G.; Stokoe, D. Inhibition of Bromodomain-Containing Protein 9 for the Prevention of Epigenetically-Defined Drug Resistance. *Bioorg. Med. Chem. Lett.* **2017**, *27*, 3534–3541.

(35) Crawford, T. D.; Tsui, V.; Flynn, E. M.; Wang, S.; Taylor, A. M.; Côté, A.; Audia, J. E.; Beresini, M. H.; Burdick, D. J.; Cummings, R.; Dakin, L. A.; Duplessis, M.; Good, A. C.; Hewitt, M. C.; Huang, H.-R.; Jayaram, H.; Kiefer, J. R.; Jiang, Y.; Murray, J.; Nasveschuk, C. G.; Pardo, E.; Poy, F.; Romero, F. A.; Tang, Y.; Wang, J.; Xu, Z.; Zawadzke, L. E.; Zhu, X.; Albrecht, B. K.; Magnuson, S. R.; Bellon, S.; Cochran, A. G. Diving into the Water: Inducible Binding Conformations for BRD4, TAF1(2), BRD9, and CECR2 Bromodomains. *J. Med. Chem.* **2016**, *59*, 5391–5402.

(36) Humphreys, P. G.; Bamborough, P.; Chung, C.; Craggs, P. D.; Gordon, L.; Grandi, P.; Hayhow, T. G.; Hussain, J.; Jones, K. L.; Lindon, M.; Michon, A.-M.; Renaux, J. F.; Suckling, C. J.; Tough, D. F.; Prinjha, R. K. Discovery of a Potent, Cell Penetrant, and Selective P300/CBP-Associated Factor (PCAF)/General Control Nonderepressible 5 (GCN5) Bromodomain Chemical Probe. *J. Med. Chem.* **2017**, *60*, 695–709.

(37) Johnson, T. W.; Gallego, R. A.; Edwards, M. P. Lipophilic Efficiency as an Important Metric in Drug Design. *J. Med. Chem.* **2018**, *61*, 6401–6420.

(38) BROMOscan recombinant protein binding assays were carried out at DiscoverX, <http://www.discoverx.com>.

(39) Nittinger, E.; Gibbons, P.; Eigenbrot, C.; Davies, D. R.; Maurer, B.; Yu, C. L.; Kiefer, J. R.; Kuglstatter, A.; Murray, J.; Ortwine, D. F.; Tang, Y.; Tsui, V. Water Molecules in Protein–Ligand Interfaces. Evaluation of Software Tools and SAR Comparison. *J. Comput. Aided. Mol. Des.* **2019**, *33*, 307–330.

(40) Zhang, X.; Chen, K.; Wu, Y.-D.; Wiest, O. Protein Dynamics and Structural Waters in Bromodomains. *PLoS One* **2017**, *12*, e0186570.

(41) Aldeghi, M.; Ross, G. A.; Bodkin, M. J.; Essex, J. W.; Knapp, S.; Biggin, P. C. Large-Scale Analysis of Water Stability in Bromodomain Binding Pockets with Grand Canonical Monte Carlo. *Commun. Chem.* **2018**, *1*, 1–12.

(42) Bamborough, P.; Chung, C.; Demont, E. H.; Bridges, A. M.; Craggs, P. D.; Dixon, D. P.; Francis, P.; Furze, R. C.; Grandi, P.; Jones, E. J.; Karamshi, B.; Locke, K.; Lucas, S. C. C.; Michon, A.-M.; Mitchell, D. J.; Pogány, P.; Prinjha, R. K.; Rau, C.; Roa, A. M.; Roberts, A. D.; Sheppard, R. J.; Watson, R. J. A Qualified Success: Discovery of a New Series of ATAD2 Bromodomain Inhibitors with a Novel Binding Mode Using High-Throughput Screening and Hit Qualification. *J. Med. Chem.* **2019**, *62*, 7506–7525.

(43) Wang, S.; Tsui, V.; Crawford, T. D.; Audia, J. E.; Burdick, D. J.; Beresini, M. H.; Côté, A.; Cummings, R.; Duplessis, M.; Flynn, E. M.; Hewitt, M. C.; Huang, H.-R.; Jayaram, H.; Jiang, Y.; Joshi, S.; Murray, J.; Nasveschuk, C. G.; Pardo, E.; Poy, F.; Romero, F. A.; Tang, Y.; Taylor, A. M.; Wang, J.; Xu, Z.; Zawadzke, L. E.; Zhu, X.; Albrecht, B. K.; Magnuson, S. R.; Bellon, S.; Cochran, A. G. GNE-371, a Potent and Selective Chemical Probe for the Second

Bromodomains of Human Transcription-Initiation-Factor TFIID Subunit 1 and Transcription-Initiation-Factor TFIID Subunit 1-Like. *J. Med. Chem.* **2018**, *61*, 9301–9315.

(44) Fedorov, O.; Castex, J.; Tallant, C.; Owen, D. R.; Martin, S.; Aldeghi, M.; Monteiro, O.; Filippakopoulos, P.; Picaud, S.; Trzupsek, J. D.; Gerstenberger, B. S.; Bountra, C.; Willmann, D.; Wells, C.; Philpott, M.; Rogers, C.; Biggin, P. C.; Brennan, P. E.; Bunnage, M. E.; Schüle, R.; Günther, T.; Knapp, S.; Müller, S. Selective Targeting of the BRG/PB1 Bromodomains Impairs Embryonic and Trophoblast Stem Cell Maintenance. *Sci. Adv.* **2015**, *1*, e1500723.

(45) Gerstenberger, B. S.; Trzupsek, J. D.; Tallant, C.; Fedorov, O.; Filippakopoulos, P.; Brennan, P. E.; Fedele, V.; Martin, S.; Picaud, S.; Rogers, C.; Parikh, M.; Taylor, A.; Samas, B.; O'Mahony, A.; Berg, E.; Pallares, G.; Torrey, A. D.; Treiber, D. K.; Samardjiev, I. J.; Nasipak, B. T.; Padilla-Benavides, T.; Wu, Q.; Imbalzano, A. N.; Nickerson, J. A.; Bunnage, M. E.; Müller, S.; Knapp, S.; Owen, D. R. Identification of a Chemical Probe for Family VIII Bromodomains Through Optimization of a Fragment Hit. *J. Med. Chem.* **2016**, *59*, 4800–4811.

(46) Sutherell, C. L.; Tallant, C.; Monteiro, O. P.; Yapp, C.; Fuchs, J. E.; Fedorov, O.; Siejka, P.; Müller, S.; Knapp, S.; Brenton, J. D.; Brennan, P. E.; Ley, S. V. Identification and Development of 2,3-Dihydropyrrolo[1,2- a ]Quinazolin-5(1 H )-One Inhibitors Targeting Bromodomains Within the Switch/Sucrose Nonfermenting Complex. *J. Med. Chem.* **2016**, *59*, 5095–5101.

(47) Peptides substituted with propionylated and butyrylated and crotonylated lysines have also been shown to be capable of binding to human bromodomains, albeit with weak affinity, see a) Vollmuth, F.; Geyer, M. Interaction of Propionylated and Butyrylated Histone H3 Lysine

Marks with Brd4 Bromodomains. *Angew. Chem. Int. Ed.* **2010**, *49*, 6768–6772. b) Flynn, E. M.; Huang, O. W.; Poy, F.; Oppikofer, M.; Bellon, S. F.; Tang, Y.; Cochran, A. G. A Subset of Human Bromodomains Recognizes Butyryllysine and Crotonyllysine Histone Peptide Modifications. *Structure* **2015**, *23*, 1801–1814.

(48) Crawford, T. D.; Audia, J. E.; Bellon, S.; Burdick, D. J.; Bommi-Reddy, A.; Côté, A.; Cummings, R. T.; Duplessis, M.; Flynn, E. M.; Hewitt, M.; Huang, H.-R.; Jayaram, H.; Jiang, Y.; Joshi, S.; Kiefer, J. R.; Murray, J.; Nasveschuk, C. G.; Neiss, A.; Pardo, E.; Romero, F. A.; Sandy, P.; Sims, R. J.; Tang, Y.; Taylor, A. M.; Tsui, V.; Wang, J.; Wang, S.; Wang, Y.; Xu, Z.; Zawadzke, L.; Zhu, X.; Albrecht, B. K.; Magnuson, S. R.; Cochran, A. G. GNE-886: A Potent and Selective Inhibitor of the Cat Eye Syndrome Chromosome Region Candidate 2 Bromodomain (CECR2). *ACS Med. Chem. Lett.* **2017**, *8*, 737–741.

(49) Robinson, M. W.; Hill, A. P.; Readshaw, S. A.; Hollerton, J. C.; Upton, R. J.; Lynne, S. M.; Besley, S. C.; Boughtflower, B. J. Use of Calculated Physicochemical Properties to Enhance Quantitative Response When Using Charged Aerosol Detection. *Anal. Chem.* **2017**, *89*, 1772–1777.

(50) Mateus, A.; Gordon, L. J.; Wayne, G. J.; Almqvist, H.; Axelsson, H.; Seashore-Ludlow, B.; Treyer, A.; Matsson, P.; Lundbäck, T.; West, A.; Hann, M. M.; Artursson, P. Prediction of Intracellular Exposure Bridges the Gap between Target- and Cell-Based Drug Discovery. *Proc. Natl. Acad. Sci.* **2017**, *114*, E6231–E6239.

(51) Gordon, L. J.; Allen, M.; Artursson, P.; Hann, M. M.; Leavens, B. J.; Mateus, A.; Readshaw, S.; Valko, K.; Wayne, G. J.; West, A. Direct Measurement of Intracellular



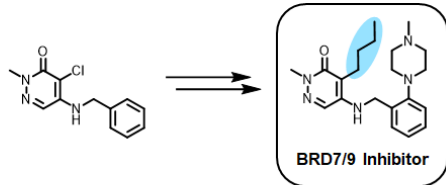
Compound Concentration by RapidFire Mass Spectrometry Offers Insights into Cell Permeability. *J. Biomol. Screen.* **2016**, *21*, 156–164.

(52) Picaud, S.; Leonards, K.; Lambert, J. P.; Dovey, O.; Wells, C.; Fedorov, O.; Monteiro, O.; Fujisawa, T.; Wang, C. Y.; Lingard, H.; Tallant, C.; Nikbin, N.; Guetzoyan, L.; Ingham, R.; Ley, S. V.; Brennan, P.; Muller, S.; Samsonova, A.; Gingras, A. C.; Schwaller, J.; Vassiliou, G.; Knapp, S.; Filippakopoulos, P. Promiscuous Targeting of Bromodomains by Bromosporine Identifies BET Proteins as Master Regulators of Primary Transcription Response in Leukemia. *Sci. Adv.* **2016**, *2*, e1600760–e1600760.

(53) Tyler, D. S.; Vappiani, J.; Cañeque, T.; Lam, E. Y. N.; Ward, A.; Gilan, O.; Chan, T.-C.; Hienzsch, A.; Rutkowska, A.; Werner, T.; Wagner, A. J.; Lugo, D.; Gregory, R.; Ramirez Molina, C.; Garton, N.; Wellaway, C. R.; Jackson, S.; MacPherson, L.; Figueiredo, M.; Stolzenburg, S.; Bell, C. C.; House, C.; Dawson, S.-J.; Hawkins, E. D.; Drewes, G.; Prinjha, R. K.; Rodriguez, R.; Grandi, P.; Dawson, M. A. Click Chemistry Enables Preclinical Evaluation of Targeted Epigenetic Therapies. *Science* **2017**, *356*, 1397–1401.

(54) Gosmini, R.; Nguyen, V. L.; Toum, J.; Simon, C.; Brusq, J.-M. G.; Krysa, G.; Mirguet, O.; Riou-Eymard, A. M.; Boursier, E. V.; Trottet, L.; Bamborough, P.; Clark, H.; Chung, C.; Cutler, L.; Demont, E. H.; Kaur, R.; Lewis, A. J.; Schilling, M. B.; Soden, P. E.; Taylor, S.; Walker, A. L.; Walker, M. D.; Prinjha, R. K.; Nicodème, E. The Discovery of I-BET726 (GSK1324726A), a Potent Tetrahydroquinoline ApoA1 Up-Regulator and Selective BET Bromodomain Inhibitor. *J. Med. Chem.* **2014**, *57*, 8111–8131.

TOC GRAPHIC



**BRD7/9 pK<sub>i</sub>: 6.3/7.2**  
**BET Selectivity: >500-fold**  
**Non-BET Selectivity: ≥285-fold**  
**Permeability: 250 nm/s**  
**Solubility: ≥228 µg/mL**

